

Spacecraft Attitude Dynamics and Control

Dispense del Corso di
Dinamica e Controllo di Assetto di Satelliti
Politecnico di Torino
Anno Accademico 2008 - 09

Ver. 3.0.0

Giulio Avanzini
Dipartimento di Ingegneria Aeronautica e Spaziale
e-mail: *giulio.avanzini@polito.it*

Nota

Le presenti dispense costituiscono parte del materiale didattico di supporto al Corso di *Dinamica e Controllo di Assetto*, da me tenuto presso il Politecnico di Torino a partire dall'Anno Accademico 2007-2008. Le presenti dispense vengono **distribuite gratuitamente**, esclusivamente a fini didattici e **ne è vietata la riproduzione** se non agli scopi di consultazione e studio per i quali sono state redatte, nell'ambito del Corso di Laurea in Ingegneria Aerospaziale del Politecnico di Torino. **Ne è vietata la vendita in qualunque forma.**

Note

The present lecture notes are part of the material for the *Attitude Dynamics and Control* course, that I have been teaching at Politecnico di Torino since the Academic Year 2007-08. The lecture notes are **freely available** exclusively to the students of Politecnico di Torino and they can be copied and reproduced only in this framework. **The lecture notes cannot be distributed or copied elsewhere and cannot be sold in any form.**

Giulio Avanzini

Torino, 1 Marzo 2009

Contents

1 Rigid Body dynamics	1
1.1 Frames of reference and transformation matrices	1
1.2 Euler's angles	3
1.2.1 Building the coordinate transformation matrix from elementary rotations	5
1.2.2 Angular velocity and the evolution of Euler's angles	9
1.2.3 The quaternions	10
1.2.4 Quaternion multiplication	14
1.2.5 The quaternion error vector	15
1.2.6 Evolution of the quaternions	15
1.3 Quaternions vs Euler angles	15
1.4 Other attitude representations	16
1.5 Time derivative of vector quantities	17
1.6 Euler's equations of motion of a rigid body	17
1.6.1 The inertia tensor	17
1.6.2 Kinetic energy	21
1.6.3 Euler's equation of motion	22
1.6.4 Conservation of angular momentum	22
1.6.5 Conservation of kinetic energy	23
1.7 Generalised Euler equation	23
1.7.1 Derivation of the generalised form of Euler equation	23
1.7.2 Use of the generalised form of Euler equation	25
2 Passive Stabilisation of Rigid Spacecraft	27
2.1 Torque-free motion of axi-symmetric satellites	27
2.1.1 Angular velocity	27
2.1.2 Attitude (in terms of Euler angles)	31
2.2 Torque-free motion of tri-inertial satellites	32
2.2.1 Drawing the polhode curves	33
2.2.2 Stability of torque-free motion about principal axes	35
2.3 Nutation Damping	36
2.3.1 Effects of energy dissipation	36
2.3.2 Equations of motion of a rigid satellite with damper	38
2.3.3 A practical case: the axial damper	42
2.4 Attitude manoeuvres of a spinning satellite	46
2.5 Gravity-gradient stabilization	49
2.5.1 Origin of the gravity-gradient torque	50
2.5.2 Equilibria of a rigid body under GG torque	52
2.5.3 Pitch motion	54

2.6	Dual-spin satellites	57
2.6.1	Mathematical model of a gyrostat	59
2.6.2	Simplified models	61
2.6.3	Stability of axial gyrostat	62
3	Active Stabilisation and Control of Spacecraft	65
3.1	Environmental torques and other disturbances	66
3.1.1	Environmental torques	66
3.1.2	Internal disturbances	67
3.2	Attitude sensors	67
3.2.1	Infrared Earth sensors (IRES)	68
3.2.2	Sun sensors	68
3.2.3	Star trackers	68
3.2.4	Rate and rate-integrating gyroscopes	68
3.2.5	Magnetometers	69
3.3	Actuators	69
3.4	Linear model of rigid satellite attitude motion	69
3.5	Linear model of gyrostat attitude motion	70
3.6	Use of thrusters for attitude control	71
3.6.1	Single axis slews (open loop)	71
3.6.2	Closed-loop control	75
3.6.3	Fine pointing control	82
3.7	Momentum exchange devices for attitude control	85
3.7.1	Open-loop control with RWs	86
3.7.2	Sizing a reaction wheel for single axis slews	87
3.7.3	Closed-loop control with RWs for single axis slews	88
3.7.4	Bias torque and reaction wheel saturation	89
3.7.5	Roll-yaw axes control in presence of momentum bias using reaction wheels	90
3.7.6	Roll-yaw axes control using a double-gimbal momentum wheel	91
3.8	Quaternion feedback control	93
3.8.1	Derivation of a globally asymptotically stabilizing controller: Lyapunov method	94
3.8.2	Application of Lyapunov method to nonlinear spacecraft attitude control	94
3.8.3	Generalization of the Quaternion Feedback Control law	95
3.9	Control Moment Gyroscopes	96
3.9.1	Dynamic model of a spacecraft controlled by a cluster of CMG's	96
3.9.2	Gimbal rate command law with Moore-Penrose pseudo-inverse	98
3.9.3	Cluster singular states	99
4	References	101

Chapter 1

Rigid Body dynamics

In order to describe the attitude of a rigid body and to determine its evolution as a function of its initial angular velocity and applied torques, Euler's angles and Euler's equations of motion need to be introduced. The transformation matrix between different reference frames will be recalled and the concept of inertia tensor will also be briefly discussed.

1.1 Frames of reference and transformation matrices

Assuming that a satellite is a rigid body is a reasonable initial model for attitude dynamics and control. However, in practice, this assumption can only be used as a first approximation. For satellites with large deployable solar arrays the structure can be quite flexible. The elastic modes in the structure can be excited through attitude control thrusters firings. This leads to vibrations which reduce the pointing accuracy of the payload. In addition, fuel consumption and fuel slosh in propellant tanks can cause the inertia properties of the satellite to be time varying, leading to a more complex control problem. But if we assume that our spacecraft is a rigid body, we can attach to it a *body frame*, \mathcal{F}_B , described by a set of unit vectors $(\hat{\mathbf{e}}_1, \hat{\mathbf{e}}_2, \hat{\mathbf{e}}_3)$. The position of \mathcal{F}_B with respect to an *inertial reference frame* \mathcal{F}_I , identified by the unit vectors $(\hat{\mathbf{E}}_1, \hat{\mathbf{E}}_2, \hat{\mathbf{E}}_3)$, completely describes the attitude of our spacecraft.

Assuming that \vec{v} is a vector quantity, it is possible to write it as

$$\vec{v} = x\hat{\mathbf{e}}_1 + y\hat{\mathbf{e}}_2 + z\hat{\mathbf{e}}_3$$

or, equivalently,

$$\vec{v} = X\hat{\mathbf{E}}_1 + Y\hat{\mathbf{E}}_2 + Z\hat{\mathbf{E}}_3$$

The column vectors $\mathbf{v}_B = (x, y, z)^T$ and $\mathbf{v}_I = (X, Y, Z)^T$ provide the component representations of the same vector quantity \vec{v} in the reference frames \mathcal{F}_B and \mathcal{F}_I , respectively.

If we now consider the components $\hat{\mathbf{e}}_{i_I} = (e_{1,i}, e_{2,i}, e_{3,i})^T$ of the i -th unit vector $\hat{\mathbf{e}}_i$ in \mathcal{F}_I , that is

$$\hat{\mathbf{e}}_i = e_{1,i}\hat{\mathbf{E}}_1 + e_{2,i}\hat{\mathbf{E}}_2 + e_{3,i}\hat{\mathbf{E}}_3$$

we can write

$$\begin{aligned}\vec{v} &= x\hat{\mathbf{e}}_1 + y\hat{\mathbf{e}}_2 + z\hat{\mathbf{e}}_3 \\ &= x(e_{1,1}\hat{\mathbf{E}}_1 + e_{2,1}\hat{\mathbf{E}}_2 + e_{3,1}\hat{\mathbf{E}}_3) + \\ &\quad + y(e_{1,2}\hat{\mathbf{E}}_1 + e_{2,2}\hat{\mathbf{E}}_2 + e_{3,2}\hat{\mathbf{E}}_3) + \\ &\quad + z(e_{1,3}\hat{\mathbf{E}}_1 + e_{2,3}\hat{\mathbf{E}}_2 + e_{3,3}\hat{\mathbf{E}}_3)\end{aligned}$$

$$\begin{aligned}\vec{v} &= (e_{1,1}x + e_{1,2}y + e_{1,3}z)\hat{\mathbf{E}}_1 + \\ &+ (e_{2,1}x + e_{2,2}y + e_{2,3}z)\hat{\mathbf{E}}_2 + \\ &+ (e_{3,1}x + e_{3,2}y + e_{3,3}z)\hat{\mathbf{E}}_3\end{aligned}$$

This means that the components of \vec{v} in \mathcal{F}_I can be expressed as a function of those in \mathcal{F}_B as follows:

$$\begin{aligned}X &= e_{1,1}x + e_{1,2}y + e_{1,3}z \\ Y &= e_{2,1}x + e_{2,2}y + e_{2,3}z \\ Z &= e_{3,1}x + e_{3,2}y + e_{3,3}z\end{aligned}$$

or, in compact matrix form,

$$\mathbf{v}_I = \mathbf{L}_{IB}\mathbf{v}_B$$

where the *transformation matrix* \mathbf{L}_{IB} is given by

$$\mathbf{L}_{IB} = \begin{bmatrix} e_{1,1} & e_{1,2} & e_{1,3} \\ e_{2,1} & e_{2,2} & e_{2,3} \\ e_{3,1} & e_{3,2} & e_{3,3} \end{bmatrix} = \begin{bmatrix} \hat{\mathbf{e}}_{1_I}^T & \hat{\mathbf{e}}_{2_I}^T & \hat{\mathbf{e}}_{3_I}^T \end{bmatrix}$$

\mathbf{L}_{IB} is made up by the components of the unit vectors $\hat{\mathbf{e}}_i$ as expressed in \mathcal{F}_I . Any matrix made up by mutually orthogonal row or column unit vectors is an *orthogonal matrix* and is characterized by several properties, among which we only recall that:

- the inverse of an orthogonal matrix \mathbf{L} is given by its transpose: $\mathbf{L}^{-1} = \mathbf{L}^T$;
- the determinant of an orthogonal matrix is $\det(\mathbf{L}) = \pm 1$ (and that of a rotation matrix is 1);
- if \mathbf{L}_1 and \mathbf{L}_2 are orthogonal matrices, their product $\mathbf{L}_1\mathbf{L}_2$ is an orthogonal matrix.

Thanks to the first property, it is possible to write the inverse coordinate transformation as

$$\mathbf{v}_B = \mathbf{L}_{BI}\mathbf{v}_I = (\mathbf{L}_{IB})^{-1}\mathbf{v}_I = (\mathbf{L}_{IB})^T\mathbf{v}_I$$

which means that it is also

$$\mathbf{L}_{BI} = \begin{bmatrix} \hat{\mathbf{e}}_{1_I}^T \\ \dots \\ \hat{\mathbf{e}}_{2_I}^T \\ \dots \\ \hat{\mathbf{e}}_{3_I}^T \end{bmatrix}$$

As an exercise, demonstrate that the dual relations

$$\mathbf{L}_{BI} = \begin{bmatrix} \hat{\mathbf{E}}_{1_B}^T & \hat{\mathbf{E}}_{2_B}^T & \hat{\mathbf{E}}_{3_B}^T \end{bmatrix}; \quad \mathbf{L}_{IB} = \begin{bmatrix} \hat{\mathbf{E}}_{1_B}^T \\ \dots \\ \hat{\mathbf{E}}_{2_B}^T \\ \dots \\ \hat{\mathbf{E}}_{3_B}^T \end{bmatrix}$$

also hold.

1.2 Euler's angles

It is possible to use the coordinate transformation matrix \mathbf{L}_{BI} to describe the attitude of the spacecraft through the unit vectors $\hat{\mathbf{e}}_i$ of the body frame attached to it, coming out with a total of 9 parameters. As a matter of fact, these 9 parameters are not free to vary at will, inasmuch as they must satisfy 6 constraints, expressed by the orthonormality condition, that is

$$\hat{\mathbf{e}}_i \cdot \hat{\mathbf{e}}_j = \delta_{i,j} = \begin{cases} 0 & \text{if } i \neq j \\ 1 & \text{if } i = j \end{cases} \quad (1.1)$$

Roughly speaking, only $9 - 6 = 3$ parameters should be sufficient to describe the attitude of \mathcal{F}_B w.r.t. \mathcal{F}_I .

One of the set of three parameters most widely used to describe the attitude of a rigid body (or equivalently the attitude of the body frame attached to it) w.r.t. a fixed frame are the Euler's angles, a sequence of three rotations that take the fixed frame and make it coincide with the body frame. The original sequence of rotations proposed by Euler to superimpose \mathcal{F}_I onto \mathcal{F}_B is the sequences 3-1-3:

1. the first rotation is about the third axis of the initial frame, that is $\hat{\mathbf{E}}_3$, in our case, and takes the first axis $\hat{\mathbf{E}}_1$ to the direction $\hat{\mathbf{e}}'_1$ perpendicular to the plane determined by the unit vectors $\hat{\mathbf{E}}_3$ and $\hat{\mathbf{e}}_3$; $\hat{\mathbf{E}}_2$ is rotated onto $\hat{\mathbf{e}}'_2$; the rotation angle is called *precession angle* Ψ ;
2. the second rotation is about the first axis transformed after the first rotation, $\hat{\mathbf{e}}'_1$, and takes the axis $\hat{\mathbf{e}}'_3$ into the position of $\hat{\mathbf{e}}_3$; $\hat{\mathbf{e}}'_2$ is moved onto $\hat{\mathbf{e}}''_2$; the rotation angle is called *nutation angle* Θ ;
3. the third and final rotation is about $\hat{\mathbf{e}}_3$ and brings $\hat{\mathbf{e}}''_1 = \hat{\mathbf{e}}'_1$ and $\hat{\mathbf{e}}''_2$ to their final positions, $\hat{\mathbf{e}}_1$ and $\hat{\mathbf{e}}_2$, respectively; the rotation angle is called *spin angle* Φ .

The three angles, representing the amplitude of the three, successive rotations Ψ, Θ, Φ , respectively about the third, the first, and again the third axis, can be used to represent the attitude of the frame \mathcal{F}_B : The nutation angle represents the inclination of the third body axis $\hat{\mathbf{e}}_3$ w.r.t. the local vertical $\hat{\mathbf{E}}_3$; The precession angle represents the angle between the first inertial axis $\hat{\mathbf{E}}_1$ and the *line of the nodes* ξ , *i.e.* the intersection between the planes perpendicular to $\hat{\mathbf{e}}_3$ and $\hat{\mathbf{E}}_3$; The spin angle is the rotation about the third body axis.

The transformation matrix \mathbf{L}_{BI} can be expressed as a function of these three angles, in terms of three elementary rotation matrices, as will be derived in the sequel.

Other sequences

It must be remembered that the sequence of rotations here described is not the only possible choice for rotating \mathcal{F}_I onto \mathcal{F}_B . Many other sequences are available and equally useful. In atmospheric flight mechanics the most widely used sequence of rotations is the 3-2-1, also known as the *Bryant's angles*.

In this case the first rotation is about the third axis, $\hat{\mathbf{E}}_3$, and its amplitude is called *yaw angle* ψ . The second rotation about the second axis $\hat{\mathbf{e}}'_2$ is the *pitch angle*, θ , and takes the first axis onto its final position. The third rotation about $\hat{\mathbf{e}}_1$ is the *roll angle*, ϕ . This set of angles is used also in space flight dynamics, to describe the attitude of a spacecraft with respect to the Local Horizontal – Local Vertical (LHLV) reference frame.

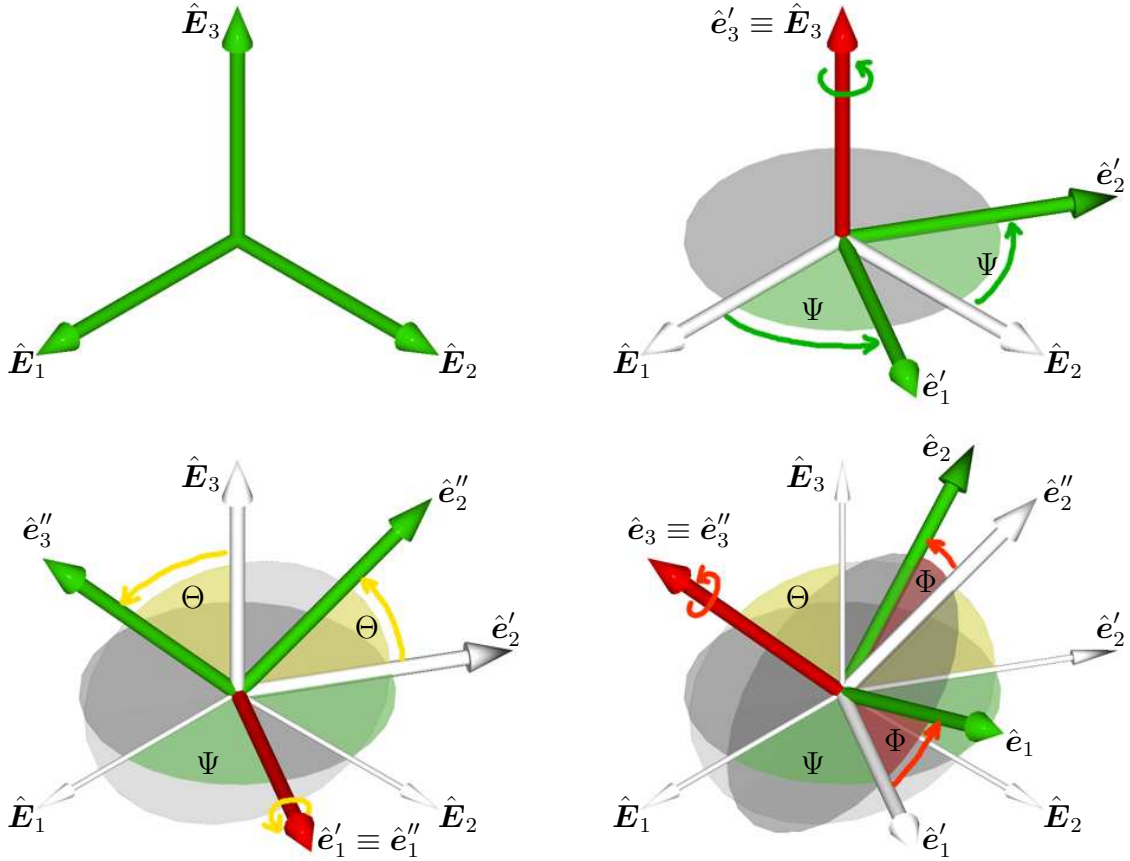


Figure 1.1: Euler's angles

In many textbooks also this latter set of rotations is often referred to as Euler's angles, and this fact may lead to some confusion.

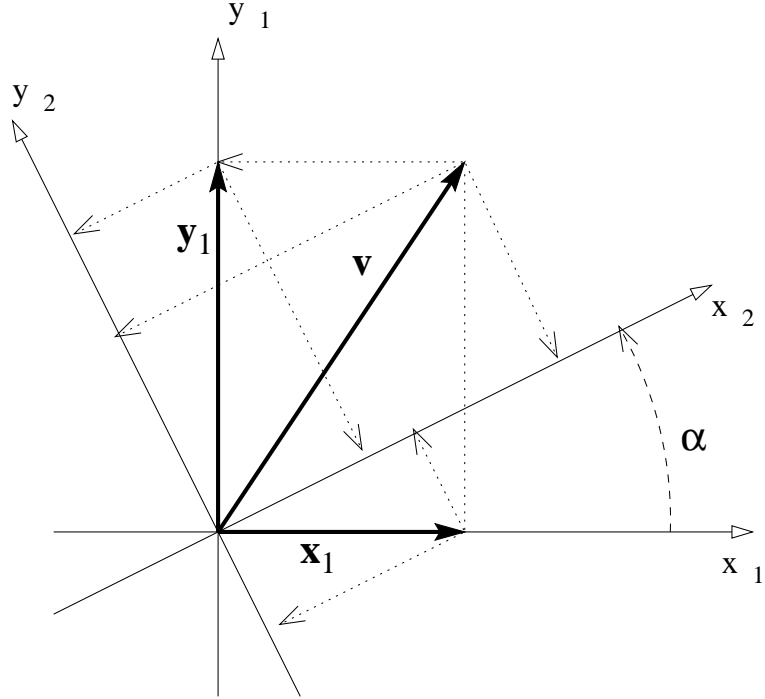
As a final observation, the order of the rotation sequence is important: Rotations do not commute! This means that the rotation sequence 1–2–3, performed with the same angles about the same axis, will take the initial frame to another one. The rotation sequence 1–2–3 is known as *Cardan angles*.

Singularity

There is another problem with the representation of rotations in a three dimensional space, that is the singularity of all the descriptions in terms of three parameters. This means that there will always be positions of the two frames that can be described in different ways, once a particular sequence of rotations is chosen. As an example, if the original Euler's angle sequence is employed, the case in which $\Theta = 0$ is singular, inasmuch as the precession and spin rotations will be about the very same axis, $\hat{\mathbf{E}}_3 \equiv \hat{\mathbf{e}}_3$. This means that all the triplets $(\Psi, 0, \Phi)$ for which $\Psi + \Phi$ is constant represent the same change of reference frame.

Similarly, when the Bryant's angles are used, the case $\theta = \pm\pi/2$ is singular, as in this case all the triplets $(\psi, \pm\pi/2, \phi)$ for which $\psi - \phi$ is constant will provide the same final attitude for \mathcal{F}_B .

The problem of coordinate transformation singularity has some unpleasant mathematical consequence that will be underlined in the following paragraphs.

Figure 1.2: Planar rotation of amplitude α .

1.2.1 Building the coordinate transformation matrix from elementary rotations

Planar rotations

Consider the sketch of Fig. 1.2, where two planar reference frames \mathcal{F}_1 and \mathcal{F}_2 , with the same origin O are represented. The angle α , assumed positive for counter-clockwise rotations, allows one to identify univocally the position of the axes X_2-Y_2 of \mathcal{F}_2 w.r.t. the frame \mathcal{F}_1 defined by the axes X_1 and Y_1 .

Given the components x_1 and y_1 of a vector \vec{v} expressed in \mathcal{F}_1 , the components x_2 e y_2 can be expressed as a function of the angle α . The following relations can be easily inferred from Fig. 1.2:

$$\begin{aligned} x_2 &= x_1 \cos(\alpha) + y_1 \sin(\alpha) \\ y_2 &= -x_1 \sin(\alpha) + y_1 \cos(\alpha) \end{aligned}$$

or, in matrix form,

$$\begin{Bmatrix} x_2 \\ y_2 \end{Bmatrix} = \begin{bmatrix} \cos(\alpha) & \sin(\alpha) \\ -\sin(\alpha) & \cos(\alpha) \end{bmatrix} \begin{Bmatrix} x_1 \\ y_1 \end{Bmatrix}$$

This relation expresses the coordinate transformation that takes the component of a vector quantity expressed in \mathcal{F}_1 into those of a reference frame \mathcal{F}_2 rotated w.r.t. \mathcal{F}_1 of an angle α .

In compact notation we can write

$$\mathbf{v}_2 = \mathbf{L}_{21}\mathbf{v}_1 = \mathbf{R}(\alpha)\mathbf{v}_1$$

where the subscript near the vector indicates the frame in which the components of the vector quantity are considered, the matrix \mathbf{L}_{21} is the coordinate transformation matrix

from \mathcal{F}_1 to \mathcal{F}_2 that in the two dimensional case coincides with the *elementary rotation matrix* $\mathbf{R}(\alpha)$.

The inverse transformation from \mathcal{F}_2 to \mathcal{F}_1 is given by

$$\mathbf{v}_1 = \mathbf{L}_{12}\mathbf{v}_2 = (\mathbf{R}(\alpha))^{-1}\mathbf{v}_2$$

Recalling the properties of orthogonal matrices, it is

$$\mathbf{L}_{12} = (\mathbf{R}(\alpha))^{-1} = (\mathbf{R}(\alpha))^T = \mathbf{R}(-\alpha)$$

Elementary rotations for the sequence 3–1–3

Each one of the Euler's rotations can be considered an elementary rotation about a given axis, that remains unchanged during the transformation. It is still possible to apply the relations derived for the planar case, adding a further equation that states that the coordinate relative to the rotation axis does not vary.

The coordinate transformation during the first rotation is given by

$$\begin{aligned} x' &= X \cos(\Psi) + Y \sin(\Psi) \\ y' &= -X \sin(\Psi) + Y \cos(\Psi) \\ z' &= Z \end{aligned}$$

that, in matrix form, can be written as:

$$\left\{ \begin{array}{l} x' \\ y' \\ z' \end{array} \right\} = \left[\begin{array}{ccc} \cos(\Psi) & \sin(\Psi) & 0 \\ -\sin(\Psi) & \cos(\Psi) & 0 \\ 0 & 0 & 1 \end{array} \right] \left\{ \begin{array}{l} X \\ Y \\ Z \end{array} \right\}$$

In an analogous way it is possible to demonstrate that, during the second rotation about $\hat{\mathbf{e}}'_1$, the coordinate transformation is given by

$$\begin{aligned} x'' &= x' \\ y'' &= y' \cos(\Theta) + z' \sin(\Theta) \\ z'' &= -y' \sin(\Theta) + z' \cos(\Theta) \end{aligned}$$

that in matrix form becomes:

$$\left\{ \begin{array}{l} x'' \\ y'' \\ z'' \end{array} \right\} = \left[\begin{array}{ccc} 1 & 0 & 0 \\ 0 & \cos(\Theta) & \sin(\Theta) \\ 0 & -\sin(\Theta) & \cos(\Theta) \end{array} \right] \left\{ \begin{array}{l} x' \\ y' \\ z' \end{array} \right\}$$

Finally, the third rotation about $\hat{\mathbf{e}}''_3$ is represented by the transformation

$$\begin{aligned} x &= x'' \cos(\Phi) + y'' \sin(\Phi) \\ y &= -x \sin(\Phi) + y'' \cos(\Phi) \\ z &= z'' \end{aligned}$$

or, in matrix form:

$$\left\{ \begin{array}{l} x \\ y \\ z \end{array} \right\} = \left[\begin{array}{ccc} \cos(\Phi) & \sin(\Phi) & 0 \\ -\sin(\Phi) & \cos(\Phi) & 0 \\ 0 & 0 & 1 \end{array} \right] \left\{ \begin{array}{l} x'' \\ y'' \\ z'' \end{array} \right\}$$

The three elementary rotation matrices of the Euler's sequence 3–1–3 can thus be defined as

$$\begin{aligned}\mathbf{R}_3(\Psi) &= \begin{bmatrix} \cos(\Psi) & \sin(\Psi) & 0 \\ -\sin(\Psi) & \cos(\Psi) & 0 \\ 0 & 0 & 1 \end{bmatrix}; \quad \mathbf{R}_1(\Theta) = \begin{bmatrix} 1 & 0 & 0 \\ 0 & \cos(\Theta) & \sin(\Theta) \\ 0 & -\sin(\Theta) & \cos(\Theta) \end{bmatrix}; \\ \mathbf{R}_3(\Phi) &= \begin{bmatrix} \cos(\Phi) & \sin(\Phi) & 0 \\ -\sin(\Phi) & \cos(\Phi) & 0 \\ 0 & 0 & 1 \end{bmatrix}\end{aligned}$$

where the subscript near the rotation matrix symbol \mathbf{R} indicates the axis around which the rotation is performed, while the argument indicates the amplitude of the rotation.

Summing up...

When passing from the inertial frame \mathcal{F}_I to the body frame \mathcal{F}_B using Euler's sequence, the coordinate transformation of vector quantities can be obtained combining in the correct order the elementary rotation matrices, as follows:

$$\begin{aligned}\mathbf{v}' &= \mathbf{R}_3(\Psi)\mathbf{v}_I \\ \mathbf{v}'' &= \mathbf{R}_1(\Theta)\mathbf{v}' \\ \mathbf{v}_B &= \mathbf{R}_3(\Phi)\mathbf{v}''\end{aligned}$$

that is

$$\mathbf{v}_B = \mathbf{R}_3(\Phi)\mathbf{R}_1(\Theta)\mathbf{R}_3(\Psi)\mathbf{v}_I$$

This means that

$$\mathbf{L}_{BI} = \mathbf{R}_3(\Phi)\mathbf{R}_1(\Theta)\mathbf{R}_3(\Psi)$$

Performing the row–column products, the following expression for \mathbf{L}_{BI} is obtained:

$$\mathbf{L}_{BI} = \begin{bmatrix} \cos \Phi \cos \Psi & \sin \Phi \cos \Theta \cos \Psi & \sin \Phi \sin \Theta \\ -\sin \Phi \cos \Theta \sin \Psi & +\cos \Phi \sin \Psi & \\ -\cos \Phi \cos \Theta \sin \Psi & \cos \Phi \cos \Theta \cos \Psi & \cos \Phi \sin \Theta \\ -\sin \Phi \cos \Psi & -\sin \Phi \sin \Psi & \\ \sin \Theta \sin \Psi & -\sin \Theta \cos \Psi & \cos \Theta \end{bmatrix}$$

As the product of orthogonal matrices is an orthogonal matrix, the inverse of which is equal to its transpose, the inverse coordinate transformation matrix \mathbf{L}_{IB} is simply given by

$$\mathbf{L}_{IB} = \mathbf{L}_{BI}^{-1} = \mathbf{L}_{BI}^T = \begin{bmatrix} \cos \Phi \cos \Psi & -\cos \Phi \cos \Theta \sin \Psi & \sin \Theta \sin \Psi \\ -\sin \Phi \cos \Theta \sin \Psi & -\sin \Phi \cos \Psi & \\ \sin \Phi \cos \Theta \cos \Psi & \cos \Phi \cos \Theta \cos \Psi & -\sin \Theta \cos \Psi \\ +\cos \Phi \sin \Psi & -\sin \Phi \sin \Psi & \\ \cos \Phi \sin \Theta & \cos \Phi \sin \Theta & \cos \Theta \end{bmatrix}$$

Elementary rotations for the sequence 3–2–1

It is left as an exercise to the reader the composition of elementary rotation matrices for the sequence 3–2–1. Adopting the same notation used above, it is

$$\mathbf{R}_3(\psi) = \begin{bmatrix} \cos(\psi) & \sin(\psi) & 0 \\ -\sin(\psi) & \cos(\psi) & 0 \\ 0 & 0 & 1 \end{bmatrix}; \quad \mathbf{R}_2(\theta) = \begin{bmatrix} \cos(\theta) & 0 & -\sin(\theta) \\ 0 & 1 & 0 \\ \sin(\theta) & 0 & \cos(\theta) \end{bmatrix};$$

$$\mathbf{R}_1(\phi) = \begin{bmatrix} 1 & 0 & 0 \\ 0 & \cos(\phi) & \sin(\phi) \\ 0 & -\sin(\phi) & \cos(\phi) \end{bmatrix}$$

and the final result is given by

$$\mathbf{L}_{BI} = \begin{bmatrix} \cos \theta \cos \psi & \cos \theta \sin \psi & -\sin \theta \\ \sin \phi \sin \theta \cos \psi & \sin \phi \sin \theta \sin \psi & \sin \phi \cos \theta \\ -\cos \phi \sin \psi & +\cos \phi \cos \psi & \\ \cos \phi \sin \theta \cos \psi & \cos \phi \sin \theta \sin \psi & \cos \phi \cos \theta \\ +\sin \phi \sin \psi & -\sin \phi \cos \psi & \end{bmatrix}$$

A first consequence of the Euler's angle singularity

When $\Theta = 0$, the coordinate transformation matrix does not depend on Ψ and Φ separately, but only on their sum. In such a case, it is

$$\mathbf{L}_{BI} = \begin{bmatrix} \cos \Phi \cos \Psi & \sin \Phi \cos \Psi & 0 \\ -\sin \Phi \sin \Psi & +\cos \Phi \sin \Psi & \\ -\cos \Phi \sin \Psi & \cos \Phi \cos \Psi & 0 \\ -\sin \Phi \cos \Psi & -\sin \Phi \sin \Psi & \\ 0 & 0 & 1 \end{bmatrix} = \begin{bmatrix} \cos(\Phi + \Psi) & \sin(\Phi + \Psi) & 0 \\ -\sin(\Phi + \Psi) & \cos(\Phi + \Psi) & 0 \\ 0 & 0 & 1 \end{bmatrix}$$

As an exercise, demonstrate that \mathbf{L}_{BI} depends on $\psi - \phi$ only, when Bryant's rotation sequence is employed and $\theta = \pm\pi/2$.

How to build elementary rotation matrices

There is a simple way to build mnemonically the elementary rotation matrices. The matrices are 3 by 3. If a rotation of an angle α about the i -th axis is being considered, place 1 in position i, i , and fill the remaining elements of the i -th row and i -th column with zeroes. All the other elements of the principal diagonal are $\cos \alpha$ and the last two outside the diagonal are $\sin \alpha$. The sin element above the row with the 1 must have a minus sign. As an example, let us consider a rotation θ about the second axis (like in the second rotation of the Bryant's sequence). We start filling the matrix with 0s along the second row and column, with a one in position 2,2:

$$\begin{bmatrix} \cdot & 0 & \cdot \\ 0 & 1 & 0 \\ \cdot & 0 & \cdot \end{bmatrix}$$

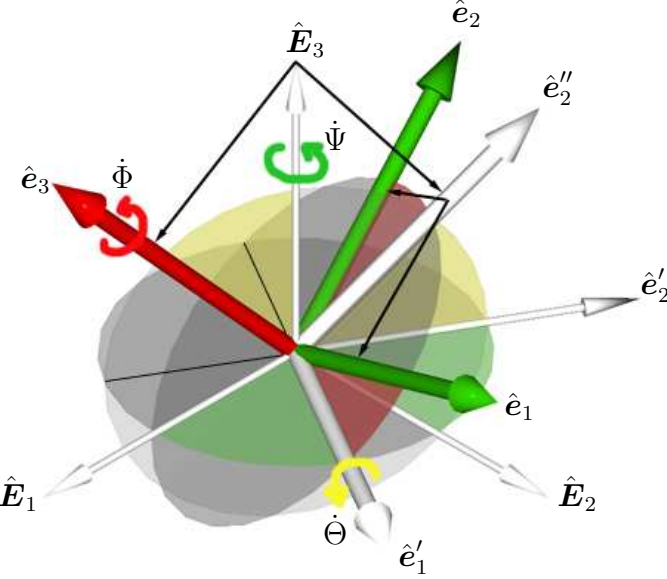


Figure 1.3: Angular velocity as a function of Euler's angle rates.

Then we fill the diagonal with $\cos \theta$:

$$\begin{bmatrix} \cos \theta & 0 & \cdot \\ 0 & 1 & 0 \\ \cdot & 0 & \cos \theta \end{bmatrix}$$

and we put $\sin \theta$ in the remaining places, with a minus sign in the row above the 1:

$$\begin{bmatrix} \cos \theta & 0 & -\sin \theta \\ 0 & 1 & 0 \\ \sin \theta & 0 & \cos \theta \end{bmatrix}$$

This is $\mathbf{R}_2(\theta)$. When a rotation about the first axis is considered, the 1 is on the first row and apparently there is no row above it. But it is sufficient to cycle and start again from the bottom: In this case the minus sign is on the sin in the third row.

1.2.2 Angular velocity and the evolution of Euler's angles

The angular velocity $\vec{\omega}$ is given by

$$\vec{\omega} = \omega_1 \hat{e}_1 + \omega_2 \hat{e}_2 + \omega_3 \hat{e}_3$$

but it is also (see Fig. 1.3)

$$\vec{\omega} = \dot{\Psi} \hat{E}_3 + \dot{\Theta} \hat{e}'_1 + \dot{\Phi} \hat{e}_3$$

The components of the unit vector \hat{E}_3 in \mathcal{F}_B are given by the third column of the matrix \mathbf{L}_{BI} , that is $\mathbf{E}_{3B} = (\sin \Phi \sin \Theta, \cos \Phi \sin \Theta, \cos \Theta)^T$, while the components of \hat{e}'_1 are $(\cos \Phi, -\sin \Phi, 0)^T$. Thus

$$\begin{aligned} \vec{\omega} &= \dot{\Psi}(\sin \Phi \sin \Theta \hat{e}_1 + \cos \Phi \sin \Theta \hat{e}_2 + \cos \Theta \hat{e}_3) + \\ &+ \dot{\Theta}(\cos \Phi \hat{e}_1 - \sin \Phi \hat{e}_2) + \\ &+ \dot{\Phi} \hat{e}_3 \\ &= (\dot{\Psi} \sin \Phi \sin \Theta + \dot{\Theta} \cos \Phi) \hat{e}_1 + \\ &+ (\dot{\Psi} \cos \Phi \sin \Theta - \dot{\Theta} \sin \Phi) \hat{e}_2 \\ &+ (\dot{\Psi} \cos \Theta + \dot{\Phi}) \hat{e}_3 \end{aligned}$$

or, in matrix form

$$\begin{Bmatrix} \omega_1 \\ \omega_2 \\ \omega_3 \end{Bmatrix} = \begin{bmatrix} \sin \Phi \sin \Theta & \cos \Phi & 0 \\ \cos \Phi \sin \Theta & -\sin \Phi & 0 \\ \cos \Theta & 0 & 1 \end{bmatrix} \begin{Bmatrix} \dot{\Psi} \\ \dot{\Theta} \\ \dot{\Phi} \end{Bmatrix}$$

Inverting the 3×3 matrix, one obtains the law of evolution of Euler's angles as a function of angular velocity components in body axis, that is

$$\begin{Bmatrix} \dot{\Psi} \\ \dot{\Theta} \\ \dot{\Phi} \end{Bmatrix} = \begin{bmatrix} \sin \Phi / \sin \Theta & \cos \Phi / \sin \Theta & 0 \\ \cos \Phi & -\sin \Phi & 0 \\ -\sin \Phi / \tan \Theta & -\cos \Phi / \tan \Theta & 1 \end{bmatrix} \begin{Bmatrix} \omega_1 \\ \omega_2 \\ \omega_3 \end{Bmatrix}$$

or, in explicit form,

$$\begin{aligned} \dot{\Psi} &= (\omega_1 \sin \Phi + \omega_2 \cos \Phi) / \sin \Theta \\ \dot{\Theta} &= \omega_1 \cos \Phi - \omega_2 \sin \Phi \\ \dot{\Phi} &= (-\omega_1 \sin \Phi - \omega_2 \cos \Phi) / \tan \Theta + \omega_3 \end{aligned}$$

These equations can be integrated to obtain the evolution of the Euler angles, if the angular velocity is known. But they also show an unpleasant feature of Euler's angle singularity, that is the spin and precession rates go to infinity when Θ approaches 0. This fact has some serious consequences on the problem of attitude representation, inasmuch as it is not possible to accept a set of attitude parameters the evolution of which cannot always be described in an accurate way.

If the Bryant's angles are used, the reader can demonstrate that

$$\vec{\omega} = \dot{\psi} \hat{\mathbf{E}}_3 + \dot{\theta} \hat{\mathbf{e}}'_2 + \dot{\phi} \hat{\mathbf{e}}_3$$

so that

$$\begin{Bmatrix} \omega_1 \\ \omega_2 \\ \omega_3 \end{Bmatrix} = \begin{bmatrix} 1 & 0 & -\sin \theta \\ 0 & \cos \phi & \cos \theta \sin \phi \\ 0 & -\sin \phi & \cos \theta \cos \phi \end{bmatrix} \begin{Bmatrix} \dot{\phi} \\ \dot{\theta} \\ \dot{\psi} \end{Bmatrix}$$

and the inverse relation is

$$\begin{aligned} \dot{\phi} &= \omega_1 + (\omega_2 \sin \phi + \omega_3 \cos \phi) \tan \theta \\ \dot{\theta} &= \omega_2 \cos \phi - \omega_3 \sin \phi \\ \dot{\psi} &= (\omega_2 \sin \phi + \omega_3 \cos \phi) / \cos \theta \end{aligned}$$

Again, in the neighborhood of the singular condition $\theta = \pm \pi/2$ the rate of change of the roll and yaw angles goes to infinity.

1.2.3 The quaternions

Euler's eigenaxis rotation theorem states that it is possible to rotate a fixed frame \mathcal{F}_I onto any arbitrary frame \mathcal{F}_B with a simple rotation around an axis $\hat{\mathbf{a}}$ that is fixed in both frames, called the *Euler's rotation axis* or *eigenaxis*, the direction cosines of which are the same in the two considered frame.

A very simple algebraic demonstration of Euler's theorem can be obtained from the following considerations:

- **The eigenvalues of any (real) orthogonal matrix \mathbf{L} have unit modulus.**

Proof: Indicating with H the Hermitian conjugate, which, for a real matrix is coincident with the transpose, one has

$$\mathbf{L}\mathbf{a} = \lambda\mathbf{a} \Rightarrow \mathbf{a}^H \mathbf{L}^T \mathbf{L}\mathbf{a} = \bar{\lambda}\lambda\mathbf{a}^H \mathbf{a} \Rightarrow (1 - \bar{\lambda}\lambda)\mathbf{a}^H \mathbf{a} = 0$$

that for any nontrivial eigenvector \mathbf{a} implies that

$$\bar{\lambda}\lambda = 1 \Rightarrow |\lambda| = 1$$

- **At least one eigenvalue is $\lambda = 1$.**

Proof: Any $n \times n$ real matrix has at least one real eigenvalue if n is an odd number, which means that a 3×3 orthogonal matrix must have at least one eigenvalue which is $\lambda_1 = \pm 1$. The other couple of eigenvalues will be, in the most general case, complex conjugate numbers of unit modulus, which can be cast in the form $\lambda_{2,3} = \exp(\pm i\phi)$. The determinant is equal to the product of the eigenvalues, which is one, for an orthogonal matrix, so that

$$\lambda_1\lambda_2\lambda_3 = 1 \Rightarrow \lambda_1 = 1$$

The eigenvector relative to the first eigenvalue satisfies the relation

$$\mathbf{L}\mathbf{a} = 1 \cdot \mathbf{a}$$

This means that there is a direction \mathbf{a} which is not changed under the action of transformation matrix \mathbf{L} . If \mathbf{L} represents a coordinate change, the vector \mathbf{a} will be represented by the same components in both the considered reference frames,

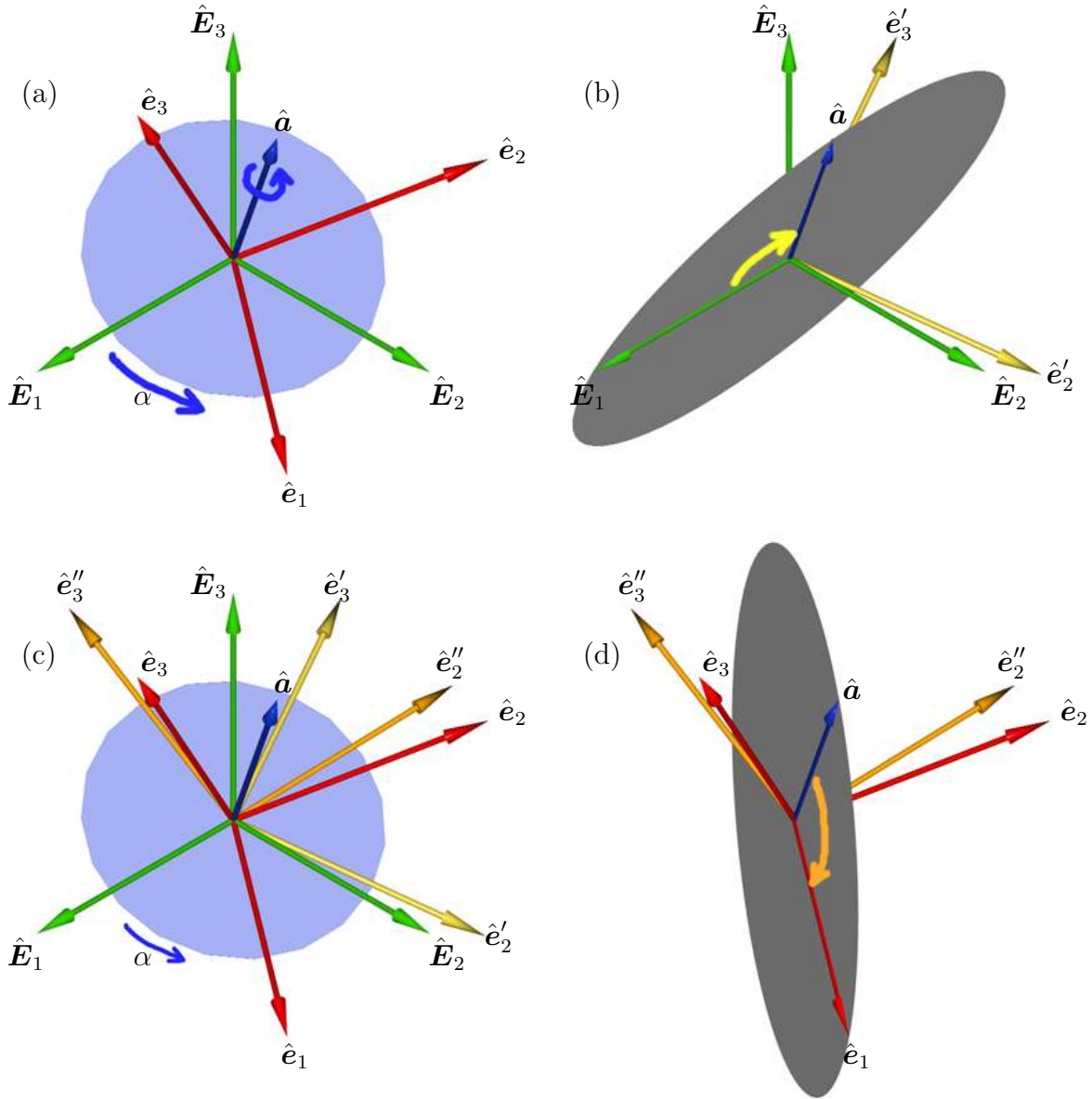
$$\begin{aligned}\hat{\mathbf{a}} &= a_1\hat{\mathbf{e}}_1 + a_2\hat{\mathbf{e}}_2 + a_3\hat{\mathbf{e}}_3 \\ &= a_1\hat{\mathbf{E}}_1 + a_2\hat{\mathbf{E}}_2 + a_3\hat{\mathbf{E}}_3\end{aligned}$$

For this reason, the transformation that takes the initial frame onto the final one can be considered as a single rotation α about the Euler axis $\hat{\mathbf{a}}$.

In order to express the coordinate transformation matrix \mathbf{L}_{BI} as a function of α and $\hat{\mathbf{a}}$ it is sufficient to consider the following sequence of rotations:¹

1. take the unit vector $\hat{\mathbf{E}}_1$ onto $\hat{\mathbf{a}}$, so that the new frame \mathcal{F}' is given by the unit vectors $\hat{\mathbf{a}}, \hat{\mathbf{e}}'_2, \hat{\mathbf{e}}'_3$; call this rotation $\bar{\mathbf{R}}$;
2. rotate both frames \mathcal{F}_I and \mathcal{F}' about the eigenaxis of the rotation angle α ; because of the definition of Euler rotation, \mathcal{F}_I goes onto \mathcal{F}_B , while \mathcal{F}' will rotate into a new frame \mathcal{F}'' given by the unit vectors $\hat{\mathbf{a}}, \hat{\mathbf{e}}''_2, \hat{\mathbf{e}}''_3$; this rotation is represented by the elementary rotation matrix $\mathbf{R}_1(\alpha)$;
3. at this point it should be noted that the rotation $\bar{\mathbf{R}}$ that takes \mathcal{F}'' onto \mathcal{F}_B has the same magnitude of $\bar{\mathbf{R}}$, but it is performed in the opposite direction so that $\bar{\mathbf{R}} = \bar{\mathbf{R}}^T$.

¹This derivation is taken from B. Wie, *Space Vehicle Dynamics and Control*, AIAA Education Series, Reston (VA), USA, 1998, Chap. 5, pp. 312–315 and 318–320.



Summing up it is

$$\mathbf{L}_{BI} = \bar{\mathbf{R}}^T \mathbf{R}_1(\alpha) \bar{\mathbf{R}}$$

where

$$\bar{\mathbf{R}} = \begin{bmatrix} a_1 & a_2 & a_3 \\ R_{21} & R_{22} & R_{23} \\ R_{31} & R_{32} & R_{33} \end{bmatrix}$$

Carrying out the calculations, one get, for the components L_{ij} of the coordinate transformation matrix \mathbf{L}_{BI} the following expressions:

$$\begin{aligned} L_{11} &= a_1^2 + (R_{21}^2 + R_{31}^2) \cos \alpha \\ L_{12} &= a_1 a_2 + (R_{21} R_{22} + R_{31} R_{32}) \cos \alpha + (R_{21} R_{32} - R_{31} R_{22}) \sin \alpha \\ L_{13} &= a_1 a_3 + (R_{21} R_{23} + R_{31} R_{33}) \cos \alpha + (R_{21} R_{33} - R_{31} R_{23}) \sin \alpha \\ L_{21} &= a_2 a_1 + (R_{22} R_{21} + R_{32} R_{31}) \cos \alpha + (R_{22} R_{33} - R_{32} R_{23}) \sin \alpha \\ L_{22} &= a_2^2 + (R_{22}^2 + R_{32}^2) \cos \alpha \end{aligned}$$

$$\begin{aligned}
L_{23} &= a_2 a_3 + (R_{22} R_{23} + R_{32} R_{33}) \cos \alpha + (R_{22} R_{33} - R_{32} R_{23}) \sin \alpha \\
L_{31} &= a_3 a_1 + (R_{23} R_{21} + R_{33} R_{31}) \cos \alpha + (R_{23} R_{31} - R_{33} R_{21}) \sin \alpha \\
L_{32} &= a_3 a_2 + (R_{23} R_{22} + R_{33} R_{32}) \cos \alpha + (R_{23} R_{32} - R_{33} R_{22}) \sin \alpha \\
L_{33} &= a_3^2 + (R_{23}^2 + R_{33}^2) \cos \alpha
\end{aligned}$$

Taking into account the orthogonality conditions for $\hat{\mathbf{R}}$, one gets

$$\begin{aligned}
a_1^2 + R_{21}^2 + R_{31}^2 &= 1 & \Rightarrow & R_{21}^2 + R_{31}^2 = 1 - a_1^2 \\
a_2^2 + R_{22}^2 + R_{32}^2 &= 1 & \Rightarrow & R_{22}^2 + R_{32}^2 = 1 - a_2^2 \\
a_3^2 + R_{23}^2 + R_{33}^2 &= 1 & \Rightarrow & R_{23}^2 + R_{33}^2 = 1 - a_3^2 \\
a_1 a_2 + R_{21} R_{22} + R_{31} R_{32} &= 0 & \Rightarrow & R_{21} R_{22} + R_{31} R_{32} = -a_1 a_2 \\
a_2 a_3 + R_{22} R_{23} + R_{32} R_{33} &= 0 & \Rightarrow & R_{22} R_{23} + R_{32} R_{33} = -a_2 a_3 \\
a_3 a_1 + R_{21} R_{23} + R_{31} R_{33} &= 0 & \Rightarrow & R_{21} R_{23} + R_{31} R_{33} = -a_1 a_2
\end{aligned}$$

while remembering that the first row of an orthogonal matrix is given by the cross product of the second and the third ones, it is

$$\begin{aligned}
a_1 &= R_{22} R_{33} - R_{23} R_{32} \\
a_2 &= R_{23} R_{31} - R_{21} R_{33} \\
a_3 &= R_{21} R_{32} - R_{22} R_{31}
\end{aligned}$$

Substituting these results into the expressions of the coefficients L_{ij} the following expression for \mathbf{L}_{BI} is obtained:

$$\mathbf{L}_{BI} = \begin{bmatrix} \cos \alpha + a_1^2(1 - \cos \alpha) & a_1 a_2(1 - \cos \alpha) + a_3 \sin \alpha & a_1 a_3(1 - \cos \alpha) - a_2 \sin \alpha \\ a_2 a_1(1 - \cos \alpha) - a_3 \sin \alpha & \cos \alpha + a_2^2(1 - \cos \alpha) & a_2 a_3(1 - \cos \alpha) + a_1 \sin \alpha \\ a_3 a_1(1 - \cos \alpha) + a_2 \sin \alpha & a_3 a_2(1 - \cos \alpha) - a_1 \sin \alpha & \cos \alpha + a_3^2(1 - \cos \alpha) \end{bmatrix} \quad (1.2)$$

or, in compact matrix form

$$\mathbf{L}_{BI} = \cos \alpha \mathbf{1} + (1 - \cos \alpha) \mathbf{aa}^T - \sin \alpha \tilde{\mathbf{A}}$$

where $\mathbf{1}$ is the 3×3 identity matrix and $\tilde{\mathbf{A}}$ is the cross product equivalent matrix form

$$\tilde{\mathbf{A}} = \begin{bmatrix} 0 & -a_3 & a_2 \\ a_3 & 0 & -a_1 \\ -a_2 & a_1 & 0 \end{bmatrix}$$

such that $\mathbf{a} \times \mathbf{b} = \tilde{\mathbf{A}}\mathbf{b}$.

We now define the *Euler parameters* or *quaternions* as

$$\begin{aligned}
q_0 &= \cos(\alpha/2) \\
q_1 &= a_1 \sin(\alpha/2) \\
q_2 &= a_2 \sin(\alpha/2) \\
q_3 &= a_3 \sin(\alpha/2)
\end{aligned}$$

By letting $\mathbf{q} = \hat{\mathbf{a}} \sin(\alpha/2)$ and rembering that $\cos \alpha = \cos^2(\alpha/2) - \sin^2(\alpha/2) = q_0^2 - \mathbf{q} \cdot \mathbf{q}$ and $\sin \alpha = 2 \cos(\alpha/2) \sin(\alpha/2) = 2q_0 \sin(\alpha/2)$, it is easy to demonstrate that the coordinate transformation matrix is given by

$$\mathbf{L}_{BI} = (q_0^2 - \mathbf{q} \cdot \mathbf{q}) \mathbf{1} + 2\mathbf{q}\mathbf{q}^T - 2q_0 \tilde{\mathbf{Q}}$$

where the \sim indicates again the cross product matrix equivalent

$$\tilde{\mathbf{Q}} = \begin{bmatrix} 0 & -q_3 & q_2 \\ q_3 & 0 & -q_1 \\ -q_2 & q_1 & 0 \end{bmatrix}$$

The quaternion $\mathbf{Q}_I = (1, 0, 0, 0)^T$ is referred to as the *unity quaternion*, and it represents the attitude of the reference fixed frame. The *conjugate quaternion* $\mathbf{Q}^* = (q_0, -\mathbf{q}^T)^T$, defined as the quaternion with the same scalar part and a sign change in the vector part, is associated to an eigenaxis rotation of equal amplitude around the same eigenaxis, but in the opposite direction. The inversion of the rotation can be seen in two different ways, either as the rotation about the same axis $\hat{\mathbf{a}}$ by an opposite angle $-\alpha$, or a rotation around the opposite axis $-\hat{\mathbf{a}}$ by the same angle α . In both case, the vector part \mathbf{q} of the corresponding quaternion achieves the same value.

On the converse, if the sign of both scalar and vector part is changed, one obtains a rotation about the opposite axis by an angle $2\pi - \alpha$. The final attitude achieved by means of the eigenaxis rotation $(\alpha, \hat{\mathbf{a}})$ is exactly the same achieved by means of the rotation $(-\alpha, 2\pi - \hat{\mathbf{a}})$, the quaternions \mathbf{Q} and $-\mathbf{Q}$ represent the same attitude. In this latter respect, note that the reference attitude, represented by the unity quaternion \mathbf{Q}_I , is also represented by $-\mathbf{Q}_I = (-1, 0, 0, 0)^T$, which describes a 360 deg revolution about an arbitrary eigenaxis.

1.2.4 Quaternion multiplication

It is possible to define a geometrically/physically meaningful quaternion multiplication operation, which combines two quaternions, namely \mathbf{Q} and \mathbf{P} , in such a way that the resulting quaternion $\mathbf{R} = \mathbf{QP}$ represents the final attitude of a frame that undergoes two successive rotations, described by \mathbf{Q} and \mathbf{P} , respectively. In other words, consider three frames \mathcal{F}_1 , \mathcal{F}_2 , and \mathcal{F}_3 , and assume that the quaternion $\mathbf{Q} = (q_0, \mathbf{q}^T)^T$,

$$q_0 = \cos(\alpha/2), \quad \mathbf{q} = \hat{\mathbf{a}} \sin(\alpha/2)$$

represents the eigenaxis rotation from \mathcal{F}_1 to \mathcal{F}_2 , while $\mathbf{P} = (p_0, \mathbf{p}^T)^T$,

$$p_0 = \cos(\beta/2), \quad \mathbf{p} = \hat{\mathbf{b}} \sin(\beta/2)$$

represents the eigenaxis rotation from \mathcal{F}_2 to \mathcal{F}_3 , then the quaternion

$$\mathbf{R} = (r_0, \mathbf{r}^T)^T = \mathbf{QP}$$

with

$$r_0 = q_0 p_0 - \mathbf{q}^T \mathbf{p} \tag{1.3}$$

$$\mathbf{r} = q_0 \mathbf{p} + p_0 \mathbf{q} + \mathbf{q} \times \mathbf{p} \tag{1.4}$$

represents the quaternion for the rotation around the eigenaxis $\hat{\mathbf{c}}$ of an angle γ that takes \mathcal{F}_1 directly onto \mathcal{F}_3 , with $\gamma = 2 \cos^{-1}(r_0) = 2 \sin^{-1}(\mathbf{r}^T \mathbf{r})$ and $\hat{\mathbf{c}} = \mathbf{r} / \|\mathbf{r}\|$.

In general, it is easy to demonstrate that the quaternion multiplication operation is not commutative (the order in which rotations are performed matters!), but it is associative. It is easy to check that the quaternion multiplication operation satisfies the following properties:

$$\mathbf{QQ}^* = \mathbf{Q}_I, \quad \mathbf{QQ}_I = \mathbf{Q}_I \mathbf{Q} = \mathbf{Q}$$

1.2.5 The quaternion error vector

Assume that the current attitude of a frame \mathcal{F}_B associated with a rigid body with respect to a given fixed frame \mathcal{F}_I is represented by the quaternion \mathbf{Q} , while \mathbf{P} represent the desired attitude \mathcal{F}_D of the body. The magnitude of the angular displacement between \mathcal{F}_B and \mathcal{F}_D , represented by the amplitude ε of the eigenaxis rotation around $\hat{\mathbf{e}}$ that takes \mathcal{F}_D onto \mathcal{F}_B , can be seen as the “error” in the current attitude with respect to the desired one. Provided that the rotation that takes \mathcal{F}_I onto \mathcal{F}_D can be combined with that that takes \mathcal{F}_D onto \mathcal{F}_B , it is possible to assess by means of the quaternion operation that

$$\mathbf{P}\mathbf{E} = \mathbf{Q}$$

where $\mathbf{E} = (\epsilon_0, \boldsymbol{\epsilon}^T)^T$ is the quaternion error, that is, the quaternion associated with the rotation that takes \mathcal{F}_D onto \mathcal{F}_B , the amplitude of which thus provides the misalignment error of \mathcal{F}_B with respect to \mathcal{F}_D . By pre-multiplication of both terms by the conjugate quaternion P^* one gets

$$\mathbf{E} = \mathbf{P}^*\mathbf{Q},$$

that is

$$\epsilon_0 = \cos(\varepsilon/2) = q_0 p_0 + \mathbf{q}^T \mathbf{p} \quad (1.5)$$

$$\boldsymbol{\epsilon} = \hat{\mathbf{e}} \sin(\varepsilon/2) = -q_0 \mathbf{p} + p_0 \mathbf{q} - \mathbf{q} \times \mathbf{p} \quad (1.6)$$

1.2.6 Evolution of the quaternions

The evolution of the quaternions is described by the set of linear differential equations, represented in matrix form as²

$$\left\{ \begin{array}{l} \dot{q}_0 \\ \dot{q}_1 \\ \dot{q}_2 \\ \dot{q}_3 \end{array} \right\} = \frac{1}{2} \begin{bmatrix} 0 & -\omega_1 & -\omega_2 & -\omega_3 \\ \omega_1 & 0 & \omega_3 & -\omega_2 \\ \omega_2 & -\omega_3 & 0 & \omega_1 \\ \omega_3 & \omega_2 & -\omega_1 & 0 \end{bmatrix} \left\{ \begin{array}{l} q_0 \\ q_1 \\ q_2 \\ q_3 \end{array} \right\}$$

The equivalent matrix form is given by

$$\begin{aligned} \dot{q}_0 &= -\frac{1}{2} \boldsymbol{\omega} \cdot \mathbf{q} \\ \dot{\mathbf{q}} &= \frac{1}{2} (q_0 \boldsymbol{\omega} - \boldsymbol{\omega} \times \mathbf{q}) \end{aligned}$$

1.3 Quaternions vs Euler angles

The quaternions allow for representing the attitude of a rigid body with several advantages over Euler’s angles, above all the absence of inherent geometric singularity. Moreover, the linear equation to be integrated in time in order to determine their evolution as a function of angular velocity components is less computationally expensive than that derived for the Euler’s angles. The price to pay is that 4 parameters are used, instead of only three, that are not independent, inasmuch as they must satisfy the constraint

$$q_0^2 + \mathbf{q} \cdot \mathbf{q} = 1$$

²See above, pp. 326–328

Truncation and discretization errors, that are randomly added up to the actual value of the quaternions during numerical integration, may lead to significant violation of the constraint on the unity value of the quaternion magnitude, which is clearly unacceptable for the geometrical meaning of the quaternion components. The constraint must thus be enforced during numerical integration. A simple yet effective technique is based on adding an auxiliary term to the evolution equation, that is

$$\begin{aligned}\dot{q}_0 &= -\frac{1}{2}\boldsymbol{\omega} \cdot \mathbf{q} + k(1 - q_0^2 - \mathbf{q}^T \mathbf{q})q_0 \\ \dot{\mathbf{q}} &= \frac{1}{2}(q_0\boldsymbol{\omega} - \boldsymbol{\omega} \times \mathbf{q}) + k(1 - q_0^2 - \mathbf{q}^T \mathbf{q})\mathbf{q}\end{aligned}$$

where a violation of the constraint results into a slight variation of quaternion dynamics, in order to keep them exactly on the unity hyper-sphere of the 4-dimensional space $(q_0, q_1, q_2, q_3)^T$.

As a further drawback, their geometric interpretation during an evolution is less immediate than that of the Euler's angles, the geometric meaning of which is intuitive. For this reason the attitude of a satellite is often integrated in *strapdown attitude determination systems* in terms of quaternions but then represented in terms of Euler angles. At the same time the quaternion multiplication operation allows for a rigorous definition of misalignment errors, that it is not possible to obtain by means of Euler angles. In this latter respect, Euler angles may be significantly different also for frames that are quite close one to the other in absolute terms.

1.4 Other attitude representations

The non-minimality of attitude representation in terms of quaternions can be solved for by use of the *Gibbs vector*, defined as

$$\mathbf{g} = (g_1, g_2, g_3)^T = \hat{\mathbf{a}} \tan(\alpha/2)$$

Gibbs parameters, also known as *Rodrigues parameters*, are strictly related to quaternions, as it is

$$(g_1, g_2, g_3)^T = (q_1/q_0, q_2/q_0, q_3/q_0)^T$$

The coordinate transformation matrix can also be represented in terms of Gibbs parameters:

$$\mathbf{L}_{BI} = (\mathbf{1} - \tilde{\mathbf{G}})(\mathbf{1} + \tilde{\mathbf{G}})^{-1}$$

Being a minimal parametrization of attitudes, Gibbs parameters must present a singularity.³ The singular configuration of the Gibbs vector is for any eigenaxis rotation with $\alpha = \pm\pi$, in which case their values diverge towards infinity. To solve for this problem, the so called set of *Modified Rodrigues parameters* (MRP) was recently introduced, defined as

$$\mathbf{p} = (p_1, p_2, p_3)^T = \hat{\mathbf{a}} \tan(\alpha/4)$$

The singularity in the attitude representation is still present, and for a spinning body the value of the MRPs will “jump” when α crosses the critical threshold placed at half of a rotation (that is, $\alpha = \pm\pi$). Nonetheless the advantage of the MRPs is that they do not diverge, but at the same time, no constraint on their value needs to be enforced in order to save their meaning. These features make the numerical integration of MRPs less critical with respect to both the quaternions case and the Gibbs vector.

³Recall that Euler demonstrated that any minimal parametrization of attitudes has at least one singular configuration

1.5 Time derivative of vector quantities

If we consider a vector quantity in an inertially fixed reference frame \mathcal{F}_I ,

$$\vec{v} = X \hat{\mathbf{E}}_1 + Y \hat{\mathbf{E}}_2 + Z \hat{\mathbf{E}}_3$$

its time derivative is given simply by

$$\frac{d\vec{v}}{dt} = \dot{X} \hat{\mathbf{E}}_1 + \dot{Y} \hat{\mathbf{E}}_2 + \dot{Z} \hat{\mathbf{E}}_3$$

that is

$$\left[\frac{d\mathbf{v}}{dt} \right]_I = \left\{ \dot{X}, \dot{Y}, \dot{Z} \right\}^T = \dot{\mathbf{v}}_I$$

When the same vector quantity \vec{v} is expressed in terms of components in a moving reference frame \mathcal{F}_B , rotating with angular velocity $\vec{\omega}^{BI} = \vec{\omega}$ with respect to \mathcal{F}_I , the time derivatives of

$$\vec{v} = x \hat{\mathbf{e}}_1 + y \hat{\mathbf{e}}_2 + z \hat{\mathbf{e}}_3$$

is given by⁴

$$\begin{aligned} \frac{d\vec{v}}{dt} &= \dot{x} \hat{\mathbf{e}}_1 + \vec{\omega} \times (x \hat{\mathbf{e}}_1) + \\ &+ \dot{y} \hat{\mathbf{e}}_2 + \vec{\omega} \times (y \hat{\mathbf{e}}_2) + \\ &+ \dot{z} \hat{\mathbf{e}}_3 + \vec{\omega} \times (z \hat{\mathbf{e}}_3) \end{aligned}$$

This means that, in terms of vector components in \mathcal{F}_B , it is

$$\left[\frac{d\mathbf{v}}{dt} \right]_B = \dot{\mathbf{v}}_B + \boldsymbol{\omega}_B \times \mathbf{v}_B$$

where

$$\begin{aligned} \dot{\mathbf{v}}_B &= \{\dot{x}, \dot{y}, \dot{z}\}^T \\ \boldsymbol{\omega}_B &= \{\omega_1, \omega_2, \omega_3\}^T \end{aligned}$$

1.6 Euler's equations of motion of a rigid body

1.6.1 The inertia tensor

The angular momentum $\delta \vec{h}$ of a mass element δm , moving with velocity \vec{v} is

$$\delta \vec{h} = \vec{r} \times (\delta m \vec{v})$$

where \vec{r} is the position vector of the mass, with respect of the pole used for the evaluation of moments of vector quantities.

For an extended rigid body (Fig. 1.4), the total angular momentum is given by

$$\vec{h} = \int_{\mathcal{B}} (\vec{r} \times \vec{v}) \delta m$$

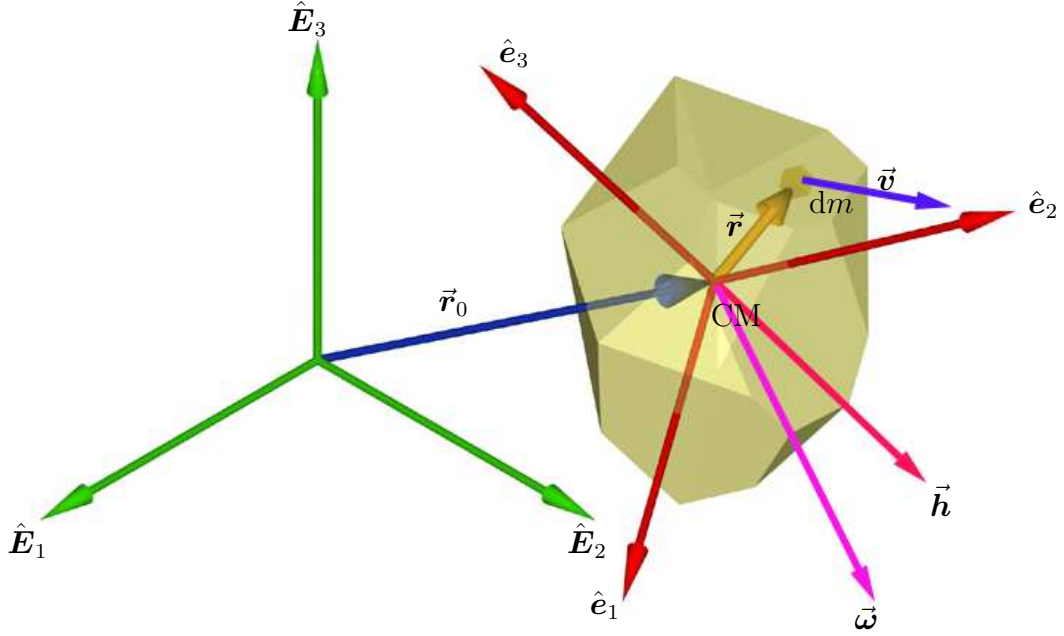


Figure 1.4: A rotating rigid body.

If the body is rotating around its center of mass, the velocity of every mass element is

$$\vec{v} = \vec{\omega} \times \vec{r}$$

so that

$$\vec{h} = \int_{\mathcal{B}} [\vec{r} \times (\vec{\omega} \times \vec{r})] \delta m$$

Expressing the vector quantities in body components as $\omega_B = (\omega_1, \omega_2, \omega_3)^T$ and $r_B = (x, y, z)^T$, the vector product $\vec{\omega} \times \vec{r}$ is given by

$$\vec{\omega} \times \vec{r} = (\omega_2 z - \omega_3 y) \hat{e}_1 + (\omega_3 x - \omega_1 z) \hat{e}_2 + (\omega_1 y - \omega_2 x) \hat{e}_3$$

Carrying on the calculations, the product $\vec{r} \times (\vec{\omega} \times \vec{r})$ is

$$\begin{aligned} \vec{r} \times (\vec{\omega} \times \vec{r}) &= [(y^2 + z^2)\omega_1 - (xy)\omega_2 - (xz)\omega_3] \hat{e}_1 + \\ &+ [-(xy)\omega_1 + (x^2 + z^2)\omega_2 - (yz)\omega_3] \hat{e}_2 + \\ &+ [-(xz)\omega_1 - (yz)\omega_2 + (x^2 + y^2)\omega_3] \hat{e}_3 \end{aligned}$$

The integration over the body \mathcal{B} of $[\vec{r} \times (\vec{\omega} \times \vec{r})] \delta m$ is strictly function of the mass distribution only, as angular velocity components are independent of body shape and location. This means that, letting

$$\vec{h} = h_1 \hat{e}_1 + h_2 \hat{e}_2 + h_3 \hat{e}_3$$

it is

$$\begin{aligned} h_1 &= I_x \omega_1 - I_{xy} \omega_2 - I_{xz} \omega_3 \\ h_2 &= -I_{xy} \omega_1 + I_y \omega_2 - I_{yz} \omega_3 \\ h_3 &= -I_{xz} \omega_1 - I_{yz} \omega_2 + I_z \omega_3 \end{aligned}$$

⁴Remeber the Poisson formula for the time derivative of a unit vector,

$$\frac{d\hat{e}_i}{dt} = \vec{\omega} \times \hat{e}_i$$

where the moments of inertia I_x , I_y , I_z , and the products of inertia I_{xy} , I_{xz} , I_{yz} , are

$$\begin{aligned} I_x &= \int_{\mathcal{B}} (y^2 + z^2) \delta m ; & I_y &= \int_{\mathcal{B}} (x^2 + z^2) \delta m ; & I_z &= \int_{\mathcal{B}} (x^2 + y^2) \delta m \\ I_{xy} &= \int_{\mathcal{B}} (xy) \delta m ; & I_{xz} &= \int_{\mathcal{B}} (xz) \delta m ; & I_{yz} &= \int_{\mathcal{B}} (yz) \delta m \end{aligned}$$

In matrix form the angular momentum components in body axes are given by

$$\mathbf{h}_B = \mathbf{I}\boldsymbol{\omega}_B$$

where the symmetric matrix

$$\mathbf{I} = \begin{bmatrix} I_x & -I_{xy} & -I_{xz} \\ -I_{xy} & I_y & -I_{yz} \\ -I_{xz} & -I_{yz} & I_z \end{bmatrix}$$

is the *inertia matrix* that represent the *inertia tensor* in body axes.

The same relations can be derived directly in a more compact vector form remembering that, for the double vector product, the following relation holds:

$$\vec{x} \times (\vec{y} \times \vec{z}) = (\vec{x} \cdot \vec{z}) \vec{y} - (\vec{x} \cdot \vec{y}) \vec{z}$$

so that, in the present case, it is

$$\vec{r} \times (\vec{\omega} \times \vec{r}) = (\vec{r} \cdot \vec{r}) \vec{\omega} - (\vec{r} \cdot \vec{\omega}) \vec{r}$$

Taking into account the definition of the dyadic tensor

$$(\vec{x}\vec{y})\vec{z} = (\vec{y} \cdot \vec{z})\vec{x}$$

and the fact that the angular velocity vector is constant and can be taken out of the integral, it is

$$\begin{aligned} \vec{h} &= \int_{\mathcal{B}} [\vec{r} \times (\vec{\omega} \times \vec{r})] \delta m \\ &= \left(\int_{\mathcal{B}} [(\vec{r} \cdot \vec{r}) - (\vec{r} \cdot \vec{r})] \delta m \right) \vec{\omega} \\ &= \tilde{\mathbf{I}}\vec{\omega} \end{aligned}$$

where $\tilde{\mathbf{I}}$ is the inertia tensor. Expressing \vec{r} in terms of body components and integrating over \mathcal{B} the previous expression for the inertia matrix \mathbf{I} is obtained.

Principal axes of inertia

The matrix \mathbf{I} is real and symmetric, so its eigenvalues are real⁵ and its eigenvectors are mutually orthogonal.⁶ This means that there exists a body reference frame \mathcal{F}_P such that the inertia matrix is diagonal,

$$\mathbf{I} = \begin{bmatrix} J_x & 0 & 0 \\ 0 & J_y & 0 \\ 0 & 0 & J_z \end{bmatrix}$$

where the *principal moment of inertia* J_x , J_y , and J_z are the eigenvalues of \mathbf{I} . The eigenvectors are called *principal axes*.

Symmetries

If the mass distribution of the body \mathcal{B} is characterized by symmetries, this property reflects onto the inertia matrix \mathbf{I} . As an example, if \mathcal{B} has a plane of symmetry, one of the principal axis will be perpendicular to the plane and the other two will lie on that plane. If this case, the products of inertia relative to the axis perpendicular to the symmetry plane will be zero. This case is typical of fixed wing aircraft, where the longitudinal plane is approximately a symmetry plane. The y body axis, directed perpendicular to the symmetry plane, is characterized by zero products of inertia, so that the inertia matrix

⁵From the definition of eigenvalue and eigenvector of a complex matrix \mathbf{A} , it is easy to derive the following equation,

$$\mathbf{Ax} = \lambda \mathbf{x} \Rightarrow \lambda = \frac{\mathbf{x}^H \mathbf{Ax}}{\mathbf{x}^H \mathbf{x}}$$

If \mathbf{A} is Hermitian (*i.e.* the linear operator represented by \mathbf{A} is self-adjoint), it is

$$\mathbf{y}^H \mathbf{Ax} = (\mathbf{Ay})^H \mathbf{x}$$

so that, remembering the properties of the hermitian inner product, such that $\mathbf{x}^H \mathbf{y} = \overline{(\mathbf{y}^H \mathbf{x})}$, it is

$$\bar{\lambda} = \frac{\overline{\mathbf{x}^H \mathbf{Ax}}}{\overline{\mathbf{x}^H \mathbf{x}}} = \frac{(\mathbf{Ax})^H \mathbf{x}}{\mathbf{x}^H \mathbf{x}} = \frac{\mathbf{x}^H \mathbf{Ax}}{\mathbf{x}^H \mathbf{x}} = \lambda$$

which means that the eigenvalue λ is equal to its conjugate, *i.e.* it must be real.

⁶Given two distinct eigenvalues $\lambda_i \neq \lambda_j$ and their respective eigenvectors \mathbf{x}_i and \mathbf{x}_j , the following relations hold:

$$\begin{aligned} \mathbf{Ax}_i &= \lambda_i \mathbf{x}_i \\ \mathbf{Ax}_j &= \lambda_j \mathbf{x}_j \end{aligned}$$

Multiplying the first equation by \mathbf{x}_j^H and the second one by \mathbf{x}_i^H , taking the complex conjugate of the second and subtracting it from the first, one gets

$$\mathbf{x}_j^H \mathbf{Ax}_i - \overline{(\mathbf{x}_i^H \mathbf{Ax}_j)} = \lambda_i \mathbf{x}_j^T \mathbf{x}_i - \overline{(\lambda_j \mathbf{x}_i^T \mathbf{x}_j)}$$

Remembering that the eigenvalues are real, it is

$$\mathbf{x}_j^H \mathbf{Ax}_i - (\mathbf{Ax}_j)^H \mathbf{x}_i = (\lambda_i - \lambda_j) \mathbf{x}_j^H \mathbf{x}_i$$

Taking into account the definition of Hermitian operator the first term of the last equation is zero and so the Hermitian product $\mathbf{x}_j^H \mathbf{x}_i$ is zero if $\lambda_i \neq \lambda_j$. Since both \mathbf{x}_j and \mathbf{x}_i are real, their Hermitian product coincides with the scalar product, so that distinct eigenvectors are real and perpendicular.

of an aircraft is typically equal to

$$\mathbf{I} = \begin{bmatrix} I_x & 0 & -I_{xz} \\ 0 & I_y & 0 \\ -I_{xz} & 0 & I_z \end{bmatrix}$$

If the body is axi-symmetric (or simply has a regular polygonal mass distribution w.r.t. an axis σ), the symmetry axis σ is a principal axis of inertia, while any couple of perpendicular axes on the plane Σ normal to σ will complete the set of principal axes. In this case the principal moments of inertia relative to the axes perpendicular to the symmetry axis will be equal. Assuming that $\sigma = \hat{\mathbf{e}}_3$ is a symmetry axis, the inertia tensor becomes

$$\mathbf{I} = \begin{bmatrix} J_t & 0 & 0 \\ 0 & J_t & 0 \\ 0 & 0 & J_s \end{bmatrix}$$

where the subscripts t and s indicate the *transverse* and *spin* (or axial) moments of inertia, respectively.

1.6.2 Kinetic energy

The rotational kinetic energy of a rigid body is given by

$$\mathcal{T} = \frac{1}{2} \int_{\mathcal{B}} (\vec{v} \cdot \vec{v}) \delta m$$

Remembering that $\vec{v} = \vec{\omega} \times \vec{r}$, the argument of the integral becomes $(\vec{\omega} \times \vec{r}) \cdot (\vec{\omega} \times \vec{r})$. Also, taking into account the permutation property of the scalar triple product

$$\vec{x} \cdot (\vec{y} \times \vec{z}) = \vec{y} \cdot (\vec{z} \times \vec{x}) = \vec{z} \cdot (\vec{x} \times \vec{y})$$

one obtains the equivalence

$$(\vec{\omega} \times \vec{r}) \cdot (\vec{\omega} \times \vec{r}) = \vec{\omega} \cdot [\vec{r} \times (\vec{\omega} \times \vec{r})]$$

Substituting this expression into the integral, and taking the (constant) angular velocity out of the integration symbol, one gets

$$\mathcal{T} = \frac{1}{2} \vec{\omega} \cdot \int_{\mathcal{B}} [\vec{r} \times (\vec{\omega} \times \vec{r})] \delta m$$

that, remembering the definition of the inertia tensor, brings

$$\mathcal{T} = \frac{1}{2} \vec{\omega} \cdot (\tilde{\mathbf{I}} \vec{\omega}) = \frac{1}{2} \boldsymbol{\omega}_B^T (\mathbf{I} \boldsymbol{\omega}_B)$$

or, equivalently,

$$\mathcal{T} = \frac{1}{2} \vec{\omega} \cdot \vec{h} = \frac{1}{2} \boldsymbol{\omega}_B^T \mathbf{h}_B$$

1.6.3 Euler's equation of motion

The second fundamental law of rigid body dynamics states that the time derivative of the angular momentum is equal to the total external torque applied to the body \mathcal{B} . In vector form, it is

$$\frac{d\vec{h}}{dt} = \vec{M}$$

Expressing the vector quantities in body axis components one gets

$$\dot{\boldsymbol{h}}_B + \boldsymbol{\omega}_B \times \boldsymbol{h}_B = \boldsymbol{M}_B$$

If the inertia matrix \boldsymbol{I} is constant, it is

$$\boldsymbol{I}\dot{\boldsymbol{\omega}}_B + \boldsymbol{\omega}_B \times (\boldsymbol{I}\boldsymbol{\omega}_B) = \boldsymbol{M}_B$$

When a set of principal axes is chosen as the body axes, the inertia tensor is diagonal and the Euler's equation of motion for a rigid body are obtained:

$$\begin{aligned} J_x \dot{\omega}_1 + (J_z - J_y) \omega_2 \omega_3 &= M_1 \\ J_y \dot{\omega}_2 + (J_x - J_z) \omega_3 \omega_1 &= M_2 \\ J_z \dot{\omega}_3 + (J_y - J_x) \omega_1 \omega_2 &= M_3 \end{aligned}$$

These equations can be integrated as a function of the applied torque to obtain the time history of the angular velocity components. These, in turn, can be used to determine the variation with time of the Euler's angles (or of the quaternions), thus describing the evolution of the rigid body attitude.

1.6.4 Conservation of angular momentum

Writing Euler's equations in a set of principal axes such that (without loss of generality) $J_x > J_y > J_z$, torque-free motion is described by the following set of ODEs,

$$\begin{aligned} J_x \dot{\omega}_1 + (J_z - J_y) \omega_2 \omega_3 &= 0 \\ J_y \dot{\omega}_2 + (J_x - J_z) \omega_3 \omega_1 &= 0 \\ J_z \dot{\omega}_3 + (J_y - J_x) \omega_1 \omega_2 &= 0 \end{aligned}$$

It is easy to demonstrate that the magnitude h of the angular momentum vector

$$\begin{aligned} \vec{h} &= h_1 \hat{\mathbf{e}}_1 + h_2 \hat{\mathbf{e}}_2 + h_3 \hat{\mathbf{e}}_3 \\ &= J_x \omega_1 \hat{\mathbf{e}}_1 + J_y \omega_2 \hat{\mathbf{e}}_2 + J_z \omega_3 \hat{\mathbf{e}}_3 \end{aligned}$$

is constant when a torque-free motion is considered. A first intuitive derivation of this property is that if the applied torque vanishes the angular momentum vector is constant in \mathcal{F}_I , and its magnitude is independent of the considered reference system. It is also possible to demonstrate analytically that $h = \|\boldsymbol{h}\|$ is constant, by taking the time derivatives of

$$h^2 = (J_x \omega_1)^2 + (J_y \omega_2)^2 + (J_z \omega_3)^2$$

in the hypothesis of torque-free motion ($M_1 = M_2 = M_3 = 0$),

$$\begin{aligned} \frac{dh^2}{dt} &= 2 (J_x^2 \omega_1 \dot{\omega}_1 + J_y^2 \omega_2 \dot{\omega}_2 + J_z^2 \omega_3 \dot{\omega}_3) \\ &= 2 [J_x \omega_1 (J_y - J_z) \omega_2 \omega_3 + J_y \omega_2 (J_z - J_x) \omega_3 \omega_1 + J_z \omega_3 (J_x - J_y) \omega_1 \omega_2] \\ &= 2 (J_x J_y - J_x J_z + J_y J_z - J_y J_x + J_z J_x - J_z J_y) \omega_1 \omega_2 \omega_3 = 0 \end{aligned}$$

Geometrically, the angular velocity vector must lie on an ellipsoid (the *angular momentum ellipsoid*) in \mathcal{F}_B , the equation of which takes the form

$$\frac{\omega_1^2}{(h/J_x)^2} + \frac{\omega_2^2}{(h/J_y)^2} + \frac{\omega_3^2}{(h/J_z)^2} = 1$$

1.6.5 Conservation of kinetic energy

In a similar way, it is also possible to demonstrate that the kinetic energy of a rigid body is constant if no external torque is applied. Again, taking the time derivative of

$$\mathcal{T} = \frac{1}{2} \boldsymbol{\omega}_B \cdot \mathbf{h} = \frac{1}{2} (J_x \omega_1^2 + J_y \omega_2^2 + J_z \omega_3^2)$$

it is

$$\begin{aligned} \frac{d\mathcal{T}}{dt} &= J_x \omega_1 \dot{\omega}_1 + J_y \omega_2 \dot{\omega}_2 + J_z \omega_3 \dot{\omega}_3 \\ &= \omega_1 (J_y - J_z) \omega_2 \omega_3 + \omega_2 (J_z - J_x) \omega_1 \omega_3 + \omega_3 (J_x - J_y) \omega_1 \omega_2 \\ &= 2(J_y - J_z + J_z - J_x + J_x - J_y) \omega_1 \omega_2 \omega_3 = 0 \end{aligned}$$

This means that the angular velocity vector must satisfy also the equation

$$\frac{\omega_1^2}{(2\mathcal{T}/J_x)} + \frac{\omega_2^2}{(2\mathcal{T}/J_y)} + \frac{\omega_3^2}{(2\mathcal{T}/J_z)} = 1$$

that is, it must point the surface of the *kinetic energy* (or *Poinsot*) *ellipsoid* in \mathcal{F}_B . The combination of these two last results demonstrate that the angular velocity vector describe the curve given by the intersection of the angular momentum ellipsoid and the kinetic energy ellipsoid, which is called the *polhode*.

1.7 Generalised Euler equation

In their original formulation, Euler equations are written in a body-fixed reference frame \mathcal{F}_B with the origin in the center of mass O of the body \mathcal{B} . On one side, the expression employed for the angular momentum \mathbf{h} of \mathcal{B} requires that \mathcal{B} is rigid, and centering \mathcal{B} in O greatly simplify the expression. At the same time, linear and angular momentum conservation laws do apply to any mechanical system (under sufficiently mild assumptions), so that it is possible to obtain a generalised formulation for the equation of motion in a frame which is non centered in O .

1.7.1 Derivation of the generalised form of Euler equation

The classical equations, referred to the center of mass O , are

$$\begin{aligned} m\vec{a}_O &= \vec{F} \\ \frac{d\vec{h}_O}{dt} &= \vec{M}_O \end{aligned}$$

where, m is the mass of \mathcal{B} and \vec{F} is the external force, producing an acceleration \vec{a}_O of the center of mass. Considering an arbitrary point A with arbitrary motion with respect

to the body, such that \vec{r}_{AO} is the position vector of the centre of mass O with respect to A , the torque acting on the body can be referred to A ,

$$\vec{M}_A = \vec{M}_O + \vec{r}_{AO} \times \vec{F}$$

As for the angular momentum relative to A , it is

$$\vec{h}_A = \int_{\mathcal{B}} \left[\vec{r}_{AP} \times \frac{d\vec{r}_{AP}}{dt} \right] \delta m$$

where \vec{r}_{AP} is the position vector of the mass element δm with respect to A , while $d\vec{r}_{AP}/dt$ its (relative) velocity. Upon substitution of $\vec{r}_{AP} = \vec{r}_{AO} + \vec{r}_{OP}$ into the expression for \vec{h}_A , one obtains

$$\begin{aligned} \vec{h}_A &= \int_{\mathcal{B}} \left[(\vec{r}_{AO} + \vec{r}_{OP}) \times \frac{d}{dt} (\vec{r}_{AO} + \vec{r}_{OP}) \right] \delta m \\ &= \int_{\mathcal{B}} \left[\vec{r}_{AO} \times \frac{d\vec{r}_{AO}}{dt} \right] \delta m + \int_{\mathcal{B}} \left[\vec{r}_{AO} \times \frac{d\vec{r}_{OP}}{dt} \right] \delta m + \\ &\quad + \int_{\mathcal{B}} \left[\vec{r}_{OP} \times \frac{d\vec{r}_{AO}}{dt} \right] \delta m + \int_{\mathcal{B}} \left[\vec{r}_{OP} \times \frac{d\vec{r}_{OP}}{dt} \right] \delta m \end{aligned}$$

The last term is the angular momentum with respect to the centre of mass

$$\vec{h}_O = \int_{\mathcal{B}} \left[\vec{r}_{OP} \times \frac{d\vec{r}_{OP}}{dt} \right] \delta m$$

while the second and the third one are both zero, from the definition of centre of mass.⁷
It is thus possible to write \vec{h}_A as

$$\vec{h}_A = \vec{h}_O + m\vec{r}_{AO} \times \frac{d\vec{r}_{AO}}{dt}$$

The acceleration of O can be rewritten as a function of the absolute acceleration of A

$$\vec{a}_O = \vec{a}_A + \frac{d^2\vec{r}_{AO}}{dt^2}$$

By substituting the above expressions in the angular momentum equation, one gets

$$\frac{d}{dt} \left(\vec{h}_A - m\vec{r}_{AO} \times \frac{d\vec{r}_{AO}}{dt} \right) = \vec{M}_A - \vec{r}_{AO} \times \left[m \left(\vec{a}_A + \frac{d^2\vec{r}_{AO}}{dt^2} \right) \right]$$

which can be rewritten as

$$\frac{d\vec{h}_A}{dt} + \vec{S}_A \times \vec{a}_A = \vec{M}_A$$

where $\vec{S}_A = m\vec{r}_A$ is the static moment of the body with respect to A .

⁷If m is the total mass of the body, the absolute position of the centre of mass is defined as

$$\vec{r}_O = \frac{1}{m} \int_{\mathcal{B}} \vec{r}_{OP} \delta m$$

so that, letting the position vector of P with respect to O be defined as $\vec{r}_{OP} = \vec{r}_P - \vec{r}_O$, it is

$$\int_{\mathcal{B}} \vec{r}_{OP} \delta m = 0.$$

Taking into account that integration is a linear operator, that can be commuted with the time derivative, both the second and the third terms vanishes.

1.7.2 Use of the generalised form of Euler equation

The generalised form of classical Euler equation allows for writing dynamic models of systems where the mass distribution is not constant. On one side, the assumption of rigidity often applies with reasonable accuracy to many spacecraft, at least over a relatively long time-scale. As an example, the slow consumption of fuel during the whole operational lifetime of the vehicle (years) causes a shift of the centre of mass, but the knowledge of the current value is usually sufficient for describing manoeuvres over a faster time-scale (minutes). On the converse, it is sometimes necessary to take into account phenomena where variations of the mass distribution affects significantly the vehicle's attitude dynamics. Flexible solar panels or other appendages or fuel sloshing in the tanks, the motion of which can be excited by an attitude or an orbit manoeuvre, may cause as a reaction oscillations of the spacecraft with respect to the desired attitude, which may harm overall pointing accuracy, unless properly damped passively by the inherent vehicle stability or actively by its automatic control system. Sometimes, a satellite may feature a nutation damper, where a mass moving within a viscous liquid induces dissipation in order to asymptotically stabilise a pure spin condition (see Chapter 3).

If the centre of mass O does not maintain a fixed position with respect to the body and one must choose whether (i) keeping the reference frame centred in O or (ii) choosing another reference point, allowing for displacements of O with respect to the origin of the frame. In the second case, the generalised form of Euler equation can be employed for the angular momentum balance, the current position of the centre of mass and the inertia tensor being usually available from the knowledge of the (current) mass distribution. The major advantage of the second approach lies in the fact that it is often possible to identify a frame which is fixed with respect to the rigid structure of the spacecraft, which allows to describe intuitively the orientation of the spacecraft itself and its equipment (antennae, sensors, and so on). If the first approach is taken, the pseudo-body frame moves with respect to the spacecraft structure because of changes in the mass distribution, so that the knowledge of its attitude does not imply the knowledge of spacecraft and sensor orientation. Moreover, the expressions of the attitude equations are usually rather complex.

Chapter 2

Passive Stabilisation of Rigid Spacecraft

Spin stabilisation is a simple, low cost and effective means of attitude stabilisation. Prior to, or just after deployment, the satellite is spun up about its axis of symmetry. For this reason, spin stabilised satellites are usually short cylinders. The angular momentum accumulated about the spin axis provides “gyroscopic stability” against external disturbance torques.

Although simple and reliable, spin stabilised satellites are inefficient for power generation. Since the satellite is continually spinning, the entire surface of the satellite must be covered with solar cells. In addition, payload efficiency is particularly low when only one direction is fixed in space and maneuvering of the spin axis complex.

When the requirement on pointing accuracy is weak (of the order of some tenths of a degree) gravity-gradient torque may be used for stabilizing an Earth pointing satellite, while the use of a dual-spin system allows one to despin a part of the satellite, while providing gyroscopic stability to the whole spacecraft.

2.1 Torque-free motion of axi-symmetric satellites

2.1.1 Angular velocity

The principal moments of inertia of an axi-symmetric satellite will be given by

$$\begin{aligned} J_t &= J_x = J_y \\ J_s &= J_z \end{aligned}$$

where the subscripts t and s stand for *transverse* and *spin*, respectively, and we assume that the symmetry axis coincides with the third ($\hat{\mathbf{e}}_3$) axis of the body frame \mathcal{F}_B .

During the spin-up manoeuvre, the satellite will accumulate angular momentum about the spin axis, but because of various perturbations or imperfections, such as thruster misalignment, the final condition at the end of the spin-up will hardly be a pure spin about the spin axis $\hat{\mathbf{e}}_3$. The imperfections will cause some (hopefully residual) nutation.

For torque-free motions

$$M_1 = M_2 = M_3 = 0$$

of axial symmetric spacecraft, Euler's equations take the following form:

$$J_t \dot{\omega}_1 + (J_s - J_t) \omega_2 \omega_3 = 0$$

$$\begin{aligned} J_t \dot{\omega}_2 + (J_t - J_s) \omega_1 \omega_3 &= 0 \\ J_s \dot{\omega}_3 &= 0 \end{aligned}$$

The first two equations are coupled, while the third one is independent of the other two. This means that the latter one can be integrated on its own. The resulting (trivial) solution is given by

$$\omega_3 = \Omega$$

where Ω is the (constant) spin rate about the spin axis.

Letting

$$\lambda = \frac{J_s - J_t}{J_t} \Omega$$

the first two equations can be rewritten as

$$\begin{aligned} \dot{\omega}_1 + \lambda \omega_2 &= 0 \\ \dot{\omega}_2 - \lambda \omega_1 &= 0 \end{aligned}$$

Multiplying the first equation by ω_1 and the second by ω_2 and summnig up, one gets

$$\dot{\omega}_1 \omega_1 + \dot{\omega}_2 \omega_2 = 0$$

that is

$$\omega_1^2 + \omega_2^2 = \omega_{12}^2 = \text{constant}$$

This means that the component of the angular velocity vector $\vec{\omega}$ that lies in the $\hat{e}_1 - \hat{e}_2$ plane, namely

$$\vec{\omega}_{12} = \omega_1 \hat{e}_1 + \omega_2 \hat{e}_2$$

has a constant magnitude. As also ω_3 is constant, we get that

$$\|\vec{\omega}\| = \omega_1^2 + \omega_2^2 + \omega_3^2 = \omega_{12}^2 + \Omega^2 = \text{constant}$$

The first two equations of motion,

$$\begin{aligned} \dot{\omega}_1 + \lambda \omega_2 &= 0 \\ \dot{\omega}_2 - \lambda \omega_1 &= 0 \end{aligned}$$

can be easily integrated. In fact, deriving the first one with respect to the time t , one gets

$$\ddot{\omega}_1 + \lambda^2 \omega_1 = 0$$

that, taking into account the second equation, becomes

$$\ddot{\omega}_1 + \lambda^2 \omega_1 = 0$$

which is formally identical to the well known equation of the linear harmonic oscillator. The general solution

$$\omega_1(t) = A \cos(\lambda t) + B \sin(\lambda t)$$

for initial conditions

$$\omega_1(t = 0) = \omega_{1,0}; \quad \dot{\omega}_1(t = 0) = \dot{\omega}_{1,0}$$

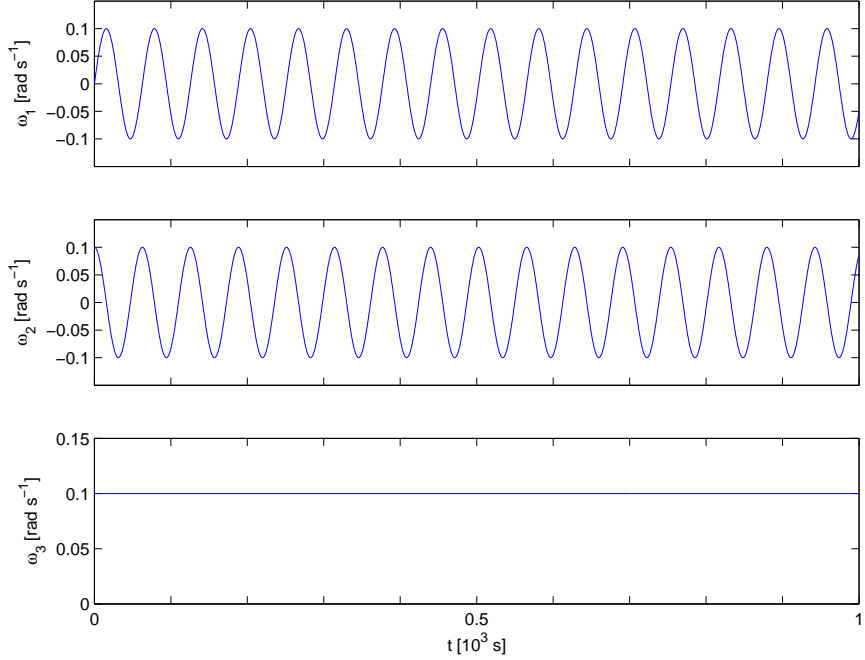


Figure 2.1: Time–history of angular velocity components for a torque–free spin condition.

becomes

$$\begin{aligned}\omega_1(t) &= \omega_1(0) \cos(\lambda t) + \frac{\dot{\omega}_1(0)}{\lambda} \sin(\lambda t) \\ &= \omega_{12} \sin[\lambda(t - t_0)]\end{aligned}$$

Deriving the solution for ω_1 w.r.t. t and substituting into the first equation, it is

$$\begin{aligned}\omega_2 = -\frac{\dot{\omega}_1}{\lambda} &= \omega_1(0) \sin(\lambda t) - \frac{\dot{\omega}_1(0)}{\lambda} \cos(\lambda t) \\ &= -\omega_{12} \cos[\lambda(t - t_0)]\end{aligned}$$

The evolution of ω_1 and ω_2 shows that $\vec{\omega}_{12}$ whirls around \hat{e}_3 with angular velocity λ . Writing the angular velocity as

$$\vec{\omega} = \vec{\omega}_{12} + \Omega \hat{e}_3$$

during the evolution, $\vec{\omega}$ describes a cone around the axis of symmetry \hat{e}_3 of the spinning body, which is called the *body cone*.

The angular momentum vector can be written in the form

$$\begin{aligned}\vec{h} &= J_1 \omega_1 \hat{e}_1 + J_2 \omega_2 \hat{e}_2 + J_3 \omega_3 \hat{e}_3 \\ &= J_t (\omega_1 \hat{e}_1 + \omega_2 \hat{e}_2) + J_s \omega_3 \hat{e}_3 \\ &= J_t \vec{\omega}_{12} + J_s \Omega \hat{e}_3\end{aligned}$$

It can be observed that \vec{h} and $\vec{\omega}$ are both a linear combination of the vectors $\vec{\omega}_{12}$ and \hat{e}_3 . Thus, during the motion of the spinning body, the vectors \vec{h} , $\vec{\omega}$ and \hat{e}_3 lie in the same plane Π , that rotates around \hat{e}_3 , if we look at the motion from \mathcal{F}_B .

In the most general case \vec{h} and $\vec{\omega}$ are not aligned. They are aligned only if $\omega_{12} = 0$, that is, if we have a pure spinning motion about the symmetry axis. This is the desired spin condition, where a sensor placed on the satellite on its symmetry axis points a fixed

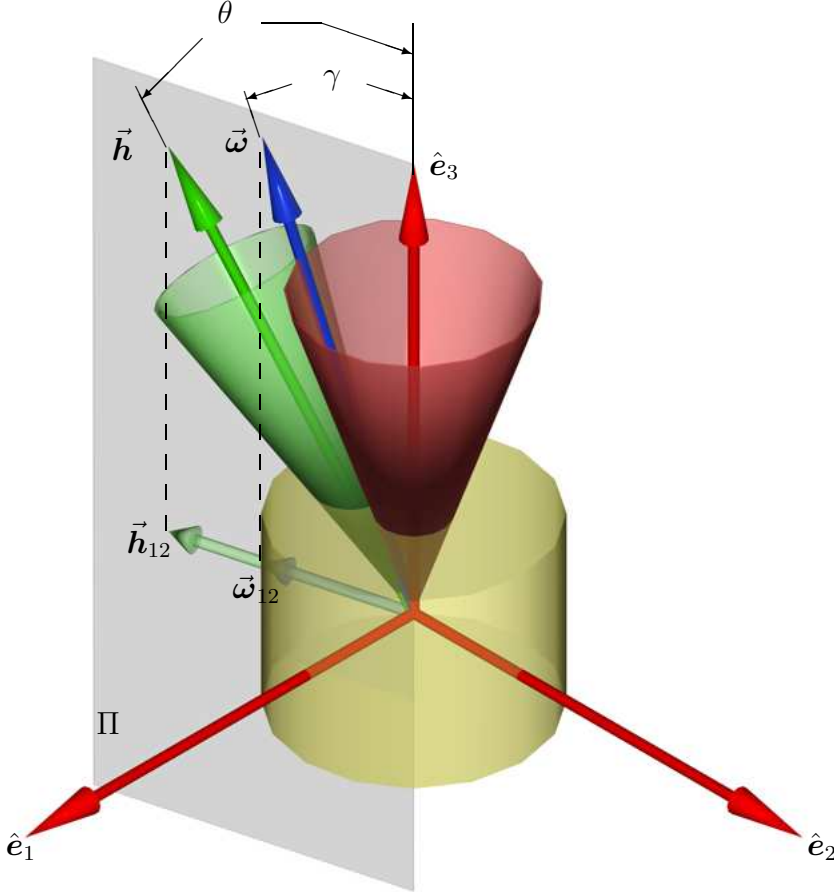


Figure 2.2: Torque-free spinning of an axi-symmetric satellite as seen in \mathcal{F}_B .

direction in space. If $\omega_{12} \neq 0$, the motion of the spinning body is more complex (and the pointing less accurate). A geometric description of this motion will now be derived.

The assumption of torque-free motion, $\vec{M} = 0$, implies that

$$\frac{d\vec{h}}{dt} = \vec{M} = 0 \implies \vec{h} = \text{constant}$$

in the inertial frame, and Π rotates around \vec{h} , if we look at the motion from \mathcal{F}_I .

It is possible to define two angles, θ and γ , that remains constant in time,

$$\left. \begin{aligned} \tan \theta &= \frac{h_{12}}{h_3} = \frac{J_t \omega_{12}}{J_s \omega_3} \\ \tan \gamma &= \frac{\omega_{12}}{\omega_3} \end{aligned} \right\} \implies \tan \theta = \frac{J_t}{J_s} \tan \gamma$$

Without loss of generality, it is possible to choose the unit vector \hat{E}_3 of the (inertially fixed) reference frame \mathcal{F}_I parallel to the (inertially constant) direction of the angular momentum vector. Under this assumption, the nutation angle Θ (that is, the angle between \hat{E}_3 and the symmetry axis \hat{e}_3) coincides with the (constant) angle θ defined above. This means that $\theta \equiv \Theta$ represents the (constant) nutation angle and it defines the orientation of the symmetry axis \hat{e}_3 in the inertial space. The angle γ is the semi-aperture of the body-cone.

As an immediate consequence, also the angle between \vec{h} and $\vec{\omega}$, equal to $|\theta - \gamma|$, is constant, and $\vec{\omega}$ describes a cone around \vec{h} , fixed in the inertial frame, the *space cone*.

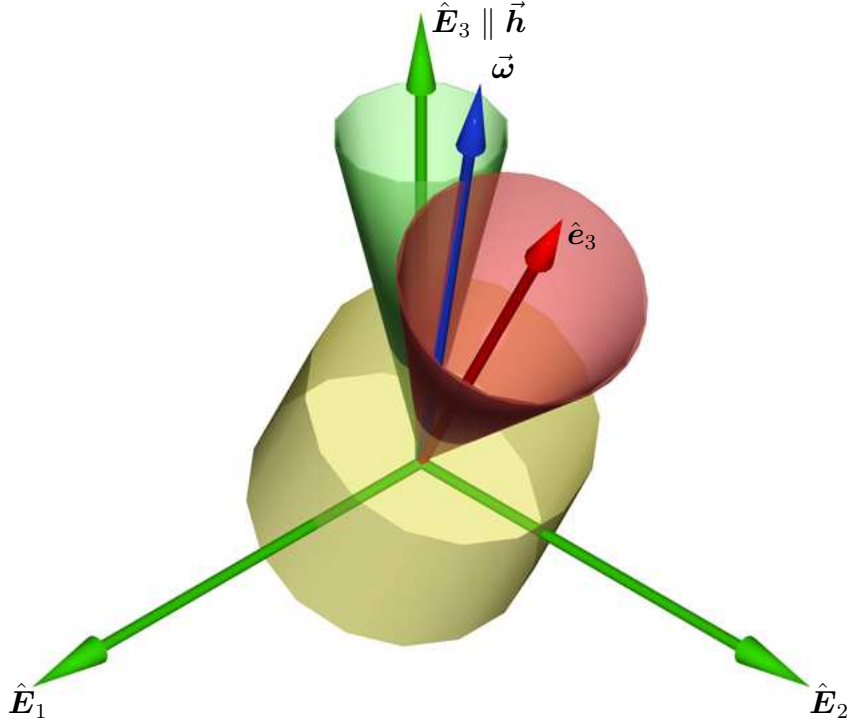


Figure 2.3: Torque-free spinning of an axi-symmetric satellite as seen in \mathcal{F}_I .

The body cone is attached to the body axes, but it is not fixed in space. On the converse, the space cone, attached to the vector \vec{h} , that is constant in the inertial frame, is fixed in \mathcal{F}_I . The two cones remains tangent along $\vec{\omega}$, that is the axis of instantaneous rotation of the body, and the motion of the satellite can be represented by the body cone rolling along the surface of the space cone.

As a final observation, it should be noted that, when $J_s > J_t$ (*oblate body*, that is a disk-shaped body), it is $\gamma > \theta$, and the space cone is inside the body cone. On the converse, when $J_s < J_t$ (*prolate body*, that is a rod-shaped body), it is $\gamma < \theta$, and the space cone is outside the body cone.

2.1.2 Attitude (in terms of Euler angles)

For what concern the attitude resulting from such a motion, substituting the expressions for the angular velocity components determined above in the following equation,

$$\begin{aligned}\omega_1 &= \dot{\Psi} \sin \Phi \sin \Theta + \dot{\Theta} \cos \Phi \\ \omega_2 &= \dot{\Psi} \cos \Phi \sin \Theta - \dot{\Theta} \sin \Phi \\ \omega_3 &= \dot{\Psi} \cos \Theta + \dot{\Phi}\end{aligned}$$

From the equivalence derived above, $\Theta \equiv \theta = \text{constant}$, one gets $\dot{\Theta} = 0$. This relation can be substituted in the above equations, together with the solution for the angular velocity components, so that one gets

$$\begin{aligned}\dot{\Psi} \sin \Phi \sin \Theta &= \omega_{12} \sin[\lambda(t - t_0)] \\ \dot{\Psi} \cos \Phi \sin \Theta &= -\omega_{12} \cos[\lambda(t - t_0)] \\ \dot{\Psi} \cos \Theta + \dot{\Phi} &= \Omega\end{aligned}$$

By squaring and summing the first two equations, it is evident that

$$\dot{\Psi}^2 \sin^2 \Theta = (\omega_{12})^2$$

so that $\dot{\Psi}$ is constant; $\dot{\Psi}$ is called *precession rate* or *coning speed*, and it is the angular velocity of the line of the nodes on the horizontal plane.

Dividing the first equation by the second, the spin angle Φ is determined,

$$\tan \Phi = -\tan[\lambda(t - t_0)] \Rightarrow \Phi = -\lambda(t - t_0)$$

Deriving w.r.t. time, the *inertial spin rate* is obtained

$$\dot{\Phi} = -\lambda$$

that is also constant. At this point, it is possible to evaluate the precession rate from the third equation,

$$\dot{\Psi} \cos \Theta + \dot{\Phi} = \Omega \Rightarrow \dot{\Psi} = \frac{\Omega - \dot{\Phi}}{\cos \Theta}$$

But from the definition of λ ,

$$\lambda = \frac{J_s - J_t}{J_t} \Omega \Rightarrow \Omega = \frac{J_t}{J_s - J_t} \lambda = \frac{J_t}{J_t - J_s} \dot{\Phi}$$

one gets

$$\dot{\Psi} = \frac{J_s}{J_t - J_s} \frac{\dot{\Phi}}{\cos \Theta}$$

If $J_t > J_s$, that is we have a prolate body, $\dot{\Psi}$ and $\dot{\Phi}$ have the same sign and we have *direct precession*, that is the precession rate is in the same direction of the spin rate. On the converse, if $J_s > J_t$ and an oblate body is dealt with, $\dot{\Psi}$ and $\dot{\Phi}$ have different signs and we have *retrograde precession*, the precession rate being in the opposite direction with respect to the spin rate.

An observation

It is important to note that the derivation presented in this paragraph are valid *for any rigid body which has two equal principal moment of inertia*. This is a category much wider than that of axi-symmetric bodies, including any prism with a basis made of a regular polygon, but also any other body of irregular shape such that there exists a set of principal axes of inertia such that $J_x = J_y \neq J_z$.

2.2 Torque-free motion of tri-inertial satellites

An analytical solution of the motion of tri-inertial rigid body can be derived in terms of Jacobi elliptic functions. Luckily there is also a geometric description of the same motion, due to Poinsot, which is much simpler, nonetheless extremely useful for the description of the dynamics of an arbitrary rigid body.

Remembering that the kinetic energy

$$\mathcal{T} = \frac{1}{2} \vec{\omega} \cdot \vec{h} = d$$

and the angular momentum vector \vec{h} are constant, it is possible to consider the (constant) dot product

$$\vec{\omega} \cdot \frac{\vec{h}}{h} = \frac{2\mathcal{T}}{h} \quad (2.1)$$

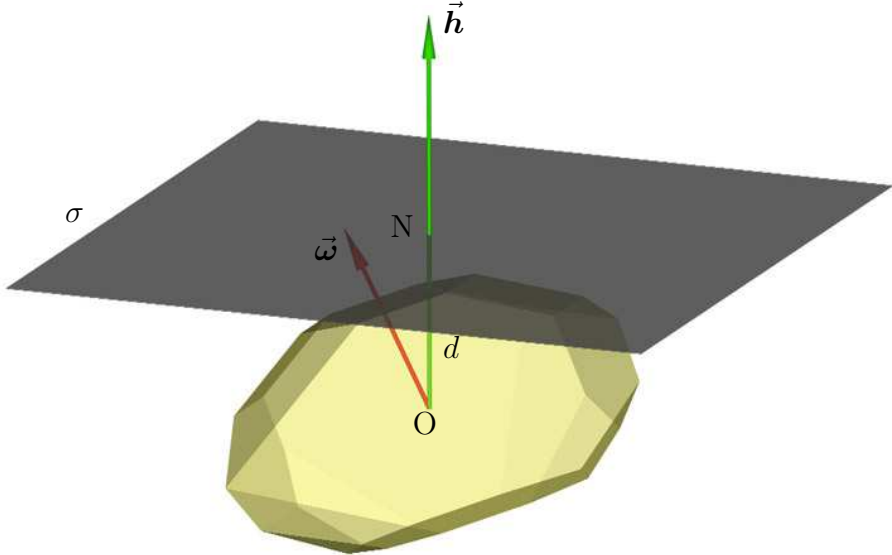


Figure 2.4: The invariable plane.

as the length d of a (constant) segment ON along the direction of \vec{h} . The *invariable plane* σ , which is the plane perpendicular to the direction of \vec{h} , placed at a distance d from the body center of mass O, is thus fixed in \mathcal{F}_I , and it represents the locus of all the possible $\vec{\omega}$ that satisfy Eq. (2.1). Remembering that the Poinsot ellipsoid is the locus of all the possible $\vec{\omega}$ that satisfy the kinetic energy equation, the intersection between the ellipsoid and the invariable plane must contain the angular velocity vector.

It is easy to demonstrate that such an intersection is a single point P , *i.e.* the Poinsot ellipsoid and the invariable plane are tangent. Since the time derivative of the kinetic energy is zero,

$$\frac{d\mathcal{T}}{dt} = \frac{1}{2} \frac{d\vec{\omega}}{dt} \cdot \vec{h}$$

the increment $d\vec{\omega}$ and \vec{h} are perpendicular, thus $d\vec{\omega}$ lie on σ . But since the vector $\vec{\omega} + d\vec{\omega}$ must be also on the Poinsot ellipsoid, $d\vec{\omega}$ must be tangent to its surface. These two conditions can be satisfied only if the Poinsot ellipsoid is always tangent to σ . Moreover, the Poinsot ellipsoid is fixed in the body frame \mathcal{F}_B , so that $d\vec{\omega}$ is the same in both \mathcal{F}_I and \mathcal{F}_B . This means that the Poinsot ellipsoid rolls without slipping on σ .

2.2.1 Drawing the polhode curves

The locus of all the possible $\vec{\omega}$ s on the Poinsot ellipsoid is given by the *polhode* curve, which is the intersection between the Poinsot ellipsoid and the angular momentum ellipsoid. Thus, during the rolling motion, the tangent point moves on the Poinsot ellipsoid along the polhode. The trajectory of the tangency point on σ is the *herpolhode*. When the body is axisymmetric, both the polhode and the herpolhode are circles and the situation can be depicted in terms of space and body cones. In general the herpolhode is not a closed curve, but the polhode must be a closed curve on the Poinsot ellipsoid, inasmuch as after a revolution around the spin axis $\vec{\omega}$ must attain again the same value, in order to satisfy conservation of both kinetic energy and angular momentum.

In order to draw the shape of the polhodes on the Poinsot ellipsoid, it is sufficient to

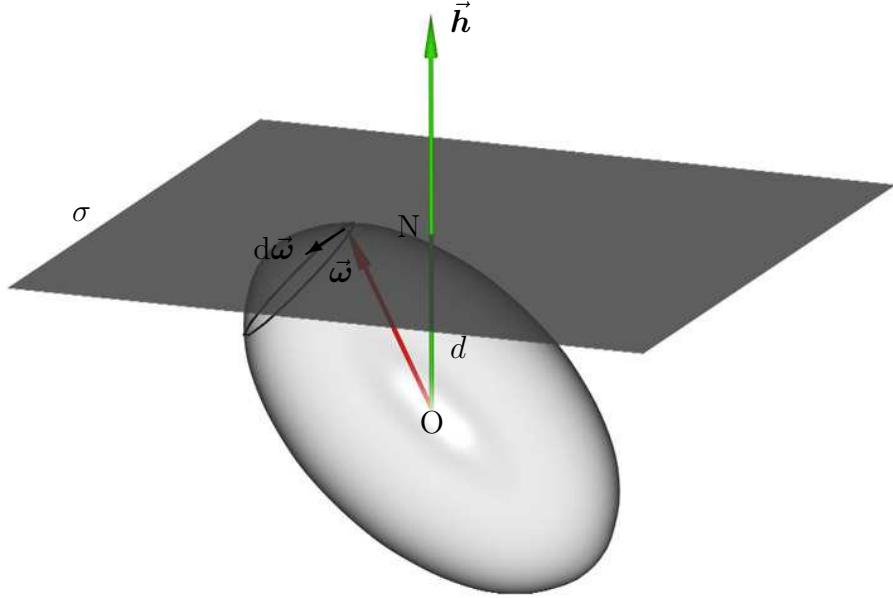


Figure 2.5: The Poinsot ellipsoid rolls on the invariable plane.

recall the equations of the Poinsot ellipsoid and the angular momentum ellipsoid, that are

$$\begin{aligned} \frac{\omega_1^2}{(2\mathcal{T}/J_x)} + \frac{\omega_2^2}{(2\mathcal{T}/J_y)} + \frac{\omega_3^2}{(2\mathcal{T}/J_z)} &= 1 \\ \frac{\omega_1^2}{(h/J_x)^2} + \frac{\omega_2^2}{(h/J_y)^2} + \frac{\omega_3^2}{(h/J_z)^2} &= 1 \end{aligned}$$

Subtracting the first equation from the second and multiplying the result by h^2 , one gets the *polhode equation*:

$$J_x \left(J_x - \frac{h^2}{2\mathcal{T}} \right) \omega_1^2 + J_y \left(J_y - \frac{h^2}{2\mathcal{T}} \right) \omega_2^2 + J_z \left(J_z - \frac{h^2}{2\mathcal{T}} \right) \omega_3^2 = 0$$

In order to have real solutions for the above equation, the three coefficients cannot have the same sign. For this reason the parameter $J^* = h^2/(2\mathcal{T})$ must lie between the maximum and the minimum moment of inertia. Assuming, without loss of generality, that $J_x > J_y > J_z$, it is

$$J_z \leq J^* \leq J_x$$

The easiest way to determine the shape of the polhodes is to consider their projection onto the planes of the three-dimensional space $\omega_1-\omega_2-\omega_3$. Eliminating ω_3 between the equations of the two ellipsoids brings the equation

$$J_x(J_x - J_z)\omega_1^2 + J_y(J_y - J_z)\omega_2^2 = 2\mathcal{T}(J^* - J_z)$$

which represents an ellipse, since all the coefficients are positive. Similarly, eliminating ω_1 one gets

$$J_y(J_y - J_x)\omega_2^2 + J_z(J_z - J_x)\omega_3^2 = 2\mathcal{T}(J^* - J_x)$$

which is again the equation of an ellipse, inasmuch as all the coefficients are negative. On the converse, eliminating ω_2 , which is the angular velocity component with respect to the intermediate axis, brings

$$J_x(J_x - J_y)\omega_1^2 + J_z(J_z - J_y)\omega_3^2 = 2\mathcal{T}(J^* - J_y)$$

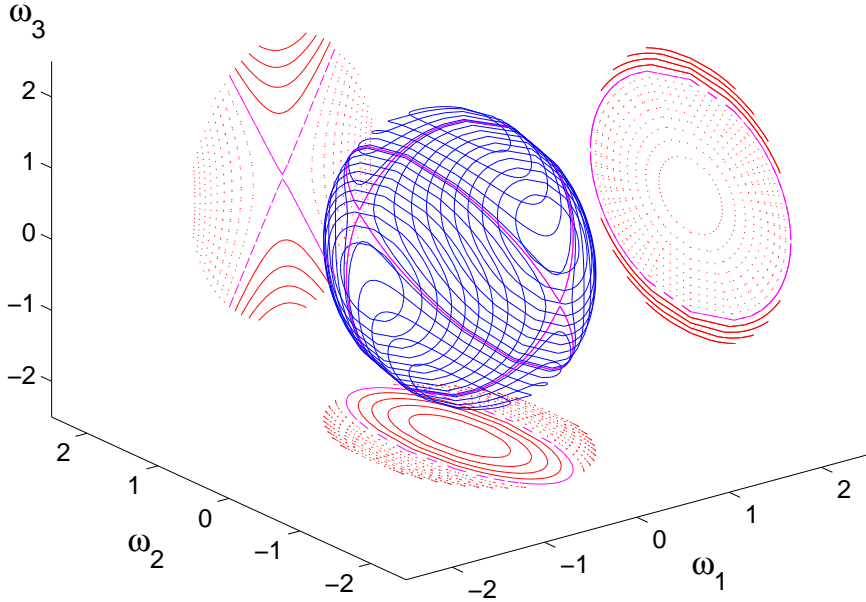


Figure 2.6: Polhode curves on the Poinsot Ellipsoid.

which represent a hyperbola, the coefficients of the left-hand side being of different sign. It should be noted that, depending on the sign of $J^* - J_y$, which can be either positive or negative, the axis of the hyperbola will be vertical or horizontal, in the $\omega_1-\omega_3$ plane. When $J^* = J_y$, the polhode equation degenerates into the form

$$J_x (J_x - J^*) \omega_1^2 + J_z (J_z - J^*) \omega_3^2 = 0$$

which represents the *separatrices*, the boundaries of motion about the axis of maximum and minimum inertia.

2.2.2 Stability of torque-free motion about principal axes

Spinning about any of the principal axis is an equilibrium condition for a rigid body of arbitrary inertias. The shape of the polhodes already provide an information about the stability of these equilibria, the axes of maximum and minimum inertia being centres surrounded by finite size orbits, while the intermediate axis is a saddle point, that is a small perturbation will take the angular velocity vector “far” from the initial point in the neighborhood of the saddle.

These facts can be demonstrated analytically. Let us consider a spinning motion about the z axis of the principal frame, such that $\vec{\omega}_0 = \Omega \hat{e}_3$. Assuming that $\vec{\omega} = \vec{\omega}_0 + \Delta\vec{\omega}$, where the body frame components of $\Delta\vec{\omega}$, given by $\Delta\vec{\omega}_B = \{\omega_1, \omega_2, \omega_3\}^T$, are small perturbations with respect to Ω , Euler’s equations can be rewritten as follows

$$\begin{aligned} J_x \dot{\omega}_1 + (J_z - J_y) \Omega \omega_2 &= 0 \\ J_y \dot{\omega}_2 + (J_x - J_z) \Omega \omega_1 &= 0 \\ J_z \dot{\omega}_3 &= 0 \end{aligned}$$

where second and higher order terms were neglected. The third equation is decoupled, thus stating that a perturbation on the spinning axis does not affect the other two. The

first two equations can be rewritten in matrix form

$$\begin{Bmatrix} \dot{\omega}_1 \\ \dot{\omega}_2 \end{Bmatrix} = \begin{bmatrix} 0 & (J_y - J_z)\Omega/J_x \\ (J_z - J_x)\Omega/J_y & 0 \end{bmatrix} \begin{Bmatrix} \omega_1 \\ \omega_2 \end{Bmatrix}$$

The characteristic equation is thus given by

$$\lambda^2 + \Omega^2 \frac{(J_y - J_z)(J_x - J_z)}{J_x J_y} = 0$$

If the spin axis is the intermediate one, the product $(J_y - J_z)(J_x - J_z)$ is negative, one of the two factor being positive and the other one negative. In this case, both roots are real,

$$\lambda = \pm \Omega \sqrt{-\frac{(J_y - J_z)(J_x - J_z)}{J_x J_y}}$$

and one of the two eigenvalues is positive. This means that spinning around the intermediate axis is an unstable equilibrium for the spinning rigid body.

On the converse, if the spin axis is the axis of maximum moment of inertia, it is $J_y < J_z$ and $J_x < J_z$, while spinning around the axis of minimum inertia makes $J_y > J_z$ and $J_x > J_z$. In both these latter two cases, the roots

$$\lambda = \pm i\Omega \sqrt{\frac{(J_y - J_z)(J_x - J_z)}{J_x J_y}}$$

are pure imaginary and the stability analysis based on the linearized model is inconclusive, inasmuch as the sufficient condition for stability requires that the real part of the eigenvalues is strictly negative. But because of conservation of energy and angular momentum, the solution is confined in a neighbourhood of the pure spin condition, so that the neglected nonlinear terms cannot induce divergence. This means that the pure spin condition about the axes of minimum and maximum inertia is Ljapunov (although not asymptotically) stable.

2.3 Nutation Damping

Nutation damping is a simple yet effective way to restore a state of pure spin, if a nutation angle different from zero should be induced by some external cause. We will now investigate how it is possible to exploit the effects of energy dissipation in order to make a pure spin condition asymptotically stable.

2.3.1 Effects of energy dissipation

As a matter of fact, the rigid body is an abstraction. Usually flexible appendages and/or fuel sloshing induce some energy dissipation the effects of which can be easily determined at least in the case of axi-symmetric satellites by use of the *energy sink model*.

The kinetic energy of a rotating rigid body is given by

$$T = \frac{1}{2} (J_x \omega_1^2 + J_y \omega_2^2 + J_s \omega_3^2)$$

The expression for \mathcal{T} can be rearranged for the axi-symmetric case in the form

$$\mathcal{T} = \underbrace{\frac{1}{2} J_t (\omega_1^2 + \omega_2^2)}_{\text{transverse}} + \underbrace{\frac{1}{2} J_s \Omega^2}_{\text{spin}}$$

At the same time, the angular momentum is

$$\vec{h} = J_t \omega_1 \hat{e}_1 + J_t \omega_2 \hat{e}_2 + J_s \omega_3 \hat{e}_3 \Rightarrow h^2 = J_t^2 (\omega_1^2 + \omega_2^2) + J_s^2 \Omega^2$$

so that the quantity $(2J_s \mathcal{T} - h^2)$ is

$$\begin{aligned} (2J_s \mathcal{T} - h^2) &= J_s J_t (\omega_1^2 + \omega_2^2) + J_s^2 \Omega^2 - J_t^2 (\omega_1^2 + \omega_2^2) - J_s^2 \Omega^2 \\ &= J_t (\omega_1^2 + \omega_2^2) (J_s - J_t) \end{aligned}$$

By taking the time derivatives of both sides of the equation, and remembering that, for zero external torque the angular momentum vector remains constant, one gets

$$\frac{d\mathcal{T}}{dt} = \frac{1}{2} \frac{J_t}{J_s} (J_s - J_t) \frac{d}{dt} (\omega_1^2 + \omega_2^2)$$

If there is no dissipation, $\dot{\mathcal{T}} = 0$ and $\omega_1^2 + \omega_2^2$ is constant (as already demonstrated in Section 2.1.1). If there is dissipation, $\dot{\mathcal{T}} < 0$, which means that, assuming an approximately constant mass distribution, so that the moments of inertia are unaffected, $\omega_1^2 + \omega_2^2$ must either grow or decrease. It should be noted that, if the body is oblate, than $J_s - J_t > 0$ and $d(\omega_1^2 + \omega_2^2)/dt < 0$, which meand that the transverse component of the angular velocity vector is decreasing. Dissipation will stop only when it is $\omega_1^2 + \omega_2^2 = 0$, that is, when a pure spin condition is reached. In such a case, dissipation turns the pure spin condition into an asymptotically stable equilibrium: a displacement from such a condition will be damped out at the expenses of a reduction of the system energy.

On the converse, if the body is prolate and $J_s - J_t < 0$, than dissipation induces an increase of the transverse angular velocity component, as in order to satisfy the equation, $d(\omega_1^2 + \omega_2^2)/dt$ must be positive. This means that the nutation angle is growing, being proportional to ω_{12}/Ω . In such a case the pure spin condition about the symmetry axis, which was stable in the sense of Lyapunov for the perfect rigid case, becomes unstable. Although divergence is usually slow, the nutation angle will steadily increase with time.

The rate of variation of the nutation angle is slow enough to make its rate negligible with respect to $\dot{\Psi}$. Under this assumption it is possible to state that

$$\omega_1^2 + \omega_2^2 \approx \dot{\Psi}^2 \sin^2 \Theta$$

and, as a consequence, it is possible to formulate the energy decay rate as

$$\frac{d\mathcal{T}}{dt} = \frac{1}{2} \frac{J_t}{J_s} (J_s - J_t) \frac{d}{dt} (\dot{\Psi}^2 \sin^2 \Theta)$$

Moreover, for small nutation angles the precession rate can also be considered approximately constant, and differentiation with respect to time bring the following expression:

$$\frac{d\mathcal{T}}{dt} = \frac{J_t}{J_s} \dot{\Psi}^2 (J_s - J_t) \sin \Theta \cos \Theta \dot{\Theta}$$

When energy is dissipated and $\dot{\mathcal{T}} < 0$, the quantity $(J_s - J_t) \sin(2\Theta)\dot{\Theta}$ must also be negative, and a nutation rate is induced by dissipation. As qualitatively shown previously,

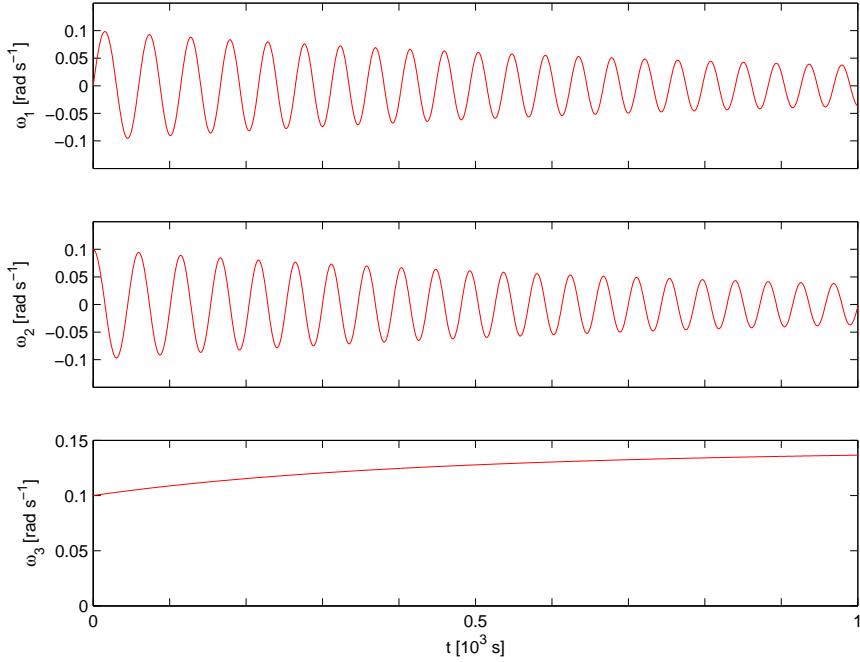


Figure 2.7: Time–history of angular velocity components with nutation damping.

if the satellite is an oblate body and $J_s > J_t$, $\dot{\Theta}$ is negative for small nutation angles, and tends to decrease with time because of dissipation. This means that spinning around the symmetry axis is asymptotically stable, as $\Theta \rightarrow 0$. For a prolate body, when $J_s < J_t$, the resulting nutation rate is positive and the nutation angle increases with time: the satellite tends towards a flat spin condition, $\Theta \rightarrow \pi/2$.

Note that both the pure–spin and flat–spin conditions are always equilibria for the satellite, regardless of its shape, inasmuch as $\dot{T} = 0$ and $\dot{\Theta} = 0$ if either $\Theta = 0$ or $\pi/2$, but the stability of these equilibria is affected by the mass distribution.

Also note that as ω_1 and ω_2 are damped out in the stable case, ω_3 increases because of conservation of angular momentum. Letting Ω_f be the final spin rate, it is

$$h^2 = J_t^2(\omega_1^2 + \omega_2^2) + J_s^2\Omega^2 = J_s^2\Omega_f^2$$

Therefore,

$$\Omega_f^2 = \Omega^2 + \frac{J_t^2}{J_s^2}(\omega_1^2 + \omega_2^2)$$

and the final spin rate results higher than the initial one, as expected (Fig. 2.7). In the unstable case, dissipation will make the spin angular velocity component drop towards zero as the angular momentum is transferred by dissipation in the transverse direction.

2.3.2 Equations of motion of a rigid satellite with damper

In a real system there are several causes that induce energy dissipation, such as fuel sloshing. Most satellites use thruster to actively remove nutation and maintain the desired pure spin condition, when the nutation angles increases beyond a prescribed threshold. For oblate bodies a nutation damper provides a very simple and useful means for passively stabilizing the pure spin motion. An example of damper is the *ball-in-tube*: a plastic tube is filled with viscous fluid and a ball bearing is free to move in the fluid, thus dissipating

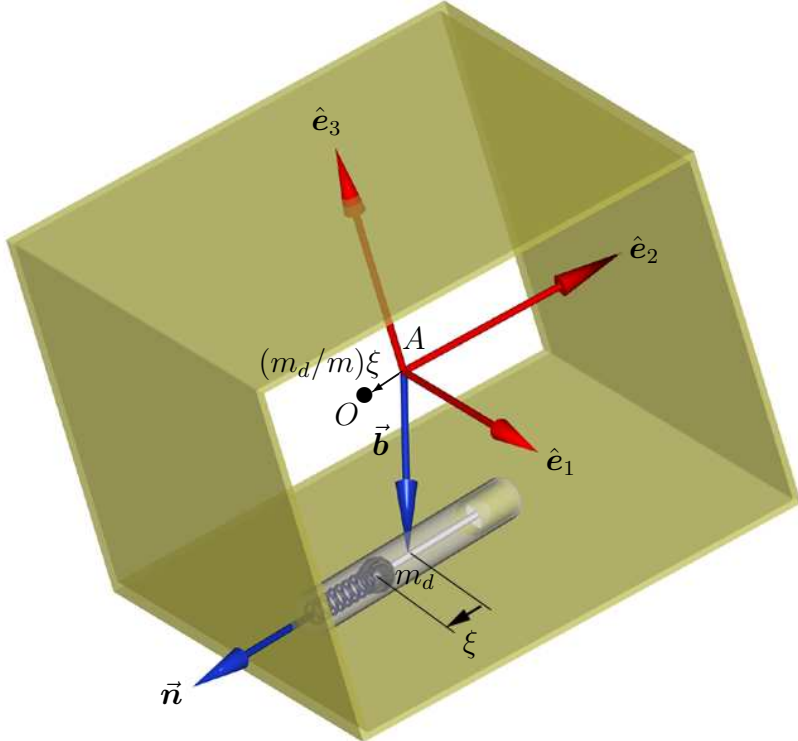


Figure 2.8: A satellite equipped with a “ball–in–tube” damper.

energy. The only drawback of this technique is that it may take several minutes (if not hours) to remove nutation.

In order to derive the equations of motion of a satellite equipped with a spring–mass–dashpot damper, it is necessary to consider the generalized form of the Euler equation,

$$\frac{d\vec{h}_A}{dt} + \vec{S}_A \times \vec{a}_A = \vec{M}_A$$

written in a reference frame \mathcal{F}_A fixed with respect to the satellite platform \mathcal{P} , with origin in the point A , which is the center of mass of the satellite when the damper mass m_d is in the undeformed position P ($\xi = 0$) for the spring. All the “moments” are taken with respect to A .

Assuming that \mathbf{I}_0 is the inertia tensor when $\xi = 0$, the inertia tensor in the general case is given by

$$\mathbf{I} = \mathbf{I}_0 + m_d \left[(\rho^2 - b^2)\mathbf{1} - (\vec{\rho}\vec{\rho} - \vec{b}\vec{b}) \right]$$

where the position vector $\vec{\rho}$ of the mass is

$$\vec{\rho} = \vec{b} + \xi \hat{n}$$

\hat{n} being the orientation of the damper and \vec{b} the position vector of P . The overall angular momentum is

$$\begin{aligned} \vec{h} &= \mathbf{I}\vec{\omega} + m_d \dot{\xi}(\vec{\rho} \times \hat{n}) \\ &= \mathbf{I}\vec{\omega} + m_d \dot{\xi}(\vec{b} \times \hat{n}) \end{aligned}$$

where $\vec{\omega}$ is the angular velocity of \mathcal{P} . It is then possible to write the time derivative of \vec{h}

in \mathcal{F}_A as

$$\begin{aligned} \left(\frac{d\vec{h}}{dt} \right)_A &= \dot{\vec{h}}_A + \boldsymbol{\omega}_A \times \vec{h}_A \\ &= \dot{\vec{I}}\boldsymbol{\omega}_A + \vec{I}\dot{\boldsymbol{\omega}}_A + m_d \ddot{\xi}(\vec{b}_A \times \vec{n}_A) + \boldsymbol{\omega}_A \times [\vec{I}\boldsymbol{\omega}_A + m_d \dot{\xi}(\vec{b}_A \times \vec{n}_A)] \end{aligned}$$

The time derivative of the inertia matrix \vec{I} is

$$\dot{\vec{I}} = m_d \left[\frac{d(\rho^2)}{dt} \mathbf{1} - (\boldsymbol{\rho}_A \dot{\boldsymbol{\rho}}_A^T + \dot{\boldsymbol{\rho}}_A \boldsymbol{\rho}_A^T) \right]$$

where, being $\rho^2 = \xi^2 + 2\xi \vec{b}_A^T \vec{n}_A + b^2$, it is

$$\frac{d(\rho^2)}{dt} t = 2\dot{\xi}(\xi + \vec{b}_A^T \vec{n}_A)$$

while

$$\dot{\boldsymbol{\rho}}_A = \dot{\xi} \vec{n}_A \Rightarrow \boldsymbol{\rho}_A \dot{\boldsymbol{\rho}}_A^T + \dot{\boldsymbol{\rho}}_A \boldsymbol{\rho}_A^T = \dot{\xi}(\vec{b}_A \vec{n}_A^T + \vec{n}_A \vec{b}_A^T + 2\xi \vec{n}_A \vec{n}_A^T)$$

Summing up, it is

$$\dot{\vec{I}} = m_d \dot{\xi} [2(\xi + \vec{b}_A^T \vec{n}_A) \mathbf{1} - \vec{b}_A \vec{n}_A^T - \vec{n}_A \vec{b}_A^T - 2\xi \vec{n}_A \vec{n}_A^T]$$

At this point, all the elements required for writing the time derivative of the angular momentum in \mathcal{F}_A are explicitly given. In order to express the term $\vec{S} \times \vec{a}_A$, it is now necessary to derive the actual position of the center of mass O , given by

$$\vec{r}_{AO} = \frac{m_d}{m} \xi \hat{\vec{n}}$$

where m is the overall satellite mass. The static moment can thus be written as

$$\vec{S}_A = m \vec{r}_{AO} = m_d \xi \hat{\vec{n}} \Rightarrow \vec{S}_A = m \vec{r}_A = m_d \xi \vec{n}_A$$

At the same time, assuming that the external force \vec{F} is zero, the absolute acceleration of the center of mass O is also zero. Writing the absolute position of the centre of mass as $\vec{r}_O = \vec{r}_A + \vec{r}_{AO}$, the resulting (absolute) acceleration of A is

$$\vec{a}_A = \vec{a}_O - \frac{d^2 \vec{r}_{AO}}{dt^2} = -\frac{d^2 \vec{r}_{AO}}{dt^2}$$

By means of a double application of the rule for the time derivative of a vector quantity in the rotating frame fixed to the spacecraft bus, \mathcal{F}_A , it is

$$\left(\frac{d^2 \vec{r}_{AO}}{dt^2} \right)_A = \ddot{\vec{r}}_{AO} + 2\boldsymbol{\omega}_A \times \dot{\vec{r}}_{AO} + \dot{\boldsymbol{\omega}}_A \times \vec{r}_A + \boldsymbol{\omega}_A \times (\boldsymbol{\omega}_A \times \vec{r}_A)$$

where

$$\dot{\vec{r}}_{AO} = \frac{m_d}{m} \dot{\xi} \hat{\vec{n}} ; \quad \ddot{\vec{r}}_{AO} = \frac{m_d}{m} \ddot{\xi} \hat{\vec{n}}$$

As a consequence, it is

$$\begin{aligned} (\vec{S} \times \vec{a}_A)_A &= -m_d \xi \vec{n}_A \times \left(\frac{m_d}{m} \right) [\ddot{\xi} \vec{n}_A + 2\dot{\xi} \boldsymbol{\omega}_A \times \vec{n}_A + \dot{\xi} \dot{\boldsymbol{\omega}}_A \times \vec{n}_A + \xi \boldsymbol{\omega}_A \times (\boldsymbol{\omega}_A \times \vec{n}_A)] \\ &= -\left(\frac{m_d^2}{m} \right) [2\xi \dot{\xi} \vec{n}_A \times (\boldsymbol{\omega}_A \times \vec{n}_A) + \xi^2 \vec{n}_A \times (\dot{\boldsymbol{\omega}}_A \times \vec{n}_A) + \xi^2 (\boldsymbol{\omega}_A^T \vec{n}_A) (\vec{n}_A \times \boldsymbol{\omega}_A)] \end{aligned}$$

In order to complete the model, it is necessary to derive the equation of motion for the damper mass m_d . The position of m_d with respect to the (inertially fixed) center of gravity O is given by

$$\vec{r}_m = -\vec{r}_{AO} + \vec{b} + \xi \hat{n}$$

so that Newton's second law can be written as

$$\frac{d^2 \vec{r}_m}{dt^2} = \frac{1}{m_d} \vec{F}_m$$

where \vec{F}_m is the overall force acting on m_d . By expressing all the vector quantities in \mathcal{F}_A one gets

$$m_d \left(\frac{d^2 \vec{r}_{mA}}{dt^2} \right)_A = \vec{F}_{mA}$$

Working out the expression of \vec{r}_{mA} , it is

$$\begin{aligned} \left(\frac{d \vec{r}_m}{dt} \right)_A &= \dot{\vec{r}}_{mA} + \boldsymbol{\omega}_A \times \vec{r}_{mA} = \\ &= -\dot{\vec{r}}_{AO} + \dot{\xi} \vec{n}_A + \boldsymbol{\omega}_A \times (-\vec{r}_A + \vec{b}_A + \xi \vec{n}_A) \\ &= (1 - m_d/m) \dot{\xi} \vec{n}_A + \boldsymbol{\omega}_A \times [(1 - m_d/m) \xi \vec{n}_A + \vec{b}_A] \\ \left(\frac{d^2 \vec{r}_m}{dt^2} \right)_A &= (1 - m_d/m) \ddot{\xi} \vec{n}_A + \dot{\boldsymbol{\omega}}_A \times [(1 - m_d/m) \xi \vec{n}_A + \vec{b}_A] + \\ &\quad + 2(1 - m_d/m) \dot{\xi} \boldsymbol{\omega}_A \times \vec{n}_A + \boldsymbol{\omega}_A \times \{ \boldsymbol{\omega}_A \times [(1 - m_d/m) \xi \vec{n}_A + \vec{b}_A] \} \end{aligned}$$

Since m_d has only one degree of freedom along the direction \hat{n} , it is sufficient to consider only the component of motion along \hat{n} itself, which is obtained by taking the scalar product of Newton's law times \vec{n}_A . Since all the terms like $\vec{n}_A^T (\boldsymbol{\omega}_A \times \vec{n}_A)$ are zero, this simplifies the expression of the absolute acceleration component of m_d along \hat{n} . The equation of motion of m_d thus becomes¹

$$\begin{aligned} -(c/m_d) \dot{\xi} - (k/m_d) \xi &= (1 - m_d/m) \ddot{\xi} + \vec{n}_A^T (\dot{\boldsymbol{\omega}}_A \times \vec{b}_A) + \\ &\quad + (\vec{n}_A^T \boldsymbol{\omega}_A) \{ \boldsymbol{\omega}_A^T [(1 - m_d/m) \xi \vec{n}_A + \vec{b}_A] \} - \omega^2 [(1 - m_d/m) \xi + \vec{n}_A^T \vec{b}_A] \end{aligned}$$

where the only forces acting on m_d along \hat{n} are the viscous damping term and the elastic force of the spring.

Collecting all the terms, it is now possible to write the equation of motion in \mathcal{F}_A of a rigid satellite equipped with a damper placed in an arbitrary position \vec{b} , with arbitrary orientation \hat{n} :

$$\begin{aligned} \vec{I} \boldsymbol{\omega}_A + \vec{I} \dot{\boldsymbol{\omega}}_A + m_d \ddot{\xi} (\vec{b}_A \times \vec{n}_A) + \boldsymbol{\omega}_A \times [\vec{I} \boldsymbol{\omega}_A + m_d \dot{\xi} (\vec{b}_A \times \vec{n}_A)] + \\ - \left(\frac{m_d^2}{m} \right) [2\xi \dot{\xi} \vec{n}_A \times (\boldsymbol{\omega}_A \times \vec{n}_A) + \xi^2 \vec{n}_A \times (\dot{\boldsymbol{\omega}}_A \times \vec{n}_A) + \xi^2 (\boldsymbol{\omega}_A^T \vec{n}_A) (\vec{n}_A \times \boldsymbol{\omega}_A)] &= \vec{M}_A \\ (1 - m_d/m) \ddot{\xi} + \vec{n}_A^T (\dot{\boldsymbol{\omega}}_A \times \vec{b}_A) + (\vec{n}_A^T \boldsymbol{\omega}_A) \{ \boldsymbol{\omega}_A^T [(1 - m_d/m) \xi \vec{n}_A + \vec{b}_A] \} + \\ - \omega^2 [(1 - m_d/m) \xi + \vec{n}_A^T \vec{b}_A] + (c/m_d) \dot{\xi} + (k/m_d) \xi &= 0 \end{aligned}$$

¹To complete the transformation, it is necessary to apply the double vector product rule

$$\vec{x} \times (\vec{y} \times \vec{z}) = (\vec{x} \cdot \vec{z}) \vec{y} - (\vec{x} \cdot \vec{y}) \vec{z}$$

to the last term.

2.3.3 A practical case: the axial damper

The equation of motion for the torque-free motion ($\vec{M}_A = 0$) of a rigid satellite equipped with a damper will now be specialized to the case where the damper is mounted parallel to the z -axis, that is $\hat{\mathbf{n}} = \hat{\mathbf{e}}_3$. Also, a set of principal axes of inertia for the configuration with $\xi = z = 0$ is chosen as the reference frame \mathcal{F}_A and it is assumed that $\vec{b} = b\hat{\mathbf{e}}_1$. This means that

$$\mathbf{n}_A = (0, 0, 1)^T ; \quad \mathbf{b}_A = (b, 0, 0)^T ; \quad \boldsymbol{\rho}_A = (b, 0, z)^T$$

Under these assumptions the inertia matrix is

$$\mathbf{I} = \begin{bmatrix} J_x + m_d z^2 & 0 & -m_d b z \\ 0 & J_y + m_d z^2 & 0 \\ -m_d b z & 0 & J_z \end{bmatrix}$$

and its time derivative is

$$\dot{\mathbf{I}} = \begin{bmatrix} 2m_d z \dot{z} & 0 & -m_d b \dot{z} \\ 0 & 2m_d z \dot{z} & 0 \\ -m_d b \dot{z} & 0 & 0 \end{bmatrix}$$

Also,

$$\mathbf{b}_A \times \mathbf{n}_A = b\hat{\mathbf{e}}_{1_A} \times \hat{\mathbf{e}}_{3_A} = -b\hat{\mathbf{e}}_{2_A} = (0, -b, 0)^T$$

The additional term of the generalized Euler equation is given by

$$(\vec{\mathbf{S}} \times \vec{\mathbf{a}}_A)_A = - \left(\frac{m_d^2}{m} \right) \left\{ \begin{array}{c} 2z\dot{z}\omega_1 + z^2\dot{\omega}_1 - z^2\omega_2\omega_3 \\ 2z\dot{z}\omega_2 + z^2\dot{\omega}_2 + z^2\omega_1\omega_3 \\ 0 \end{array} \right\}$$

Collecting all the terms, one gets the following system of ordinary differential equations,

$$\begin{aligned} J_x \dot{\omega}_1 + (J_z - J_y)\omega_2\omega_3 + m_d(1 - m_d/m)z^2\dot{\omega}_1 - m_d b z \dot{\omega}_3 + 2m_d(1 - m_d/m)z\dot{z}\omega_1 + \\ - m_d b z \omega_1 \omega_2 - m_d(1 - m_d/m)z^2\omega_2\omega_3 = 0 \end{aligned}$$

$$\begin{aligned} J_y \dot{\omega}_2 + (J_x - J_z)\omega_1\omega_3 + m_d(1 - m_d/m)z^2\dot{\omega}_2 - m_d b \ddot{z} + 2m_d(1 - m_d/m)z\dot{z}\omega_2 + \\ + m_d b z (\omega_1^2 - \omega_3^2) + m_d(1 - m_d/m)z^2\omega_1\omega_3 = 0 \end{aligned}$$

$$J_z \dot{\omega}_3 + (J_y - J_x)\omega_1\omega_2 - m_d b z \dot{\omega}_1 - 2m_d b \dot{z} \omega_1 + m_d b z \omega_2 \omega_3 = 0$$

As for the motion of the damper mass, it is

$$(1 - m_d/m)\ddot{z} - b\dot{\omega}_2 + b\omega_1\omega_3 - (1 - m_d/m)z(\omega_1^2 + \omega_2^2) + (c/m_d)\dot{z} + (k/m_d)z = 0$$

Equilibria and stability of a spinning satellite with axial damper

It is easy to show that a condition of spin about the z -axis with the damper mass in its rest position is an equilibrium for a rigid satellite equipped with a damper such that $\hat{\mathbf{n}} = \hat{\mathbf{e}}_3$. In the considered condition, it is $\boldsymbol{\omega}_B = (0, 0, \Omega)^T$ and $z = \dot{z} = 0$. Upon substitution of $\omega_1 = \omega_2 = 0$, $\omega_3 = \Omega$ in the equations of motion, it is immediate to see that all the acceleration terms, $\dot{\omega}_1$, $\dot{\omega}_2$, $\dot{\omega}_3$, and \ddot{z} vanish. Please note that this fact is independent of the relative size of the principal moment of inertia J_z with respect to the other ones, J_x and J_y . It is thus possible to state that spinning around any principal axis of inertia for the satellite with the damper in its rest condition is an equilibrium for the system.

In order to investigate the stability of this equilibria, it is possible to linearize the equations of motion in the neighborhood of such a spin condition. Letting $\omega_B = (\omega_1, \omega_2, \Omega + \omega_3)^T$ and assuming that $\omega_1, \omega_2, \omega_3 \ll \Omega$, $z \ll b$ and \dot{z} are first order perturbations, a set of linear ordinary differential equation that describe the evolution of the perturbation in the neighborhood of the nominal spin condition is obtained when higher order terms are neglected. The linearized form of the model of a spinning satellite with damper is

$$\begin{aligned} J_x \dot{\omega}_1 + (J_z - J_y) \Omega \omega_2 &= 0 \\ J_y \dot{\omega}_2 + (J_x - J_z) \Omega \omega_1 - m_d b \ddot{z} - m_d b \Omega^2 z &= 0 \\ J_z \dot{\omega}_3 &= 0 \\ m_d (1 - m_d/m) \ddot{z} - m_d b \dot{\omega}_2 + m_d b \Omega \omega_1 + c \dot{z} + k z &= 0 \end{aligned}$$

In order to simplify the above expression the following parameters can be defined:

$$\lambda_1 = \frac{J_z - J_y}{J_x} \Omega ; \quad \lambda_2 = \frac{J_x - J_z}{J_y} \Omega ; \quad \mu = m_d/m ; \quad p^2 = \frac{k}{m_d} ; \quad \beta = \frac{c}{m_d} ; \quad \zeta = \frac{z}{b} ; \quad \delta = \frac{m_d b^2}{J_y}$$

so that the linear system can be rewritten in the form

$$\begin{aligned} \dot{\omega}_1 + \lambda_1 \omega_2 &= 0 \\ \dot{\omega}_2 - \lambda_2 \omega_1 - \delta \ddot{\zeta} - \delta \Omega^2 \zeta &= 0 \\ (1 - \mu) \ddot{\zeta} - \dot{\omega}_2 + \Omega \omega_1 + \beta \dot{\zeta} + p^2 \zeta &= 0 \end{aligned}$$

where the third equation (relative to perturbations of the spin condition) is not included, as it is decoupled from the others.

Taking the Laplace transform \mathcal{L} of the time-varying states, such that $\mathcal{L}\{\omega_i(t)\} = \bar{\omega}_i(s)$ and $\mathcal{L}\{\zeta(t)\} = \bar{\zeta}(s)$, one gets the following transformed system:

$$\begin{aligned} s \bar{\omega}_1 + \lambda_1 \bar{\omega}_2 &= 0 \\ s \bar{\omega}_2 - \lambda_2 \bar{\omega}_1 - s^2 \delta \bar{\zeta} - \delta \Omega^2 \bar{\zeta} &= 0 \\ s^2 (1 - \mu) \bar{\zeta} - s \bar{\omega}_2 + \Omega \bar{\omega}_1 + s \beta \bar{\zeta} + p^2 \bar{\zeta} &= 0 \end{aligned}$$

which becomes, in matrix form

$$\begin{bmatrix} s & \lambda_1 & 0 \\ -\lambda_2 & s & -(s^2 + \Omega^2) \delta \\ \Omega & -s & s^2 (1 - \mu) + s \beta + p^2 \end{bmatrix} \begin{Bmatrix} \bar{\omega}_1 \\ \bar{\omega}_2 \\ \bar{\zeta} \end{Bmatrix} = \begin{Bmatrix} 0 \\ 0 \\ 0 \end{Bmatrix}$$

The characteristic equation

$$\begin{vmatrix} s & \lambda_1 & 0 \\ -\lambda_2 & s & -(s^2 + \Omega^2) \delta \\ \Omega & -s & s^2 (1 - \mu) + s \beta + p^2 \end{vmatrix} = 0$$

can be thus written in polynomial form as

$$\begin{aligned} (1 - \mu - \delta) s^4 + \beta s^3 + [p^2 - \delta \lambda_1 \Omega - \delta \Omega^2 + \lambda_1 \lambda_2 (1 - \mu)] s^2 + \\ + \lambda_1 \lambda_2 \beta s + (\lambda_1 \lambda_2 p^2 - \lambda_1 \delta \Omega^3) = 0 \end{aligned}$$

If the real part of all the roots of the characteristic polynomial is strictly negative, the satellite equipped with an axial damper is stable, when spinning around \hat{e}_3 .

Routh's criteria

Once the coefficients of the polynomial characteristic equation are known, nowadays classic numerical root finding techniques can be easily applied, using the particular set of satellite parameters of interest. The drawback of this approach is that it does not offer any physical insight into the influence of each parameter on the global stability properties of the system.

Routh's criteria for asymptotic stability can be easily applied, and when the system order is sufficiently low, it is possible to determine analytically the stability condition and, as a consequence, stability boundaries in the parameter space. Given the polynomial characteristic equation

$$a_n s^n + a_{n-1} s^{n-1} + \dots + a_2 s^2 + a_1 s + a_0 = 0$$

Routh's criteria states that a *necessary condition for stability* is that all the coefficients have the same sign. Assuming that the coefficient are normalized with respect to a_n , so that $a_n = 1$, the condition $a_0 > 0$ is the generalized static stability requirement.

In order to evaluate *necessary and sufficient condition for asymptotic stability*, it is necessary to build the Routhian matrix, which has the form

$$\begin{array}{cccc} a_n & a_{n-2} & a_{n-4} & \dots \\ a_{n-1} & a_{n-3} & a_{n-5} & \dots \\ b_{3,1} & b_{3,2} & b_{3,3} & \dots \\ b_{4,1} & b_{4,2} & b_{4,3} & \dots \end{array}$$

where the first two rows are build using the coefficients of the polynomial, while those of the following ones are evaluated as

$$b_{i,j} = \frac{b_{i-1,j} b_{i-2,j+1} - b_{i-2,j} b_{i-1,j+1}}{b_{i-1,j}}$$

The number of non zero elements of each row decreases of one unit as the row index i is increased by two, until the last two rows are reached such that only one element on each row is non-zero. The following row will be made entirely of zeroes.

The Routh's condition for asymptotic stability guarantees that the real part of all the roots of the characteristic equation are negative if and only if all the elements in the first column of the Routhian matrix are not null and have the same sign. If the polynomial equation is normalized with respect to a_n this condition requires that all the terms $b_{i,1}$ are positive, with $b_{1,1} = 1$ and $b_{2,1} = a_{n-1}$.

Routh's criterion for asymptotic stability fails when there is one zero term in the first column of the Routhian matrix. In such a case one or more of the roots of the polynomial has a zero real part and stability analysis with eigenvalues of the characteristic polynomial is inconclusive.

Conclusions of the stability analysis

Application of Routh's criteria to the present case, *i.e.* the spinning satellite with axial damper, brings to the following Routhian matrix:

$$\begin{array}{ccccc}
(1 - \mu - \delta) & [p^2 - \delta\lambda_1\Omega - \delta\Omega^2 + \lambda_1\lambda_2(1 - \mu)] & (\lambda_1\lambda_2p^2 - \lambda_1\delta\Omega^3) & 0 \\
\beta & \lambda_1\lambda_2\beta & 0 & 0 \\
(p^2 - \delta\Omega^2 - \lambda_1\delta\Omega + \delta\lambda_1\lambda_2) & (\lambda_1\lambda_2p^2 - \lambda_1\delta\Omega^3) & 0 & 0 \\
\frac{\delta\beta\lambda_1(\lambda_2 - \Omega)(\lambda_1\lambda_2 - \Omega^2)}{p^2 - \delta\Omega^2 - \lambda_1\delta\Omega + \delta\lambda_1\lambda_2} & 0 & 0 & 0 \\
\lambda_1(\lambda_2p^2 - \delta\Omega^3) & 0 & 0 & 0
\end{array}$$

Since $\beta > 0$ for all dissipative dampers, the conditions for asymptotic stability of the spin condition about the z -axis are

$$\begin{aligned}
1 - \mu - \delta &> 0 \\
p^2 - \delta(\Omega^2 + \lambda_1\Omega - \lambda_1\lambda_2) &> 0 \\
\delta\beta\lambda_1(\lambda_2 - \Omega)(\lambda_1\lambda_2 - \Omega^2) &> 0 \\
\lambda_1(\lambda_2p^2 - \delta\Omega^3) &> 0
\end{aligned}$$

Since usually $m_d \ll m$, so that $\mu \ll 1$ and $\delta \ll 1$, we can consider the limiting case $\mu \rightarrow 0$ and $\delta \rightarrow 0$, so that most of the inequalities become trivial. Taking into account that p^2 and β are strictly positive for a real damper, the only conditions left are

$$\begin{aligned}
\lambda_1(\lambda_2 - \Omega)(\lambda_1\lambda_2 - \Omega^2) &> 0 \\
\lambda_1\lambda_2 &> 0
\end{aligned}$$

Taking into account the definitions of λ_1 and λ_2 , the first inequality can be rewritten in the form

$$\Omega^4 J_z \left(\frac{J_z - J_x - J_y}{J_x J_y} \right)^2 (J_z - J_y) > 0$$

which is equivalent to the condition

$$J_z > J_y$$

As a consequence, because of the second condition, it must also be

$$J_z > J_x$$

so that only spinning about the axis of maximum inertia is a stable condition for a satellite equipped with a damper. It should be noted that the presence of the damper makes such a spin condition asymptotically stable.

A comment

The presence of a damper makes the spin condition around the principal axis of minimum inertia an unstable one, while for a perfectly rigid body it was shown that spinning around the axis on minimum inertia was locally stable, although in a weak form. At the same time, spinning around the axis of intermediate inertia remains unstable (which is little surprise, as far as dissipation was unlikely to affect an exponential instability), while spinning around the axis of maximum inertia acquires a stronger form of stability, as far

as dissipation will align in the long run the spin axis with the inertially fixed direction of the angular momentum vector.

These results are of general validity, whichever the source of the dissipation, so that the structure of the solutions in the $\omega_1 - \omega_1 - \omega_3$ space thus changes significantly with respect to the rigid-body case. In particular, the separatrices disappear, while the ellipses surrounding the pure spin condition around the axes of maximum and minimum inertia are substituted by spirals, converging onto the pure spin condition in the first case, diverging from it in the latter one.

2.4 Attitude manoeuvres of a spinning satellite

One of the major drawbacks of spin stabilisation, together with the inefficient power generation, lies in the complexity of the technique necessary for performing attitude manoeuvres, that is, changing the direction of the spin axis of the satellite in a controlled way. In order to rotate the spin axis of a spinning spacecraft, it is possible to exploit the precession rate induced by a properly sized nutation angle. This requires a variation of the angular momentum vector that can be obtained by applying a proper control torque to the spacecraft.

If we consider a thruster generating a force \vec{F} at position \vec{r} in the body frame centered in the center of mass O, the resulting moment acting on the satellite is

$$\vec{M} = \vec{r} \times \vec{F}$$

Given a firing time of Δt_{on} seconds, starting at t_0 , the overall change of angular momentum is equal to

$$\Delta \vec{h} = \int_{t_0}^{t_0 + \Delta t_{\text{on}}} (\vec{r} \times \vec{F}) dt.$$

If the firing time is sufficiently small with respect to the period of rotation of the spinning spacecraft $T_{\text{spin}} = 2\pi/\Omega$, it is possible to approximate $\Delta \vec{h}$ as

$$\Delta \vec{h} = (\vec{r} \times \vec{F}) \Delta t_{\text{on}}$$

The control torque is usually delivered by use of coupled pairs of thrusters, in such a way that a net torque is produced, with no force perturbing the orbit motion of the spacecraft. The torque pulse changes almost instantaneously the direction of the spacecraft's angular momentum vector, thus creating a nutation angle θ . At this point the spacecraft is no longer spinning around its symmetry axis, and a precession rate builds up, equal to

$$\dot{\Psi} = \frac{J_s}{J_t - J_s \cos \Theta} \frac{\dot{\Phi}}{\cos \Theta} = \frac{J_s}{J_t} \frac{\Omega}{\cos \Theta}$$

where $\Theta \equiv \theta$ is assumed.²

²It must be remembered that the direction of the precession motion depends on whether an oblate or a prolate body is considered. In the latter case, the instability of the spin condition around the axis of minimum inertia when dissipation is present must also be taken into account. Only if the dissipation rate is sufficiently small the manoeuvre technique is of practical interest. In this latter case, attitude manoeuvres are required not only for changing the direction of the spin axis for aligning sensors or antennas with a new target, but also for compensating long term effects of attitude perturbations on the spin condition.

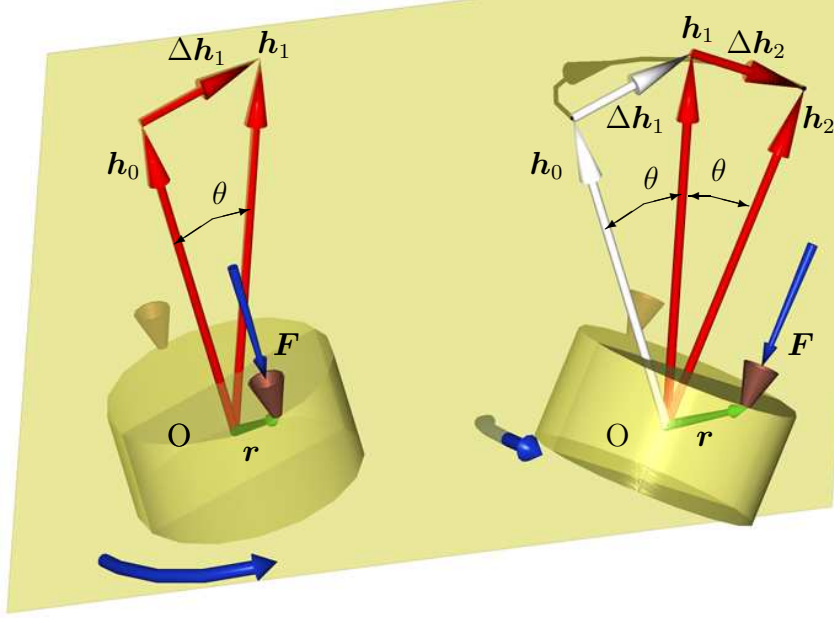


Figure 2.9: Changing the spin axis direction with nutation angle and precession rate.

Since the precession rate is constant, the precession angle will vary by

$$\Delta\Psi = \frac{J_s}{J_t} \frac{\Omega}{\cos\theta} (t - t_1)$$

where t_1 is the time of the first thruster impulse that starts the manoeuvre. After an interval equal to

$$T = \pi \frac{(J_t) \cos\theta}{J_s \dot{\Omega}}$$

the precession angle is varied by π rad, and the direction of the symmetry axis of the spinning satellite has changed of 2θ . If the firing time Δt_{on} is such that the resulting nutation angle is half of the desired variation of the spin axis direction and the thruster activation time t_0 is chosen in such a way that the resulting angular momentum increment lies in the manoeuvre plane (that is, the plane containing both the initial and final position of the satellite spin axis), then after T seconds the spin axis will be in the desired position, although moving at the coning speed $\dot{\Psi}$. At this point a second thruster firing is required to stop the precession and achieving again a pure spin condition about the new re-oriented axis.

From simple trigonometric consideration, it is easy to show that

$$||\Delta\mathbf{h}_1|| = ||\Delta\mathbf{h}_2|| = h_0 \tan\theta = J_s \Omega \tan\theta$$

where $h_0 = J_s \Omega$ is the magnitude of the initial angular momentum. But being also

$$||\Delta\mathbf{h}|| = M \Delta t$$

the required firing time for each pulse is equal to

$$\Delta t_{\text{on}} = \frac{J_s \Omega \tan\theta}{M}$$

If ℓ is the thruster moment arm (*i.e.* the distance between the thruster axis and the satellite centre of mass; in Fig. 2.9 this distance is equal to the radius of the spinning body) and only one thruster is employed, it is $M = F\ell$. In general at least two thrusters are activated in order to obtain a balanced control torque, as stated before, in which case it is $M = 2F\ell$

In order to estimate the amount of propellant necessary to perform the reorientation, it must be remembered that the specific impulse of an engine is given by

$$I_{sp} = \frac{F}{\Delta mg/\Delta t_{on}}$$

that is the thrust delivered divided by the weight of propellant burned in a unit time. The specific impulse is one of the most important characteristics of rocket engines of any size, and from its value it is possible to determine

$$\Delta m = \frac{F\Delta t_{on}}{gI_{sp}}$$

The total propellant mass required to rotate the spin axis of an angle equal to 2θ is

$$\Delta m_{tot} = 4 \frac{J_s \Omega \tan \theta}{g I_{sp} \ell}$$

if two thrusters are employed for delivering the control torque M .

For small reorientation angles it is $\tan \theta \approx \theta$, and the propellant consumption is roughly proportional to the reorientation angle itself. But as θ increases, the fuel consumption gets larger, so that it is more convenient to perform the overall reorientation in several smaller steps. Moreover, for a given I_{sp} , the pulse duration may become a not negligible fraction of the spin period, thus reducing the change in angular momentum. The drawback of a large reorientation performed in N steps is that the manoeuvre time is increased and the overall manoeuvre is usually less accurate.

Figure 2.10 shows the results for reorientation 2θ angles between 0 and 70 deg, for a satellite with $J_s = 20 \text{ kg m}^2$, $J_t = 15 \text{ kg m}^2$, spinning at $\Omega = 2 \text{ rad s}^{-1}$, that is controlled by pair of thrusters with a 1 m moment arm, which produce 10 N of thrust each, with a specific impulse $I_{sp} = 120 \text{ s}$.

The minimum pulse duration considered is 10 ms, that puts a limit on the resolution of the reorientation, the minimum manoeuvre angle being 0.573 deg. On the other side, a thruster firing time longer than one tenth of the spin period cannot be considered a “pulse”. This limits the maximum reorientation angle that can be achieved by a single nutation manoeuvre, that is 17.9 deg. A stricter requirement on the pulse duration will reduce the maximum available reorientation angle with a single manoeuvre. Using 2 steps, the propellant savings at low angles are negligible (less than 1%), but it is possible to achieve spin axis reorientation up to 35 deg. With 4 steps the maximum reorientation angle becomes as high as 71 deg. Of course, the manoeuvre duration will increase accordingly.

The correct timing of the thruster pulses is of very important in order to obtain an accurate reorientation. In this framework it should be noted that, unless a very particular case is dealt with, where the precession and the spin rate are in a rational ratio, the pair of thrusters used for starting the manoeuvre will not be in the correct position for delivering the required torque in the manoeuvre plane after half of the precession revolution. This means that two pairs of thrusters need to be activated for the second pulse, delivering a

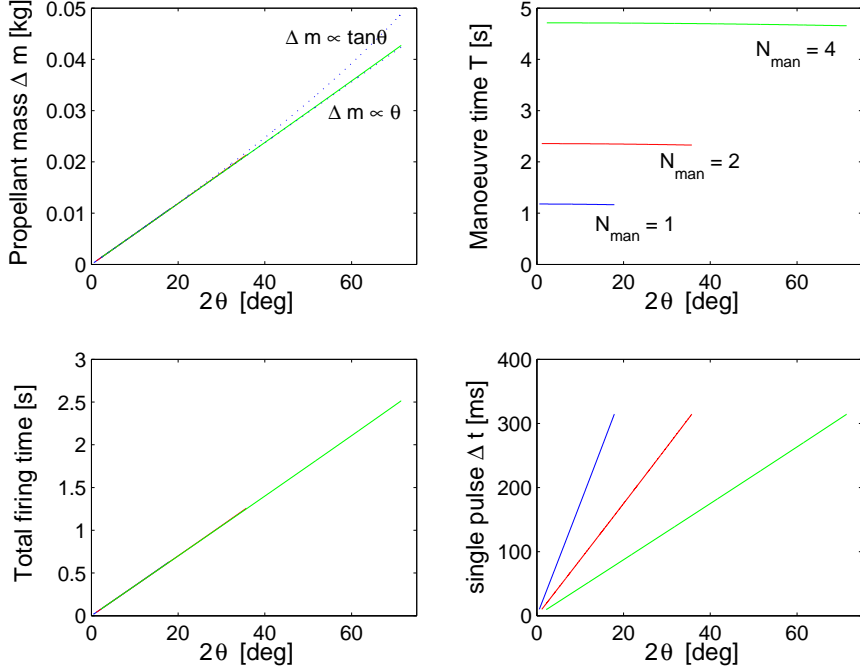


Figure 2.10: Spinning satellite manoeuvre: Fuel consumption (a), Total manoeuvre time (b), Total firing time (c), single pulse duration (d).

total net torque equal to the required one. As a consequence, the above description of the manoeuvre technique will provide an estimate of fuel consumption slightly optimistic and the overall complexity of the manoeuvre technique is, if possible, even higher in the actual implementation.

2.5 Gravity-gradient stabilization

Spin stabilization allows one to provide the satellite with gyroscopic stability, which can be made asymptotic, by a proper use of dissipative devices. At the same time, some significant disadvantages affects the operational use of spin stabilized satellites, that are

- the presence of only one inertially fixed direction along which to point the payload;
- the inefficient production of electric power, inasmuch as the entire surface of the satellite must be covered with photovoltaic cells, only half of which faces the sun during the spinning motion (with less than one fourth at an angle greater than 45 deg with respect to the direction of the sun rays);
- the complexity, limited accuracy and cost in terms of fuel of attitude maneuvers for reorientation of the spin axis.

A very interesting possibility for stabilizing an Earth facing satellite in low Earth orbit is to exploit the gravitational torque that acts on any rigid body of finite size. The differential gravitational acceleration across the satellite provides a small, but non negligible torque. Simply put, the side of the satellite closest to the Earth experiences a slightly greater gravitational acceleration than the opposite side. The resulting torque will tend to align the satellite with the local vertical direction. For some mission applications the gravity gradient torque provides a disturbance which must be countered. However, for

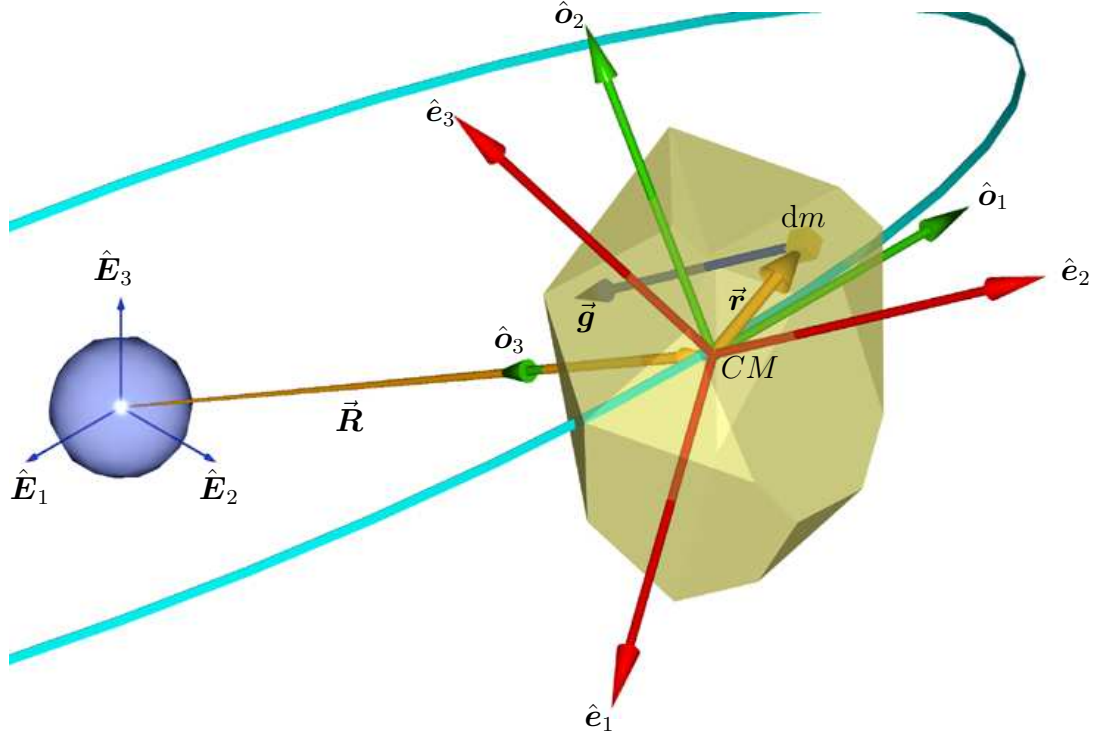


Figure 2.11: Gravity on a finite-size rigid body.

an Earth facing satellite, the gravity gradient provides a simple, low cost means of attitude stabilization, albeit rather inaccurate. The great advantage is that no fuel nor energy dissipation is required to maintain the desired attitude, if a proper stability condition is met.

2.5.1 Origin of the gravity-gradient torque

The gravity acceleration acting on a mass element \$dm\$ is given by

$$\vec{g} = -GM \frac{\vec{R} + \vec{r}}{\|\vec{R} + \vec{r}\|^3}$$

where \$G\$ is the universal gravity constant, \$M\$ is the mass of the primary body (the Earth, for an Earth orbiting satellite), while \$\vec{R}\$ and \$\vec{r}\$ are the position vectors of the center of mass of the satellite, CM, w.r.t. the center \$O\$ of the primary and the position vector of the mass element \$dm\$ w.r.t. CM, respectively. Letting \$\mu = GM\$, the total moment w.r.t. CM is given by

$$\begin{aligned} \vec{G} &= \int_{\mathcal{B}} (\vec{r} \times \vec{g}) dm \\ &= -\mu \int_{\mathcal{B}} \left[\frac{\vec{r} \times (\vec{R} + \vec{r})}{\|\vec{R} + \vec{r}\|^3} \right] dm \end{aligned}$$

Since \$\vec{r} \times \vec{r}\$ is zero, it is

$$\vec{G} = -\mu \int_{\mathcal{B}} \left(\frac{\vec{r} \times \vec{R}}{\|\vec{R} + \vec{r}\|^3} \right) dm$$

As a first observation, it is possible to note that $\vec{G} \cdot \vec{R} = 0$, *i.e.* the gravity torque around the local vertical is always zero. In the above expression, it is possible to write

$$\|\vec{R} + \vec{r}\|^{-3} = \left[(\vec{R} + \vec{r}) \cdot (\vec{R} + \vec{r}) \right]^{-3/2} = \left[R^2 + 2\vec{r} \cdot \vec{R} + r^2 \right]^{-3/2}$$

where r and R are the magnitude of \vec{r} and \vec{R} , respectively. The latter expression can be rewritten as

$$\|\vec{R} + \vec{r}\|^{-3} = R^{-3} \left(1 + \frac{2}{R^2} \vec{r} \cdot \vec{R} + \frac{r^2}{R^2} \right)^{-3/2}$$

Being $r \ll R$, the third term inside the parentheses can be neglected, and the second one is a first order perturbation compared to 1. Moreover, we can expand a term like $(1 + \varepsilon)^n$ in the neighbourhood of $\varepsilon = 0$ as

$$(1 + \varepsilon)^n = 1 + n\varepsilon + \mathcal{O}(\varepsilon^2)$$

that in the present case gives

$$R^{-3} \left(1 + \frac{2}{R^2} \vec{r} \cdot \vec{R} + \frac{r^2}{R^2} \right)^{-3/2} \approx R^{-3} \left(1 - 3 \frac{\vec{r} \cdot \vec{R}}{R^2} \right)$$

Using this latter expression in the definition of the gravity torque, one gets

$$\begin{aligned} \vec{G} &= -\frac{\mu}{R^3} \int_B \left[\left(1 - 3 \frac{\vec{r} \cdot \vec{R}}{R^2} \right) (\vec{r} \times \vec{R}) \right] dm \\ &= -\frac{\mu}{R^3} \left(\int_B \vec{r} dm \right) \times \vec{R} + \frac{3\mu}{R^5} \left[\int_B (\vec{r} \cdot \vec{R}) \vec{r} dm \right] \times \vec{R} \end{aligned}$$

The first term is zero from the definition of center of mass. Remembering the definition of *dyadic*,³ the second term can be rewritten as

$$\vec{G} = \frac{3\mu}{R^5} \left[\left(\int_B \vec{r} \vec{r} dm \right) \vec{R} \right] \times \vec{R}$$

Remembering that the inertia tensor can be written as

$$\mathbf{I} = \int_B (r^2 \mathbf{1} - \vec{r} \vec{r}) dm$$

and noting that

$$\left[\left(\int_B r^2 \mathbf{1} dm \right) \vec{R} \right] \times \vec{R} = 0$$

³The dyadic $\vec{x}\vec{y}$ is a tensor such that

$$(\vec{x}\vec{y})\vec{z} = (\vec{y} \cdot \vec{z})\vec{x}$$

Expressing the vector components in a frame \mathcal{F}_F , it is

$$(\vec{x}\vec{y})_F = \mathbf{x}_F \mathbf{y}_F^T$$

it is possible to write the gravity gradient torque as

$$\vec{G} = \frac{3\mu}{R^3} \hat{\mathbf{o}}_3 \times (\mathbf{I} \hat{\mathbf{o}}_3)$$

where $\hat{\mathbf{o}}_3 = -\vec{\mathbf{R}}/R$ is the unit vector along the local vertical passing through the satellite center of mass. Since the orbit rate is $\omega_0 = \sqrt{\mu/R^3}$, it is possible to rewrite the above expression as

$$\vec{G} = 3\omega_0^2 \hat{\mathbf{o}}_3 \times (\mathbf{I} \hat{\mathbf{o}}_3)$$

2.5.2 Equilibria of a rigid body under GG torque

The equation of motion of a satellite under the action of the gravity-gradient torque can thus be written as

$$\frac{d\vec{h}}{dt} - 3\omega_0^2 \hat{\mathbf{o}}_3 \times (\mathbf{I} \hat{\mathbf{o}}_3) = 0$$

It can be observed that the gravity gradient torque is zero whenever

$$\hat{\mathbf{o}}_3 \times (\mathbf{I} \hat{\mathbf{o}}_3) = 0$$

which requires that one of the principal inertia axes is oriented along the local vertical $\hat{\mathbf{o}}_3$. Such a condition can be maintained on a circular orbit if the satellite is purely spinning about an axis perpendicular to the orbit plane at an angular velocity which is equal to the orbit rate, so that $\vec{\omega} = -\omega_0 \hat{\mathbf{o}}_3$. In such a case a relative equilibrium with respect to the orbit frame is obtained, with the satellite principal axes aligned with the orbit frame. Expressing the equation in terms of body frame components gives the following equation of motion

$$\mathbf{I}\dot{\omega}_B + \boldsymbol{\omega}_B \times (\mathbf{I}\boldsymbol{\omega}_B) - 3\omega_0^2 \mathbf{o}_{3_B} \times (\mathbf{I}\mathbf{o}_{3_B}) = 0$$

If the attitude of the satellite is expressed in terms of Bryan angles (roll, pitch and yaw) with respect to the orbit frame $\mathcal{F}_O = \{\hat{\mathbf{o}}_1; \hat{\mathbf{o}}_2; \hat{\mathbf{o}}_3\}$, the body frame components of $\hat{\mathbf{o}}_3$ are given by the third column of the matrix \mathbf{L}_{BO} , *i.e.*

$$\mathbf{o}_{3_B} = (-\sin \theta, \cos \theta \sin \phi, \cos \theta \cos \phi)^T$$

which, assuming that all the angles remain “small”, becomes

$$\mathbf{o}_{3_B} = (-\theta, \phi, 1)^T$$

The (absolute) angular velocity components are

$$\boldsymbol{\omega}_B = \boldsymbol{\omega}_B^r - \omega_0 \mathbf{o}_{2_B}$$

where $\boldsymbol{\omega}_B^r = (\omega_1, \omega_2, \omega_3)^T$ is the angular velocity of the satellite with respect to \mathcal{F}_O and \mathbf{o}_{2_B} is given by

$$\mathbf{o}_{2_B} = (\psi, 1, -\phi)^T$$

for small perturbation. As a result, angular velocity components in body frame can be expressed as

$$\boldsymbol{\omega}_B = (\dot{\phi} - \omega_0\psi, \dot{\vartheta} - \omega_0, \dot{\psi} - \omega_0\phi)^T$$

Substituting this perturbation expressions for ω_B and \mathbf{o}_{3B} in the equation of motion and neglecting second order terms, one gets

$$\begin{aligned} J_x \ddot{\phi} - (J_z + J_x - J_y) \omega_0 \dot{\psi} + 4(J_y - J_z) \omega_0^2 \phi &= 0 \\ J_y \ddot{\vartheta} + 3(J_x - J_z) \omega_0^2 \vartheta &= 0 \\ J_z \ddot{\psi} + (J_z + J_x - J_y) \omega_0 \dot{\phi} + (J_y - J_x) \omega_0^2 \psi &= 0 \end{aligned}$$

First of all, it can be noted how the pitch motion is decoupled from the roll–yaw motion. The equation of motion of pitch (harmonic) oscillation can be rewritten in the form

$$\ddot{\vartheta} - a\vartheta = 0$$

where the quantity

$$a = 3 \frac{J_z - J_x}{J_y} \omega_0^2$$

must be negative, in order to have finite size oscillations, the amplitude of which depends on the initial conditions $\vartheta(t = 0)$ and $\dot{\vartheta}(t = 0)$. The stability condition for pitch motion simply requires that

$$J_z < J_x$$

If this condition is not met, the coefficient a becomes positive and the characteristic equation $\lambda^2 = a$ has two real solutions, $\lambda = \pm\sqrt{a}$, so that the pitch angle will exponentially grow after a perturbation from the equilibrium condition $\vartheta = \dot{\vartheta} = 0$.

As for the roll–yaw equation, taking the Laplace transform, we have, in matrix form, the following equation

$$\begin{bmatrix} J_x s^2 + 4(J_y - J_z) \omega_0^2 & -(J_z + J_x - J_y) \omega_0 s \\ (J_z + J_x - J_y) \omega_0 s & J_z s^2 + (J_y - J_x) \omega_0^2 \end{bmatrix} \begin{Bmatrix} \bar{\phi}(s) \\ \bar{\psi}(s) \end{Bmatrix} = \begin{Bmatrix} 0 \\ 0 \end{Bmatrix}$$

so that the characteristic polynomial $p(s) = \det(\mathbf{A})$ can be written in the form

$$p(s) = b_0 s^4 + b_1 s^2 + b_2$$

where

$$\begin{aligned} b_0 &= J_x J_z \\ b_1 &= (J_y^2 - 3J_z^2 - J_x J_y + 2J_y J_z + 2J_x J_z) \omega_0^2 \\ b_2 &= 4(J_y - J_z)(J_y - J_x) \omega_0^4 \end{aligned}$$

Given the structure of the polynomial coefficients, it is not possible to apply Routh's criteria, as the coefficient of the third order term, which appears in the first column of the Routhian matrix, is zero, thus making the analysis inconclusive. But it is still possible to derive some conclusions. Let

$$x_{1,2} = \frac{-b_1 \pm \sqrt{b_1^2 - 4b_0 b_2}}{2b_0}$$

denote the roots of the equation $b_0 x^2 + b_1 x + b_2 = 0$. If $x_{1,2}$ is a pair of complex conjugate roots $x = \alpha \pm i\beta$, the poles of the system can be written as $s_{1,2} = \pm\sqrt{\alpha - i\beta} = \pm a \pm ib$, and $s_{3,4} = \pm\sqrt{\alpha + i\beta} = \pm a \mp ib$. In both cases, two of the resulting roots of the characteristic equation have a positive real part. So, the discriminant of the characteristic equation

$$\Delta = b_1^2 - 4b_0 b_2$$

must be positive for stability, so that both solutions x_1 and x_2 are real. Under this condition, if one (or both) of the solutions x_i is (are) also positive, one (or two) pole(s) of the system is (are) real and positive and the equilibrium is unstable. As b_0 is the product of two positive quantities, $x_{1,2}$ are negative only if $-b_1 \pm \sqrt{b_1^2 - 4b_0b_2} < 0$. If b_1 is negative, this condition cannot be satisfied, and at least one of the solutions x_i will be positive. If $b_1 > 0$, both solutions will be negative if and only if b_2 is also positive, in which case $\Delta < b_1^2$. Summarizing, the set of stability conditions can be written in the following form:

$$\begin{aligned} b_1 &> 0 \\ b_2 &> 0 \\ \Delta = b_1^2 - 4b_0b_2 &> 0 \end{aligned}$$

Letting

$$k_1 = \frac{J_y - J_z}{J_x}; \quad k_3 = \frac{J_y - J_x}{J_z}$$

it is possible to write the stability condition as a function of the two inertia parameters k_1 and k_3 only, as

$$\begin{aligned} b_1 &\propto 1 + 3k_1 + k_1k_3 > 0 \\ b_2 &\propto k_1k_3 > 0 \\ \Delta &\propto (1 + 3k_1 + k_1k_3)^2 - 16k_1k_3 > 0 \end{aligned}$$

The requirement for pitch stability, $J_x > J_z$ can be rewritten as $k_1 > k_3$.

If all the four conditions stated above are satisfied, the linearized equation of motion will have only purely imaginary eigenvalues, which means that the small perturbations will remain bounded, in the linear model. Exponential divergence is thus ruled out, but the stability analysis of the system is inconclusive, as far as the original nonlinear system is concerned. As a matter of fact, the neglected nonlinear terms does not harm stability and oscillation in roll, pitch and yaw, although coupled, remain bounded also for the nonlinear system, which is rather reasonable, as far as the gravity field in conservative and, as such, does not change the total energy of the system during its evolution. The resulting stability region, where all the four stability conditions are satisfied, is plotted in Fig. 2.12.

2.5.3 Pitch motion

If one considers purely pitching motion ($\omega_1 = \omega_3 = 0$, $\psi = \phi = 0$), only the second component of Euler's equation is required, with $\omega_2 = \dot{\theta} - \omega_0$. By taking into account the expressions of $\hat{\mathbf{o}}_{2B} = \hat{\mathbf{e}}_2 = (0, 1, 0)^T$ and $\hat{\mathbf{o}}_{3B} = (-\sin \theta, 0, \cos \theta)^T$, the single-axis equation of motion achieves the simple form

$$\ddot{\theta} + 3\omega_0^2 \frac{J_x - J_z}{J_y} \cos \theta \sin \theta = 0$$

There are two equilibrium solutions, for $\theta = 0$ and $\theta = \pi/2$, the stability of which is determined by the sign of the term $J_x - J_z$. It was already stated previously that equilibrium under the action of the gravity-gradient torque requires that the principal axes of inertia are aligned with the orbit frame. Clearly, a rotation of 90 deg around the pitch axis changes the alignment, leaving the three principal axes parallel to different orbit axes.

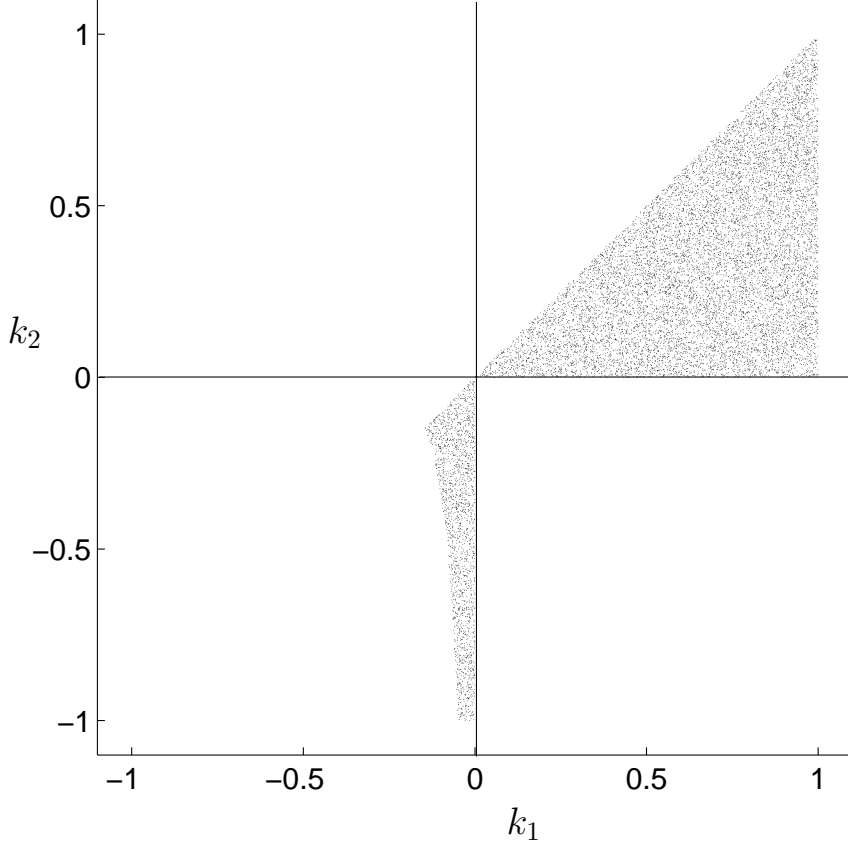


Figure 2.12: Stability region of the Earth–pointing attitude for a rigid satellite under gravity gradient torque.

For small perturbations about the local vertical – local horizontal reference frame it is $\sin \theta \approx \theta$ and $\cos \theta \approx 1$, and we get the second order linear equation of motion

$$\ddot{\theta}_3 + \left(3\omega_0^2 \frac{J_x - J_z}{J_y} \right) \theta = 0$$

which, of course, matches exactly the second equatoin in the linearized form.

If $J_x > J_z$ the term $3\omega_0^2(J_x - J_z)/J_y$ is positive and we can write

$$\lambda^2 = 3\omega_0^2 \frac{J_x - J_z}{J_y}$$

The equation of motion becomes

$$\ddot{\theta}_3 + \lambda^2 \theta = 0$$

the solution of which is given by

$$\theta(t) = \alpha_1 \cos(\lambda t) + \alpha_2 \sin(\lambda t)$$

where the coefficient α_1 and α_2 can be determined from the initial conditions. The satellite is thus stable and oscillates in the neighborhood of the condition $\theta = 0$ with a period equal to

$$T = \frac{2\pi}{\lambda} = \frac{2\pi}{\omega_0 \sqrt{3}} \sqrt{\frac{J_y}{J_x - J_z}}$$

If on the converse $J_x < J_z$, it is $3\omega_0^2(J_x - J_z)/J_y < 0$, and letting

$$\mu^2 = 3\omega_0^2 \frac{J_z - J_x}{J_y}$$

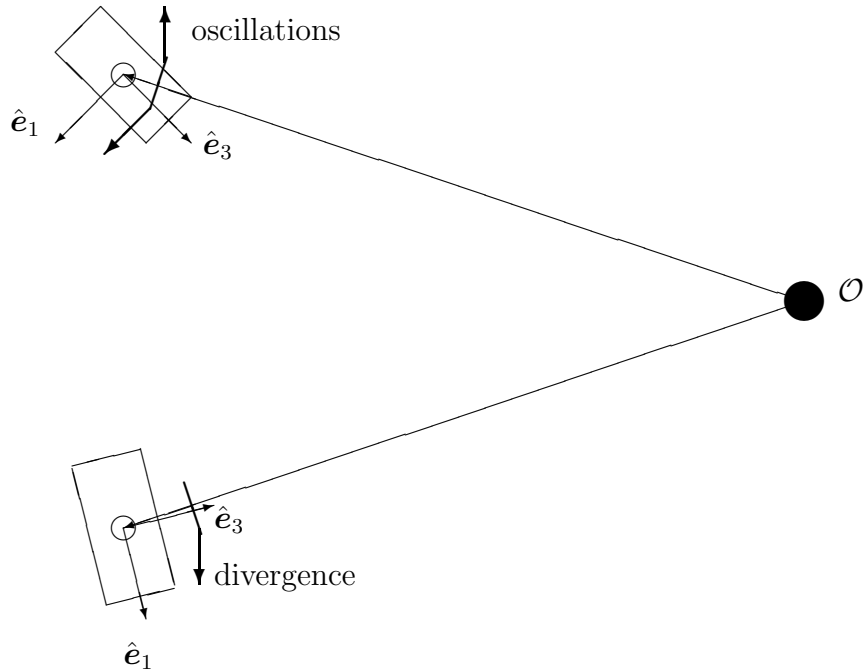


Figure 2.13: Stable and unstable equilibria around the pitch axis under the action of gravity-gradient torque.

the equation of motion can be rewritten as

$$\ddot{\theta} - \mu^2\theta = 0$$

The evolution of the pitch angle with time is thus expressed by

$$\theta(t) = \alpha_1 \exp(-\mu t) + \alpha_2 \exp(\mu t)$$

which is clearly unstable, because of the presence of a divergent exponential term. Because of such an instability, the satellite will rotate away from the neighborhood of the initial condition $\theta \approx 0$, and will acquire a periodic motion around the other equilibrium solution, for $\theta = \pi/2$. In this case. It is left to the reader as an exercise to demonstrate that, if $J_x < J_z$, the equilibrium solution for $\theta = \pi/2$ is stable.

As an example of the resulting motion, Fig. 2.14 shows the behaviour of the Space Shuttle ($\mathbf{I} = \text{diag}(1.29, 9.68, 10.01)10^6 \text{ kg m}^2$) on a low orbit with a period of 1 hour and 35 minutes. The first simulation is performed starting from an Earth pointing attitude ($\alpha = 10 \text{ deg}$), that is the nose of the Shuttle faces the Earth, with a perturbation from the vertical of 10 deg. The resulting motion is confined and the angular velocity is less than 0.015 deg s^{-1} . Internal dissipation (modeled as a term proportional to $\dot{\theta}$, with a damping constant $C = 1.5 \cdot 10^{-6} \text{ s}^{-1}$) damps very slowly the oscillation in the neighbourhood of the local vertical.

If on the converse, the motion is started near the second equilibrium condition, for $\alpha = 90 \text{ deg}$ (that is the nose of the Shuttle points the direction of the orbital velocity), the resulting motion is unstable and large amplitude oscillation will build up. From the simulation it can be seen how the vehicle will reverse its attitude, and will oscillate around the equilibrium at $\alpha = -90 \text{ deg}$, with the nose pointing towards the external space. It should also be noted how the effect of the nonlinear term in $\sin \theta \cos \theta$ in the gravity-gradient torque affects the oscillation frequency, when the amplitude is large. In the last two plots, the stable motion of the first case is reported as a comparison.

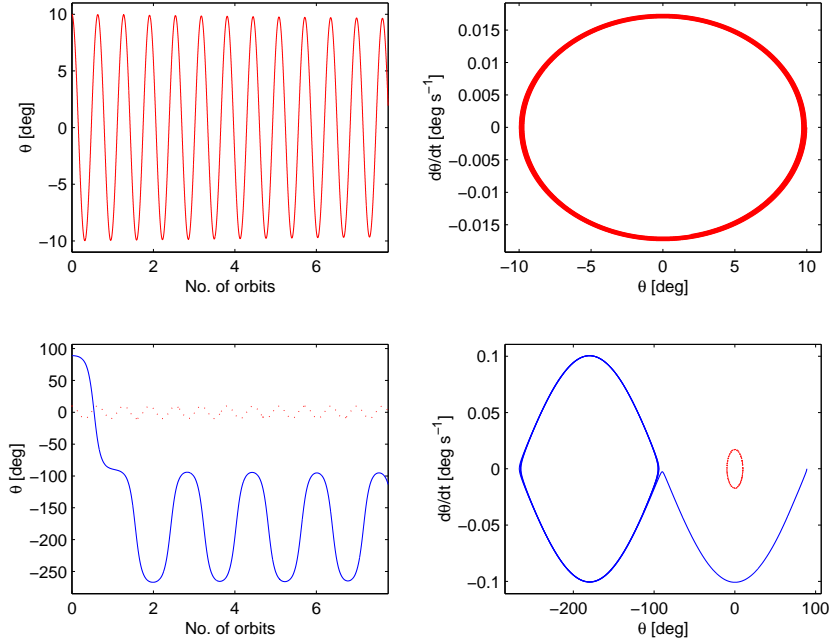


Figure 2.14: Stable and unstable motion of the Space Shuttle under gravity-gradient torque.

2.6 Dual-spin satellites

The presence of only one single inertially fixed direction on board of gyroscopically stabilized satellites greatly limits their use, as far as it is possible to mount a sensor payload or a communication antenna only along that direction. Moreover, maneuvering the satellite in order to reorient the spin axis is both difficult and expensive in terms of fuel consumption, the required propellant being proportional to the amount of angular momentum stored in the spinning satellite.

In order to overcome this negative features, an alternative satellite configuration was proposed and used in the past, where the payload and the communication hardware is mounted on a platform \mathcal{P} which has a relative rotational degree of freedom with respect to the spinning part of the satellite, the rotor \mathcal{R} . During orbit injection the two elements are locked and the satellite behaves like a standard rigid body. After the operational orbit is reached, the spin-up motor accelerates the rotor, with respect to the platform, in order to transfer on the rotor the entire vehicle angular momentum, thus despining the platform. The de-spin maneuver is ended when the platform is fixed in space, while the rotor provides gyroscopic stability to the entire vehicle. The main advantage of such a solution is that, pivoting the payload mounted on the platform allows aiming it in any direction in space, with great flexibility, without changing the direction of the rotor spin axis.

From the configuration point of view, the first dual-spin satellites were made of a large rotor, containing most of the satellite equipment, with solar cells mounted on the surface of the rotor, the configuration of which resembled that of a standard (for that time) spinning satellite. A small platform was attached to it, as represented in Fig. 2.15, where only antennas and sensors were located. Later on, the platform became larger, as in the Intelsat IV satellite, depicted in Fig. 2.16. This was the first prolate dual spin satellite, where the platform represents approximately half of the satellite total mass. In

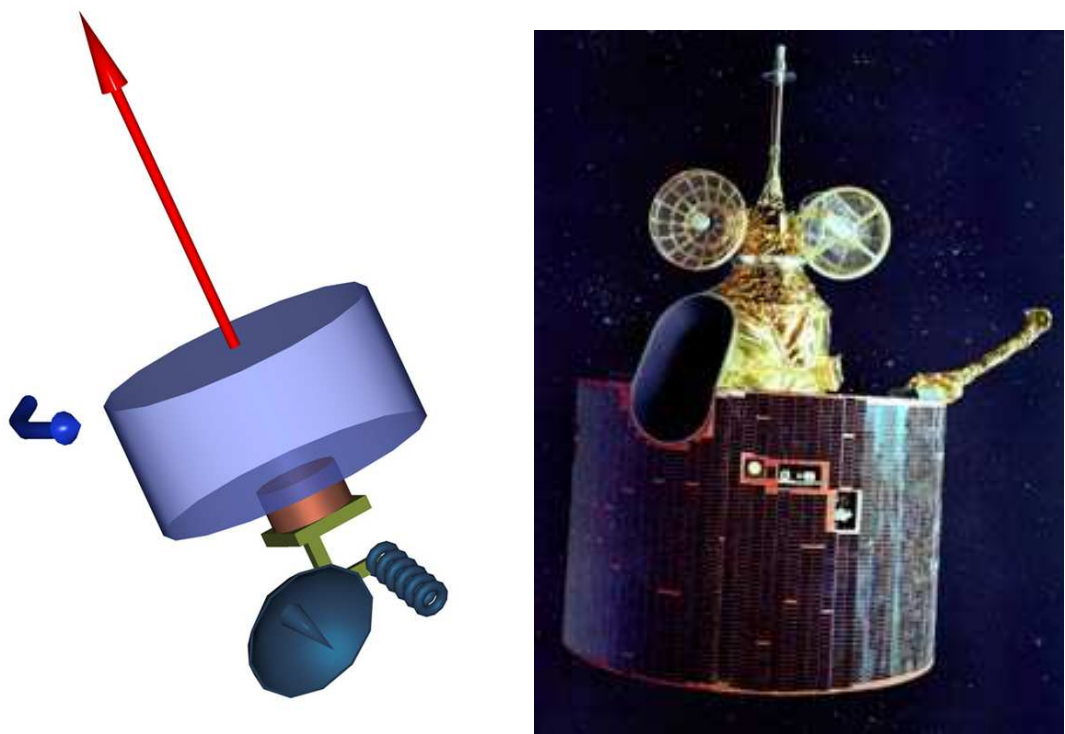


Figure 2.15: Dual spin satellite: configuration with large rotor (e.g. GOES-7 satellite).

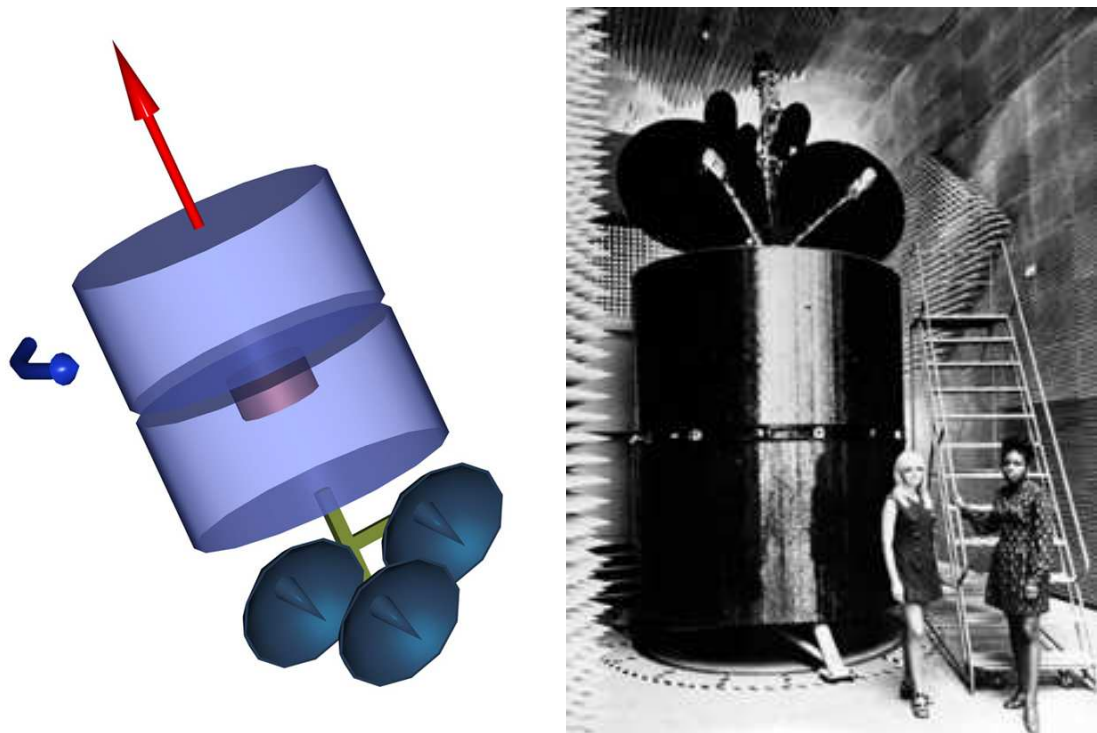


Figure 2.16: Dual spin satellite: configuration with equivalent rotor and platform (e.g. Intelsat IV satellite).

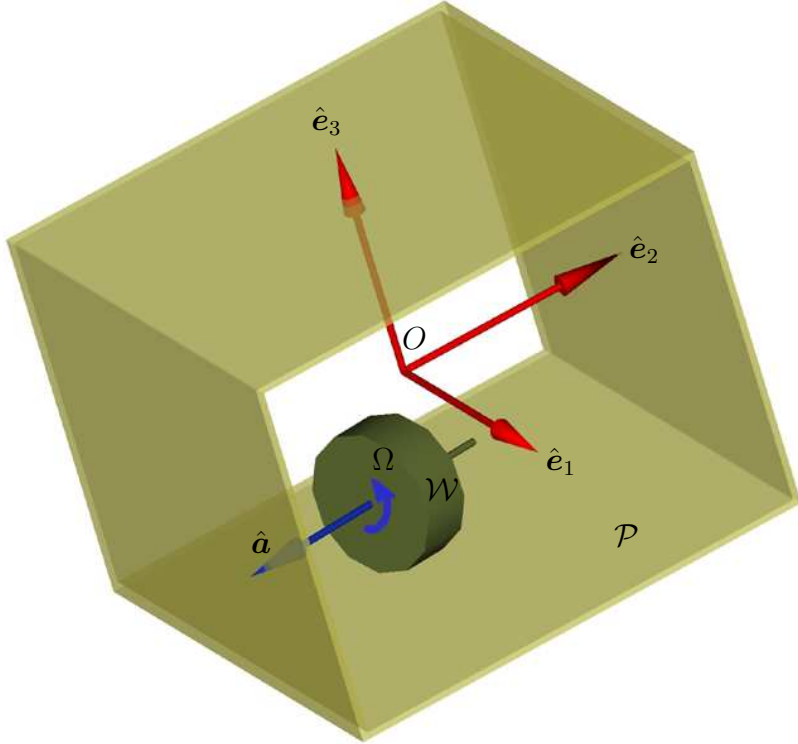


Figure 2.17: Sketch of a satellite equipped with a momentum wheel.

more recent times, the rotor was substituted by a momentum wheel, which is a small (and light) wheel spinning at a very high speed, placed inside the platform. In this latter case, the satellite is referred to as a momentum–bias satellite.

The mathematical model that will be derived in the next section is not affected by the relative size of platform and rotor. In this framework, both configurations (the dual–spinner, with a large rotor attached outside of the platform, and the momentum bias satellite, with a small spin–wheel inside the spacecraft bus) can be referred to as gyrostats. The presence of a relative rotational degree of freedom between the platform and the rotor (or spin–wheel) of the gyrostat makes it necessary to derive a new formulation for the angular momentum balance, since the body, featuring a rotating element, is no longer rigid.

2.6.1 Mathematical model of a gyrostat

Figure 2.17 shows the generic arrangement of a momentum wheel \mathcal{W} spinning about the spin axis $\hat{\mathbf{a}}$ at an angular rate Ω with respect to the satellite platform \mathcal{P} . The mathematical model is derived under the assumption that both the platform and the wheel are perfectly rigid. Moreover, a perfectly balanced and axi–symmetric wheel is assumed, the centre of mass of which lies on the spin axis. As a result, the presence of a relative degree of freedom between \mathcal{W} and \mathcal{P} does not affect the mass distribution of the spacecraft, which is independent of the angular displacement of \mathcal{W} about $\hat{\mathbf{a}}$. For this reason it is still possible to define a body frame \mathcal{F}_B , fixed with respect to the platform, the inertia tensor \mathbf{I} of the gyrostat $\mathcal{P} + \mathcal{W}$ being constant in \mathcal{F}_B as for a standard rigid body. This means that \mathbf{I} represents the total moment of inertia of the gyrostat, including the wheel.

Angular momentum formulation

If the wheel is locked to the platform, the angular momentum is given (as usual) by $\vec{h} = \mathbf{I}\vec{\omega}$, but if the wheel is spinning, than the overall angular momentum features a second term,

$$\vec{h} = \mathbf{I}\vec{\omega} + I_s\Omega\hat{\mathbf{a}}$$

where, letting I_s be the moment of inertia of \mathcal{W} about $\hat{\mathbf{a}}$, the quantity $h_r = I_s\Omega$ is the relative angular momentum. The absolute angular momentum stored in the spinning rotor

$$h_a = h_r + I_s\hat{\mathbf{a}} \cdot \vec{\omega}$$

is made up of two contributions: (i) the relative angular momentum due to the spin motion with respect to \mathcal{P} , and (ii) the angular momentum related to the motion of the platform. Writing the components in body frame, it is

$$\begin{aligned} \mathbf{h}_B &= \mathbf{I}\boldsymbol{\omega}_B + I_s\Omega\mathbf{a}_B \\ h_a &= I_s(\Omega + \mathbf{a}_B^T\boldsymbol{\omega}_B) \end{aligned}$$

The equation of motion of the gyrostat can be written in terms of evolution of the angular momentum vector as

$$\begin{aligned} \dot{\mathbf{h}}_B &= -\boldsymbol{\omega}_B \times \mathbf{h}_B + \mathbf{M}_B \\ \dot{h}_a &= g_a \end{aligned}$$

where \mathbf{M}_B is the external torque acting on the satellite, while g_a is the torque applied by the de-spin engine to the rotor. It should be noted how g_a , which is an internal torque, does not appear in the equation of the time evolution of the overall angular momentum. Nonetheless its effects on the overall dynamics are significant.

Also, the presence of the additional rotational degree of freedom increases the order of the system of first order nonlinear differential equations with respect to the rigid-body case, from 3 to 4 (three components for the total angular momentum plus the absolute wheel angular momentum about the spin axis). In order to integrate this fourth-order system and to evaluate the Euler angle rates, it is necessary to determine the angular velocity $\boldsymbol{\omega}_B$. Integrating the Euler angle rate equation (or the quaternion evolution equation), one gets the time evolution of satellite attitude.

The kinematic problem for the attitude of the satellite is solved expressing $\boldsymbol{\omega}_B$ as a function of the total and wheel angular momentum, that is

$$\boldsymbol{\omega}_B = \mathbf{I}^{-1}(\mathbf{h}_B - I_s\Omega\mathbf{a}_B)$$

The value of $\boldsymbol{\omega}_B$ thus depends on both \mathbf{h}_B and Ω . The rotor angular speed can be expressed as

$$\Omega = h_a/I_s - \mathbf{a}_B^T\boldsymbol{\omega}_B$$

where $\boldsymbol{\omega}_B$ appears, so that the two equations must be solved simultaneously, but this can be done easily, since the two equations are linear in the angular velocity components. If one assumes a set of principal axes of inertia, such that $\mathbf{I} = \text{diag}(J_x, J_y, J_z)$, the resulting linear system is given by

$$\begin{bmatrix} J_x & 0 & 0 & I_s a_1 \\ 0 & J_y & 0 & I_s a_2 \\ 0 & 0 & J_z & I_s a_3 \\ I_s a_1 & I_s a_2 & I_s a_3 & I_s \end{bmatrix} \begin{pmatrix} \omega_1 \\ \omega_2 \\ \omega_3 \\ \Omega \end{pmatrix} = \begin{pmatrix} h_1 \\ h_2 \\ h_3 \\ h_a \end{pmatrix}$$

Note that the 4×4 matrix with the moments of inertia must be inverted only once.

Angular velocity formulation

An alternative formulation of the equations of motion is also available, where gyrostat dynamics is expressed directly in terms of the angular velocity components and rotor spin rate. In this case, the angular momentum vector is written as

$$\begin{aligned}\mathbf{h}_B &= \mathbf{I}\boldsymbol{\omega}_B + (h_a - I_s\mathbf{a}_B^T\boldsymbol{\omega}_B)\mathbf{a}_B \\ &= (\mathbf{I} - I_s\mathbf{a}_B\mathbf{a}_B^T)\boldsymbol{\omega}_B + h_a\mathbf{a}_B\end{aligned}$$

The time derivative of the angular momentum vector components are thus expressed as

$$\dot{\mathbf{h}}_B = (\mathbf{I} - I_s\mathbf{a}_B\mathbf{a}_B^T)\dot{\boldsymbol{\omega}}_B + g_a\mathbf{a}_B$$

At the same time it is

$$\dot{h}_a = g_a = I_s(\dot{\Omega} + \mathbf{a}_B^T\dot{\boldsymbol{\omega}}_B)$$

so that, upon substitution of $\dot{\mathbf{h}}_B$ and \dot{h}_a into the angular momentum formulation, the equations of motion of the gyrostat become

$$\begin{aligned}\dot{\boldsymbol{\omega}}_B &= \tilde{\mathbf{I}}^{-1}[\mathbf{M}_B - \boldsymbol{\omega}_B \times (\mathbf{I}\boldsymbol{\omega}_B + I_s\Omega\mathbf{a}_B) - g_a\mathbf{a}_B] \\ \dot{\Omega} &= g_a/I_s - \mathbf{a}_B^T\dot{\boldsymbol{\omega}}_B\end{aligned}$$

where $\tilde{\mathbf{I}} = (\mathbf{I} - I_s\mathbf{a}_B\mathbf{a}_B^T)$ is the pseudo-inertia tensor. These equations of motion can be used for describing the gyrostat spin-up dynamics, during platform de-spin, that is, a spin axis torque g_a is applied until the platform angular velocity drops to zero. The knowledge of $\boldsymbol{\omega}_B$ allows for a direct evaluation of Euler angle or quaternion rates.

2.6.2 Simplified models

The Kelvin gyrostat

In many applications, especially once the de-spin manoeuvre is completed, it is possible to assume that the rotor relative spin rate remains constant, under the action of a control system that drives the motor torque in order to compensate for possible fluctuations induced by perturbations.

If one assumes that the angular speed of the rotor remains exactly constant, the system loses one degree of freedom, as $\Omega(t) = \text{const}$ and the associated dynamics can be neglected. In this case the so-called Kelvin gyrostat is obtained. The variable $h_r = I_s\Omega$ becomes a system parameter and the platform equation of motion decouples from rotor spin dynamics. In such a case, it is

$$\mathbf{I}\dot{\boldsymbol{\omega}}_B = -\boldsymbol{\omega}_B \times (\mathbf{I}\boldsymbol{\omega}_B + h_r\mathbf{a}_B) + \mathbf{M}_B$$

In order to keep Ω constant (that is, $\dot{\Omega} = 0$), it is necessary to apply a certain spin torque to the rotor, which, from the equation of motion of rotor spin dynamics can be evaluated as

$$g_a = I_s\mathbf{a}_B^T\dot{\boldsymbol{\omega}}_B$$

In real applications it is not possible to keep the rotor speed exactly constant and a simple feed-back loop is employed for determining the required spin torque. A tachometer is mounted on the wheel shaft, which measures the actual rotor spin rate Ω . The error

with respect to the nominal (desired) rotor speed Ω_{des} is the input for the rpm regulator. As an example, the spin torque can be set equal to

$$g_a = K(\Omega_{\text{des}} - \Omega)$$

where K is the gain of the rotor control system. In this way the rotor is accelerated ($g_a > 0$) whenever the angular speed is lower than the prescribed one, and decelerated when $\Omega > \Omega_{\text{des}}$. Of course, if the spin wheel dynamics is modeled including this simple control scheme, it is no longer possible to treat Ω as a constant in the platform angular velocity equations, and the full system equations must be accounted for.

The apparent gyrostat

If the rotor spin-up torque is zero ($g_a = h_a = 0$), the rotor absolute angular momentum becomes constant and the apparent gyrostat model is dealt with. Also in this case one state variable is lost, since it can be determined from the knowledge of a constant parameter, namely h_a . The equation of motion can thus be rewritten as

$$\tilde{\mathbf{I}}\dot{\boldsymbol{\omega}}_B = -\boldsymbol{\omega}_B \times (\tilde{\mathbf{I}}\boldsymbol{\omega}_B + h_a \mathbf{a}_B) + \mathbf{M}_B$$

with the usual meaning for the symbols.

Note that, provided that the spacecraft moment of inertia, \mathbf{I} , and wheel relative angular momentum, h_r , are replaced by the pseudo-inertia matrix, $\tilde{\mathbf{I}}$, and the absolute angular momentum, h_a , respectively, the two reduced order models for the Kelvin and the apparent gyrostats share the same expression.

2.6.3 Stability of axial gyrostat

Although of little practical use, the apparent gyrostat model is interesting for the derivation of analytical results on the stability of the de-spun condition. The simple axial case is discussed in this paragraph.

Assuming that \mathcal{F}_B is a set of principal axes of inertia and that the spin axis is parallel to $\hat{\mathbf{e}}_3$ (axial rotor), the satellite and rotor absolute angular momentum can be written, respectively, as

$$\mathbf{h}_B = \begin{Bmatrix} J_x \omega_1 \\ J_y \omega_2 \\ J_z \omega_3 + I_s \Omega \end{Bmatrix}; \quad h_a = I_s(\Omega + \omega_3)$$

The equation of motion of the axial gyrostat can be written as follows:

$$\begin{aligned} J_x \dot{\omega}_1 + (J_z - J_y) \omega_2 \omega_3 + I_s \Omega \omega_2 &= M_1 \\ J_y \dot{\omega}_2 + (J_x - J_z) \omega_1 \omega_3 - I_s \Omega \omega_1 &= M_2 \\ J_z \dot{\omega}_3 + (J_y - J_x) \omega_1 \omega_2 + I_s \dot{\Omega} &= M_3 \\ I_s(\dot{\Omega} + \dot{\omega}_3) &= g_a \end{aligned}$$

When $\Omega = 0$, the dual-spin satellite behaves like a standard rigid body. This situation is called all-spun condition. After platform de-spin, the satellite angular velocity must be zero and all the satellite angular momentum must be stored in the rotor. The stability of the equilibrium for the de-spun condition of a Kelvin gyrostat with axial rotor can be analyzed as usual assuming the components $\boldsymbol{\omega}_B = (\omega_1, \omega_2, \omega_3)$ as small and neglecting

second order terms in the equation of motion, which can be written for the torque-free case as

$$\begin{aligned} J_x \dot{\omega}_1 + I_s \Omega \omega_2 &= 0 \\ J_y \dot{\omega}_2 - I_s \Omega \omega_1 &= 0 \\ J_z \dot{\omega}_3 &= 0 \end{aligned}$$

The third equation is decoupled from the others, stating that a perturbation about \hat{e}_3 will remain constant. The first and the second equations can be recast in matrix form as

$$\left\{ \begin{array}{l} \dot{\omega}_1 \\ \dot{\omega}_2 \end{array} \right\} = \left[\begin{array}{cc} 0 & -(I_s/J_x)\Omega \\ (I_s/J_y)\Omega & 0 \end{array} \right] \left\{ \begin{array}{l} \omega_1 \\ \omega_2 \end{array} \right\}$$

It is easy to show that the eigenvalues of the state matrix are a pair of conjugate imaginary numbers, provided that $\Omega \neq 0$. No unstable eigenvalues are present for any value of Ω , so that exponential divergence is ruled out. It is possible to show, on angular momentum conservation grounds, that the variation of ω_1 and ω_2 remains confined in a neighborhood of the origin, so that the system is stable in the sense of Lyapunov. This means that the rotor provides the required gyroscopic stability to the entire satellite.

Adding damping (*e.g.* under the action of a nutation damper) it is possible to transform the L-stable de-spun condition into an asymptotically stable equilibrium.

Chapter 3

Active Stabilisation and Control of Spacecraft

For many applications where accurate payload pointing is required full three-axis control is used. The satellite does not spin (except for slew manoeuvres) and is stabilised by reaction wheels (gyros) and/or thruster relative to an Earth (or other direction) facing attitude. Since the satellite is not spinning, large Sun facing solar panels can be used for power generation. The satellite is also capable of fast reorientation manoeuvres (*slews*) in any arbitrary direction. However, due to the added complexity, 3-axis stabilised satellites are far more expensive than simple spin-stabilised ones. The application and its accuracy requirements must justify the increase in costs and the reduced life expectation of the vehicle.

In order to actively stabilize the satellite in the presence of external disturbances and allow for autonomous manoeuvres, the satellite must be equipped with a suitable set of sensors, which provide the on-board computer with the necessary information on the current attitude. The precision of the control action depends on the accuracy of the attitude measurement.

Moreover, the control law itself depends on the type of actuators available. During the station-keeping phase, a 3-axis stabilised spacecraft featuring only a reaction control system will continuously bounce back-and-forth between the edges of the allowed dead-band, under the alternating action of a (small) disturbance torque and the quick reversal provided by a (large) control pulse at one of the edges of the dead-band. On the converse, when the spacecraft is either gyroscopically stabilised or it is characterised by a considerable momentum bias the perturbation requires a longer time for producing a sizable variation of the spacercraft attitude. In any case, sooner or later, some compensation is required. The control action can be continuous, if momentum exchange devices are employed, althoug the amount of angular momentum stored in the wheel is expected to grow during the station-keeping phase, so that a wheel desaturation manoeuvre is usually necessary, which requires the use of external torques, usually provided by a set of thrusters.

A brief outline on the more common external disturbances, on attitude sensors for evaluating spacecraft orientation and control actuator for implementing the necessary control action is given in the first part of this chapter, prior to the discussion on active attitude control.

3.1 Environmental torques and other disturbances

Together with gravity-gradient, the effects of which on an orbiting spacecraft were described in the previous chapter, there are other environmental disturbance torques. Although small in terms of absolute value, disturbance torques act on a spacecraft for a very long period of time, thus producing in the long run a sizable displacement of the satellite from the desired attitude, if no proper compensating action is taken. As shown, gravity gradient has the interesting property of stabilising an Earth pointing attitude, provided that a certain alignment condition between orbit and principal frame is satisfied, but the restoring moment is of the same order of magnitude of other disturbance torque, so that gravity gradient is a viable passive stabilization technique only when the requirement on pointing accuracy is weak (of the order of some tenths of a degree).

Disturbances of different nature may affect spacecraft attitude, especially when flying a Low Earth Orbit. At the same time, internal sources of disturbances are also present, which either affect the dynamic behaviour of the satellite with respect to the ideal one, or directly affect sensor pointing precision because of oscillations induced by flexible appendages or fuel sloshing.

3.1.1 Environmental torques

The major sources of external disturbances that may influence the dynamic behaviour of a satellite are:

- **gravity gradient:** the variation of gravity pull acting on different mass elements of the spacecraft provide a small yet significant torque; in Low Earth Orbit (LEO) this torque can stabilise an Earth pointing attitude, although the resulting motion is not naturally damped;
- **atmospheric drag:** in Low Earth Orbit (LEO) the air density is small but not null; the centre of pressure is usually not aligned with the center of mass and this fact will produce a torque acting on the spacecraft;
- **magnetic field:** the satellite, with its metallic parts and currents flowing in the electric system produces a magnetic field that interacts with the magnetic field of the Earth, especially in LEO; again a torque on the satellite is produced by this interaction; this coupling between a magnetic field produced by the satellite and the environmental magnetic field can be used beneficially to provide a simple and effective means of attitude control; a magneto-torquer is made of a magnetic coil (or a permanent magnet) the orientation of which inside the satellite bus can be changed so as to produce a control torque; as an alternative, to coils at an angle can be activated with different currents so as to provide an arbitrary torque in a plane; no torque can be delivered in the direction of the magnetic field, so that magnetic torques alone are not sufficient for three-axis control;
- **solar radiation:** the solar radiation produce a light pressure force on the satellite parts exposed to the flow of nuclear particles emitted by the sun; again the force offset will determine a small torque, that is insignificant in LEO, but is the main disturbance at higher distances from the Earth, such as in GEostationary Orbit (GEO).

A simple mathematical formulation is available only for the gravity gradient torque, that will be discussed later in this chapter. Atmospheric and solar radiation torques depend strongly on the shape of the spacecraft, and in particular on how the solar panels and the spacecraft bus face the flow of the rarified gas molecule or the stream of high energy particles from the Sun. The magnetic torque, on the converse, depend on the electric system architecture. As a consequence no general model is available for these disturbances.

3.1.2 Internal disturbances

There are also some sources of internal disturbances, that can be due to the uncertainty of some parameters or to some simplifying assumptions the effect of which is not null on the actual spacecraft:

- **uncertain center of gravity:** there can be an uncertainty on the position of the center of gravity up to some centimeters (1 to 3 cm);
- **thruster misalignment:** the direction of the thruster can be different from the design one up to 1 deg;
- **run-run thrust variation:** there can be sizable variation (up to 5%) in the thrust produced by a thruster in different firings;
- **fuel slosh:** fuel sloshing in the propellant tanks causes both shift in the position of the centre of mass and in the mass distribution (that is, affects the value of the moments of inertia); moreover, as propellant is burned, a long term variation in mean mass properties is also experienced by the satellite;
- **rotating parts:** rotating parts inside the satellite (gyroscopes, reaction wheels, but also tape recorders) produce microvibrations which in turn cause loss in pointing accuracy;
- **elastic modes of flexible appendages:** several flexible items, such as antennas, booms and solar arrays can be attached to the spacecraft bus, and their flexibility can interact with the rigid body motion of the main platform, resonating at the bending frequencies, if properly excited, with serious consequences for the pointing accuracy.

3.2 Attitude sensors

In order to implement some feedback control law for actively stabilizing a spacecraft, it is necessary to have an information on the current satellite attitude. This information is provided by sensors that can be based on significantly different principles, depending on the satellite application and the related pointing accuracy requirements. Roughly speaking, it is possible to group the attitude determination hardware into 5 categories:

- Earth sensors;
- Sun sensors;
- star sensors (and star trackers);

- gyroscopic sensors;
- magnetometers.

3.2.1 Infrared Earth sensors (IRES)

Earth sensors are capable of determining the attitude of the satellite with respect to the Earth, by sensing the Earth's horizon. For this reason they are also referred to as "horizon sensors". Two techniques can be used: (i) the dynamic crossing of the horizon, with precise determination of the crossing points, and (ii) the static determination of the horizon inside the field of view of the instrument.

In principle the sensor could be based on any radiation source coming from the Earth, but the radiation in the visual wavelength region depends too strongly on the characteristics of the reflecting surface. Infrared (IR) radiation provides a range of wavelengths in which the energy is more uniform. Still some problems remains on how to model the Earth's surface and how to take into account the thickness of the atmosphere, which also gives a sizable contribution to the IR radiation of the Earth.

Horizon-crossing sensor (IRHCES)

Static Horizon sensor (IRSES)

3.2.2 Sun sensors

Sun sensors detect the line-of-sight of the Sun. Only the attitude around the Sun-direction remains unknown. The major advantage is that the Sun is a bright object easily identified, providing at the same time an angular resolution which is sufficient for most mission operations. The major drawback, especially when flying a LEO, is that the Sun is not visible during passes in the shadow of the Earth, in which case different sensors are required for providing the necessary attitude information.

Single-axis analogic sun sensor

Two-axis analogic sun sensor

Digital sun sensor

3.2.3 Star trackers

Star trackers are the most accurate and complex attitude sensors. They are based on a simple principle, that is, the attitude of the spacecraft is determined by comparing the position of a known set of stars with a catalogue, so that whole information on three attitude degree of freedom is readily available. The technological problems are that (i) stars provide a very faint reference and (ii) a significant amount of memory (to store the star catalogue) and processing capabilities (for matching the current view with the catalogue) are required.

3.2.4 Rate and rate-integrating gyroscopes

A wholly gimballed, friction-less spinning body will maintain its spin direction fixed with respect to an inertial frame. This well-known physical principle is at the basis of gyroscopic sensors, which being inertial instrument, do not require optical head and are not

affected by line-of-sight and shadow problems. The sensor is based on the determination of the gyroscopic torque produced by the spinning wheel on its support. Letting $\hat{\mathbf{a}}$ be the spin axis, an angular speed component ω around the axis $\hat{\mathbf{i}}$ perpendicular to $\hat{\mathbf{a}}$ will produce an apparent gyroscopic torque $-(\omega \hat{\mathbf{i}}) \times (I_w \Omega \hat{\mathbf{a}})$, where Ω is the wheel spin speed. By measuring the apparent gyroscopic torque around the output axis $\hat{\mathbf{k}} = \hat{\mathbf{i}} \times \hat{\mathbf{a}}$ it is possible to evaluate ω , assuming I_w and Ω known.

By means of three, mutually perpendicular gyroscopes it is thus possible to evaluate all the angular velocity components and, integrating their signal, the current spacecraft attitude, if the initial one is known by means of some other sensor. Updating of the attitude estimate is always necessary as far as real gyroscopes are affected by noise and signal drift.

3.2.5 Magnetometers

Also the Earth magnetic field can provide a reference for attitude measurements.

3.3 Actuators

Spacecraft control actuators can be based on different physical principles. The choice in the type of actuator installed on board of the satellite greatly affects its configuration, the resulting pointing accuracy, and even the implementation of the control laws themselves.

A control action can be delivered to the satellite by either a direct torque produced by a (set of) thruster(s), by exchanging angular momentum between parts in relative rotational motion or by application of a magnetic torque, obtained from the interaction of an electric coil and the Earth magnetic field.

- Reaction control system (RCS)
 - Cold gas jets
 - Chemical propulsion (Mono-propellant or Bi-propellant propulsion system; can be used also for orbit control)
- Momentum exchange devices
 - Reaction wheels
 - Bias-momentum wheel
 - Double-gimbal bias-momentum wheel
 - Control Moment Gyroscopes
- Magneto-torquers

3.4 Linear model of rigid satellite attitude motion

For a general three axis motion, Euler's equation states that

$$\dot{\mathbf{h}}_B + \boldsymbol{\omega}_B \times \mathbf{h}_B = \mathbf{M}_B \quad (3.1)$$

If there are no internal moving parts (e.g. no spinning rotors) this equation can be written in the form

$$\mathbf{I}\dot{\boldsymbol{\omega}}_B + \boldsymbol{\omega}_B \times (\mathbf{I}\boldsymbol{\omega}_B) = \mathbf{M}_B$$

Assuming that the rotation is slow, the angular velocity can be considered as a first order perturbation of the steady state $\boldsymbol{\omega}_B = 0$, so that $\|\boldsymbol{\omega}_B\| \ll 1$ and $\boldsymbol{\omega}_B \times (\mathbf{I}\boldsymbol{\omega}_B)$ is a second order (negligible) term in the equations of motion. Euler's equation thus becomes

$$\mathbf{I}\dot{\boldsymbol{\omega}}_B = \mathbf{M}_B$$

When dealing with a stabilization problem, that is small perturbations with respect to a prescribed nominal attitude are considered, also the angular displacement is “small”. In such a case, it is possible to demonstrate that, letting the variation of the Bryan's angles be equal respectively to

$$\Delta\psi = \theta_3 ; \quad \Delta\theta = \theta_2 ; \quad \Delta\phi = \theta_1$$

and defining $\boldsymbol{\theta} = \{\theta_1, \theta_2, \theta_3\}^T$, it is

$$\dot{\boldsymbol{\theta}} = \boldsymbol{\omega}_B$$

Euler's equation in linear form become simply

$$\mathbf{I}\ddot{\boldsymbol{\theta}} = \mathbf{M}_B \quad (3.2)$$

Finally, assuming that a set of principal axes of inertia is chosen as the body frame, the inertia matrix is in diagonal form, $\mathbf{I} = \text{diag}(J_1, J_2, J_3)$, and three independent second order linear ordinary differential equations are obtained, one for each axis,

$$J_i \ddot{\theta}_i = M_i , \quad i = 1, 2, 3$$

It should be noted that for single axis rotations, a scalar equation in the same form as Eq. (3.2) is obtained, regardless of the angular speed and angular displacement, that is

$$J \ddot{\theta} = M$$

This equation will be the starting point for the analysis of attitude slew maneuvers.

3.5 Linear model of gyrostat attitude motion

If the satellite is equipped with a momentum wheel with a moment of inertia I_s spinning about the axis $\hat{\mathbf{a}}$ with a relative spin rate Ω , the total satellite angular momentum is

$$\mathbf{h}_B = \mathbf{I}\boldsymbol{\omega}_B + h_r \mathbf{a}_B$$

where $h_r = I_s \Omega$ is the relative angular momentum; Ω can be written as

$$\Omega = \Omega_0 + \Delta\Omega$$

being $\Delta\Omega \ll \Omega_0$, i.e. $\Delta\Omega$ is a “small perturbation” of the reference wheel spin rate Ω_0 . Equation (3.1) thus becomes

$$\mathbf{I}\dot{\boldsymbol{\omega}}_B + I_s \Delta\dot{\Omega} \mathbf{a}_B + \boldsymbol{\omega}_B \times [\mathbf{I}\boldsymbol{\omega}_B + I_s (\Omega_0 + \Delta\Omega) \mathbf{a}_B] = \mathbf{M}_B$$

Neglecting higher order term one gets

$$\mathbf{I}\dot{\boldsymbol{\omega}}_B + I_s \Delta\dot{\Omega} \mathbf{a}_B + I_s \Omega_0 \boldsymbol{\omega}_B \times \mathbf{a}_B = \mathbf{M}_B$$

The evolution of the perturbations of Euler's angles is again

$$\dot{\theta} = \omega_B$$

so that the equations of motion becomes can be expressed in scalar form as follows:

$$\begin{aligned} J_1\ddot{\theta}_1 + I_s\Delta\dot{\Omega}a_1 + I_s\Omega_0(\dot{\theta}_2a_3 - \dot{\theta}_3a_2) &= M_1 \\ J_2\ddot{\theta}_2 + I_s\Delta\dot{\Omega}a_2 + I_s\Omega_0(\dot{\theta}_3a_1 - \dot{\theta}_1a_3) &= M_2 \\ J_3\ddot{\theta}_3 + I_s\Delta\dot{\Omega}a_3 + I_s\Omega_0(\dot{\theta}_1a_2 - \dot{\theta}_2a_1) &= M_3 \end{aligned}$$

This set of equations is coupled with the dynamics of the spin-wheel, described by the (linear) equation

$$\dot{\Omega} \equiv \Delta\dot{\Omega} = \frac{g_a}{I_s} - \dot{\omega}_B^T \mathbf{a}_B$$

When the rotor spin axis is parallel to the i -th principal axis of inertia ($\hat{\mathbf{a}} \equiv \hat{\mathbf{e}}_i$), the i -th equation of motion becomes decoupled from the others, because $a_j = a_k = 0$, for $j, k \neq i$. As an example, let us assume that $\hat{\mathbf{a}} \equiv \hat{\mathbf{e}}_2$, so that $a_1 = a_3 = 0$ and $a_2 = 1$. The equations of motion become

$$\begin{aligned} J_1\ddot{\theta}_1 - I_s\Omega_0\dot{\theta}_3 &= M_1 \\ J_2\ddot{\theta}_2 + I_s\Delta\dot{\Omega} &= M_2 \\ J_3\ddot{\theta}_3 + I_s\Omega_0\dot{\theta}_1 &= M_3 \end{aligned}$$

The pitch dynamics is decoupled from the roll and yaw motions, but is coupled with the spin-wheel dynamics

$$\Delta\dot{\Omega} = \frac{g_a}{I_s} - \dot{\omega}_2$$

Summing up, the torque-free pitch dynamics ($M_2 = 0$) is described by the equations

$$\begin{aligned} (J_2 - I_s)\ddot{\theta} &= -g_a \\ \Omega &= \Omega_0 - \frac{J_2}{I_s}\dot{\theta} \end{aligned}$$

On the converse, roll and yaw motions are coupled by the gyroscopic term. Moreover, if the rotor spin speed is time-varying and $\Delta\Omega$ is not negligible, the roll and yaw coupling terms depend on the pitch dynamics through Ω .

3.6 Use of thrusters for attitude control

3.6.1 Single axis slews (open loop)

If we consider a constant torque acting around the generis i -th axis, the angular acceleration is

$$\alpha_i = \ddot{\theta}_i = M_i/J_i$$

Integrating from the initial condition $\theta(t_0) = \theta_0$, $\dot{\theta}(t_0) = \dot{\theta}_0$ (and dropping the subscript i), one has

$$\begin{aligned} \dot{\theta}(t) &= \dot{\theta}_0 + \alpha(t - t_0) \\ \theta(t) &= \theta_0 + \dot{\theta}_0(t - t_0) + \frac{1}{2}\alpha(t - t_0)^2 \end{aligned}$$

The same equation can be integrated in the phase plane θ vs $\dot{\theta}$. By application of the derivation chain rule it is

$$\ddot{\theta} = \frac{d\dot{\theta}}{d\theta} \frac{d\theta}{dt}$$

so that one gets

$$\alpha = \dot{\theta} \frac{d\dot{\theta}}{d\theta}$$

Integrating the previous equation in θ , one gets

$$\int_{\dot{\theta}_0}^{\dot{\theta}} \dot{\vartheta} d\vartheta = \int_{\theta_0}^{\theta} \alpha d\vartheta$$

that, for constant applied torque, becomes

$$\frac{1}{2} (\dot{\theta}^2 - \dot{\theta}_0^2) = \alpha(\theta - \theta_0)$$

or,

$$\dot{\theta}^2 = \dot{\theta}_0^2 + 2\alpha(\theta - \theta_0)$$

Starting from a rest position in the nominal attitude ($\dot{\theta} = 0$ and $\theta = 0$), one gets

$$\dot{\theta}^2 = 2\alpha\theta \implies \dot{\theta}(t) = \sqrt{2\alpha\theta}$$

A single-axis rotation manoeuvre can thus be performed in three phases: an initial acceleration phase (i) during which the spacecraft achieves the desired slew rate $\dot{\theta}_d$ for the reorientation; the acceleration is followed by a drifting phase (ii), during which a constant angular velocity remains constant with no action from the thrusters, until, at a proper time instant, the drifting motion is stopped during the deceleration phase (iii) by a second impulse from the thrusters. Representing the manoeuvre in the phase plane, the state variables evolve as reported in Fig. 3.1.

The configuration of the thrusters used for spinning the satellite up to the drift angular velocity can be different. As reported in Fig. 3.2, a single thruster delivering a force \vec{F} with a moment arm ℓ with respect to the spacecraft centre of mass produces a torque the magnitude of which is $F\ell$. Unfortunately, also a net force F is produced which will affect orbit parameters, thus coupling the orbit and the attitude control problems.

On the converse, if a balanced configuration is employed, the simultaneous firing of two thrusters in opposite directions will produce only a torque $M = 2F\ell$, with a zero net force, so that the orbit motion of the spacecraft is unaffected by attitude control pulses.

An approximate evaluation of the total manoeuvre time and the propellant necessary for performing it can be derived by neglecting the duration of the thruster firings for accelerating and decelerating the angular motion of the vehicle, taking into account only the drift phase. Assuming that the drift angular velocity is $\dot{\theta}_d$, the time required for a manoeuvre of amplitude equal to θ_f is simply given by $T = \theta_f/\dot{\theta}_d$.

Assuming a sharp thrust profile, it is

$$\dot{\theta}_d = \frac{2F\ell}{J} \Delta t$$

and the pulse width (thruster on-time) for the spin-up is given by

$$\Delta t_{on,1} = \frac{J\dot{\theta}_d}{2F\ell}$$

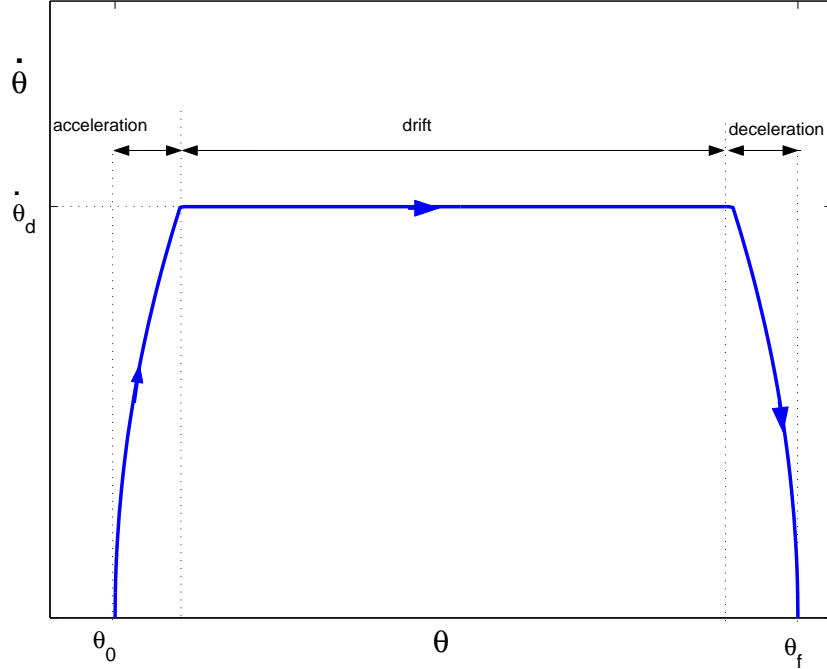


Figure 3.1: Evolution of θ and $\dot{\theta}$ for a rest-to-rest manoeuvre.

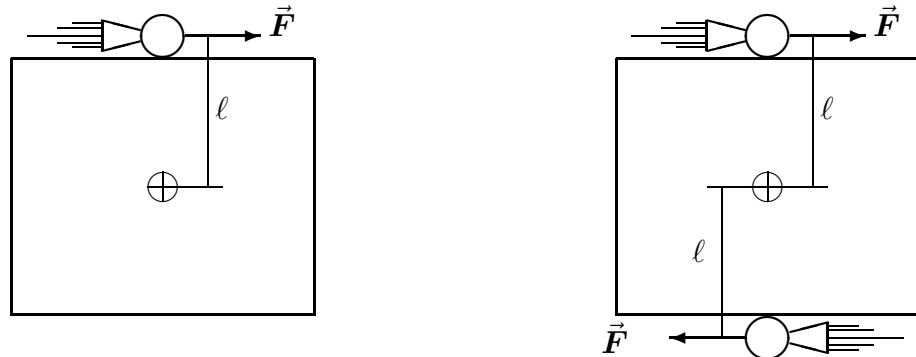


Figure 3.2: Unbalanced and balanced thruster configurations.

From the definition of the thruster specific impulse

$$I_{sp} = \frac{F \Delta t_{on}}{g \Delta m_f}$$

(that is the ratio between the momentum gained and the weight of the propellant used) the mass of propellant necessary for the acceleration is

$$\Delta m_1 = 2 \frac{F \Delta t_{on,1}}{g I_{sp}} = \frac{J \dot{\theta}_d}{g \ell I_{sp}}$$

The drift angular velocity can be determined as a function of the manoeuvre time, that is, $\dot{\theta}_d = \theta_f/T$, so that the propellant mass necessary for the spin-up becomes equal to

$$\Delta m_1 = \frac{J \theta_f}{g \ell I_{sp} T}$$

At the end of the drift interval, a second pulse of equal duration in the opposite direction will stop the motion of the satellite and the new attitude will be acquired. The total

propellant mass is thus equal to

$$\Delta m_{\text{tot}} = \Delta m_1 + \Delta m_2 = 2 \frac{J\theta_f}{g\ell I_{sp}T}$$

It can be observed that allowing larger manoeuvre times, the same angle variation can be achieved with a significantly smaller amount of fuel. Moreover, low energy thrust pulses are less likely to excite vibrations in the structure and/or in flexible appendages attached to the spacecraft (such as antennas or solar panels). For large values of T , smaller on-time for the thruster are required, and the initial assumption that the acceleration and deceleration phases have a negligible duration with respect to the overall manoeuvre time is confirmed.

On the other side, for agile spacecraft that achieve high angular velocities, it is possible to improve the accuracy of the estimate of manoeuvre time taking into account the duration of the initial and terminal phases. The time for accelerating the satellite up to $\dot{\theta}_d$ is again given by

$$\Delta t_1 = \frac{J\dot{\theta}_d}{F\ell} = \frac{\dot{\theta}_d}{\alpha}$$

which is still equal to the time Δt_2 necessary for bringing it back to rest at the end of the maneuver, with the difference that for fast manoeuvres the total firing time $\Delta t_1 + \Delta t_2$ is a not negligible fraction of the total manoeuvre time T .

During the acceleration, the variation of θ is

$$\theta_1 = \frac{1}{2}\alpha\Delta t_1^2 = \frac{1}{2}\frac{\dot{\theta}_d^2}{\alpha}$$

and the total variation during the manoeuvre is given by

$$\theta_f = \dot{\theta}_d t_d + \theta_1 + \theta_2$$

where the angle variation during the acceleration and deceleration phases, θ_1 and θ_2 , are equal. The drift time is $t_d = T - 2\Delta t_1$, where T is the total manoeuvre time, so that

$$\begin{aligned} \theta_f &= \dot{\theta}_d(T - 2\Delta t_1) + \alpha\Delta t_1^2 \\ &= \dot{\theta}_d \left(T - 2\frac{\dot{\theta}_d}{\alpha} \right) + \frac{\dot{\theta}_d^2}{\alpha} \end{aligned}$$

The total manoeuvre time becomes thus

$$T = \frac{\theta_f}{\dot{\theta}_d} + \frac{\dot{\theta}_d}{\alpha}$$

In the limit, the minimum-time bang-bang control law brings to zero the drift time t_d . The reader can demonstrate that in this limit case it is

$$T = 2\sqrt{\theta_f/\alpha}$$

In both cases, the faster manoeuvres are performed at the expenses of a significant increase in propellant consumption.

3.6.2 Closed-loop control

The ideal case: thrust modulation

If the satellite is equipped with a set of sensors that provides the necessary information on the attitude motion, it is possible to implement a control law which provides a torque command that drives the satellite towards the prescribed attitude.

If the torque command is simply proportional to the attitude error, $e = \theta_{\text{des}} - \theta$, the closed-loop equation of motion becomes

$$\left. \begin{aligned} \ddot{\theta} &= M/J \\ M &= K(\theta_{\text{des}} - \theta) = Ke \end{aligned} \right\} \implies \ddot{\theta} = \frac{K}{J}(\theta_{\text{des}} - \theta) \implies \ddot{\theta} + p^2\theta = p^2\theta_{\text{des}}$$

where $p^2 = K/J$. The solution of this second order equation for an initial condition of rest for $\dot{\theta} = 0$ is

$$\theta(t) = \theta_{\text{des}} [1 - \cos(pt)]$$

i.e. an unacceptable undamped oscillation of amplitude θ_{des} about the desired condition. In order to damp the oscillation and asymptotically reach the desired condition, it is necessary to add a damping term in the control law, proportional to the angular rate $\dot{\theta}$. The command torque is thus

$$M = K(\theta_{\text{des}} - \theta) + K_d\dot{\theta} \quad (3.3)$$

and the closed-loop equation of motion becomes

$$\ddot{\theta} + c\dot{\theta} + p^2\theta = p^2\theta_{\text{des}}$$

where the coefficient of the damping term $c = 2\zeta p = -K_d/J$ is positive (damped oscillations) if the gain associated to the angular rate is negative.

There are two possible resulting closed-loop behaviours. For $0 < \zeta < 1$, the time-history of the angular motion is

$$\theta(t) = \theta_{\text{des}} [1 - \exp(-\zeta pt) \cos(p_d t)]$$

where $p_d = p\sqrt{1 - \zeta^2}$, that is, damped oscillations with an exponentially decaying amplitude.

If on the converse $\zeta > 1$, the characteristic equation has two real solutions $\lambda_{1,2} = p(-\zeta \pm \sqrt{\zeta^2 - 1})$, which are both negative. In this case the evolution of the rotation angle is

$$\theta(t) = \theta_{\text{des}} \left[1 - \frac{\lambda_2}{\lambda_2 - \lambda_1} \exp(\lambda_1 t) + \frac{\lambda_1}{\lambda_2 - \lambda_1} \exp(\lambda_2 t) \right]$$

Two important issues need to be considered, at this point. The first one is the choice of the gains. The case with $\zeta < 0$ is not considered at all, inasmuch as one of the poles of the closed loop system would be a positive real number, that is, the closed loop system would be unstable. When $\zeta < 1$ (sub-critical damping), the time τ to damp out 99% of the initial oscillation amplitude increases as ζ gets smaller according to the equation

$$\exp(-\zeta p \tau) = 0.01 \implies \tau = -\log(0.01)/(\zeta p)$$

At the same time, if $\zeta > 1$ (super-critical damping) the time constant of the slowest mode becomes larger, being approximately equal to ζ/p , for large values of ζ . This means that a largely super-critical damping coefficient will cause a slower convergence.

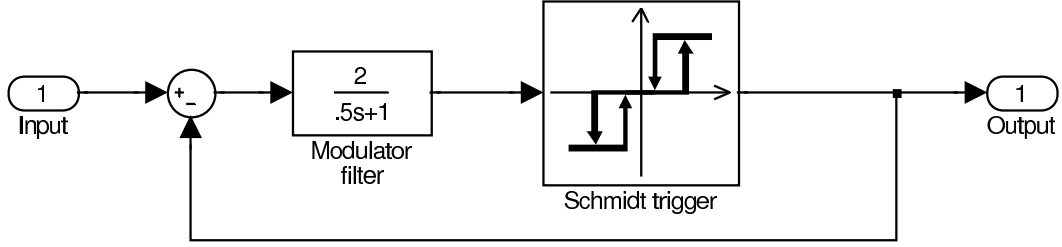


Figure 3.3: Pulse–Width/Pulse–Frequency (PWPF) modulator.

The best performance in terms of maneuver agility are obtained for the critical damping $\zeta = 1$, which guarantees the fastest convergence time to the desired position. The over-damped case may be of interest in those cases when fuel consumption is more a stringent concern than maneuver time. On the contrary, the under-damped case, which exhibits some overshoot, is of no practical interest, since it is characterized by a longer settling time and an increased fuel consumption, because of the thrusting system firing alternatively in both directions, during the oscillations.

The second issue concerns the actual implementation of a control law in the form (3.3). Such a control law would be realistic only if the control torque provided by the thruster could be modulated. Unfortunately direct thrust modulation would require a complex hardware and, at the same time, would be extremely inefficient in large portions of the required thrust range. For these reason, thruster are always *on/off* devices. As a consequence, some form of pulse modulation is required to provide a feasible implementation of the control torque demand. Two techniques will be presented, the Pulse–Width/Pulse–Frequency (PWPF) modulator, which is an analogic device, and the Pulse–Width Modulator (PWM), which lends itself to a discrete time implementation.

Pulse–Width/Pulse–Frequency modulation

Figure 3.3 shows the structure of a Pulse–Width/Pulse–Frequency (PWPF) modulator. The main element of the modulator is the Schmidt trigger, which consist of a double relay with hysteresis, separated by a dead band. In order to provide a quasi-linear steady-state response, a modulation filter is added, the input of which is the signal $\tilde{e} = e_m - y_m$, i.e. the difference between the feed-back signal error and the modulator output. The output of the filter v is the activation signal for the Schmidt trigger.

The modulator filter is represented by a linear first order system, the dynamics of which is

$$\dot{v} = \frac{1}{\tau} (K e_m - v)$$

The response of the modulator filter to a steady input \tilde{e} is

$$v(t) = v_0 \exp(-t/\tau) + K e_m [1 - \exp(-t/\tau)]$$

until $y = 0$.

The output y of the modulator remains zero until the signal v remains below the activation threshold U_{on} . This threshold is never crossed if the error variable e_m remains smaller than U_{on}/K , that is, the asymptote of $v(t) \rightarrow K e_m$ lies below U_{on} .

If on the converse $K e_m > U_{\text{on}}$, there will be a time t_{om} when v reaches U_{on} and the trigger output switches from 0 to U_m (Fig. 3.4), so that the thruster is activated by the

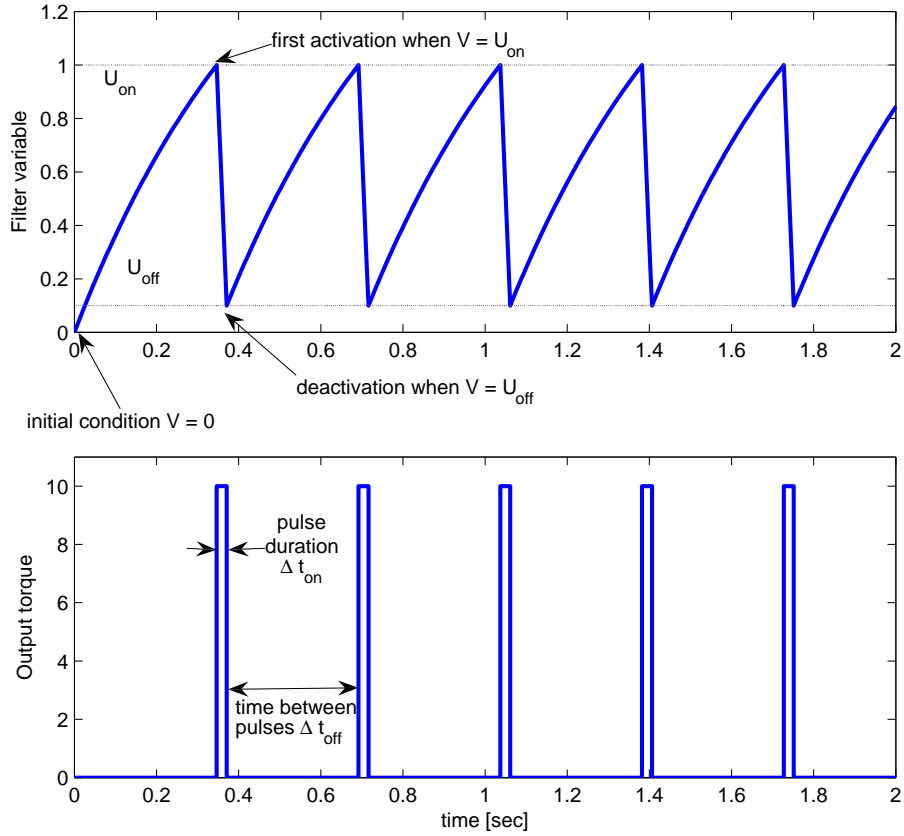


Figure 3.4: Activation/deactivation sequence of a PWPF modulator.

trigger. At this point, the modulator input changes to $\tilde{e} = e_m - U_m$. Assuming that e_m is unaffected by y , integration of the filter linear dynamics starting from the initial condition $v(t_{\text{on}}) = U_{\text{on}}$ for $\tilde{e} = e_m - U_m$ brings to the following expression for the activation function

$$\begin{aligned} v(t) &= U_{\text{on}} \exp\left(-\frac{t-t_{\text{on}}}{\tau}\right) + K(e_m - U_m) \left[1 - \exp\left(-\frac{t-t_{\text{on}}}{\tau}\right)\right] \\ &= K(e_m - U_m) + [U_{\text{on}} - K(e_m - U_m)] \exp\left(-\frac{t-t_{\text{on}}}{\tau}\right) \end{aligned}$$

The thruster is switched off when the activation function becomes equal to U_{off} , that is when

$$\begin{aligned} \exp\left(-\frac{t_{\text{off}}-t_{\text{on}}}{\tau}\right) &= \frac{U_{\text{off}} - K(e_m - U_m)}{U_{\text{on}} - K(e_m - U_m)} \\ &= 1 - \frac{U_{\text{on}} - U_{\text{off}}}{U_{\text{on}} - K(e_m - U_m)} \end{aligned} \quad (3.4)$$

It should be noted that, if $K(e_m - U_m) > U_{\text{off}}$, i.e. $e_m > U_{\text{off}}/K + U_m$, the above equation has no real solution, that is the input is so great that the modulator calls for a continuous thruster engagement. This level constitutes the saturation level of the modulator. On the converse, if e_m becomes less than $U_{\text{off}}/K + U_m$, the thrusters are switched off when $t = t_{\text{off}}$. Calling $\Delta t_{\text{on}} = t_{\text{off}} - t_{\text{on}}$ the on-time of the thruster, and assuming that it is sufficiently small, it is possible to approximate $\exp(-\Delta t_{\text{on}}/\tau) = 1 - \Delta t_{\text{on}}/\tau$, so that

$$\Delta t_{\text{on}} \approx \tau \frac{U_{\text{on}} - U_{\text{off}}}{U_{\text{on}} - K(e_m - U_m)}$$

After the thruster pulse, the modulator input becomes again $\tilde{e} = e_m$ and the response of the filter for an initial condition given by $v(t_{\text{off}}) = U_{\text{off}}$ is

$$v(t) = U_{\text{off}} \exp\left(-\frac{t - t_{\text{off}}}{\tau}\right) + K e_m \left[1 - \exp\left(-\frac{t - t_{\text{off}}}{\tau}\right)\right]$$

The thruster will be activated again when $v = U_{\text{on}}$, that is when

$$\exp\left(-\frac{t - t_{\text{off}}}{\tau}\right) = \frac{U_{\text{on}} - K e_m}{U_{\text{off}} - K e_m}$$

Assuming again that the off time is also sufficiently small, one gets

$$\Delta t_{\text{off}} = \tau \frac{U_{\text{on}} - U_{\text{off}}}{K e_m - U_{\text{off}}}$$

Figure 3.5 shows the activation sequence of a PWPF modulator for increasingly higher values of the error signal e_m . In the first case it is clear how the error signal is so small that the thruster are not activated. For an error slightly above the activation threshold, a sequence of small pulses (25 ms) separated by wide deactivation intervals ($\Delta t_{\text{off}} \approx 0.6$ s) are present. This correspond to a small average control torque. A higher error signal increase the duration of the pulses, while decreasing the time between the pulses, so that the average torque increases almost linearly until the saturation level is reached. Beyond saturation (bottom-right corner in Figure 3.5) the deactivation threshold is no longer crossed and the thruster are not switched off.

The average output of the thruster, given by

$$\bar{y} = U_m \frac{\Delta t_{\text{on}}}{\Delta t_{\text{off}} + \Delta t_{\text{on}}}$$

is represented in Fig. 3.6. Its variation is almost linear for $U_{\text{on}}/K < e_m < U_{\text{off}}/K + U_m$, it is zero below the activation threshold and equal to the thruster force beyond the saturation value. The proper sizing of the trigger and filter characteristics through tuning of filter and trigger parameters allows for realizing a modulator which takes into account the physical characteristics of the thrusters, such as the minimum pulse time and the minimum time between pulses.

Figure 3.7 shows the response of a satellite controlled by a set of thruster driven by a PWPF modulator (continuous blue line). The response is compared with that obtained by thrust modulation (red dashed line). In the initial part of the reorientation manoeuvre ($t < 100$ s), the modulator reproduce almost exactly the behaviour of the ideal linear PD controller.

In the following part of the simulation, shown in Fig. 3.8, the angular velocity of the ideal case goes asymptotically towards 0, while the small residual angular velocity (-0.002 deg/s) visible in the more realistic case, where the modulator is present, causes a slow drift towards the negative side of the dead-band. Since the error signal is within the dead-band no control action is produced, until for $t = 273.36$ s a pulse is fired which revert the motion. The minimum pulse provides the required reversal, but the resulting angular velocity is significantly higher (0.025 deg/s) so that after few seconds, $t = 286.43$ s, a new pulse in the opposite direction is required to revert again the motion on the positive side of the dead-band. This bouncing between the edges of the dead-band characterizes the steady-state condition of a spacecraft controlled with a reaction control system.

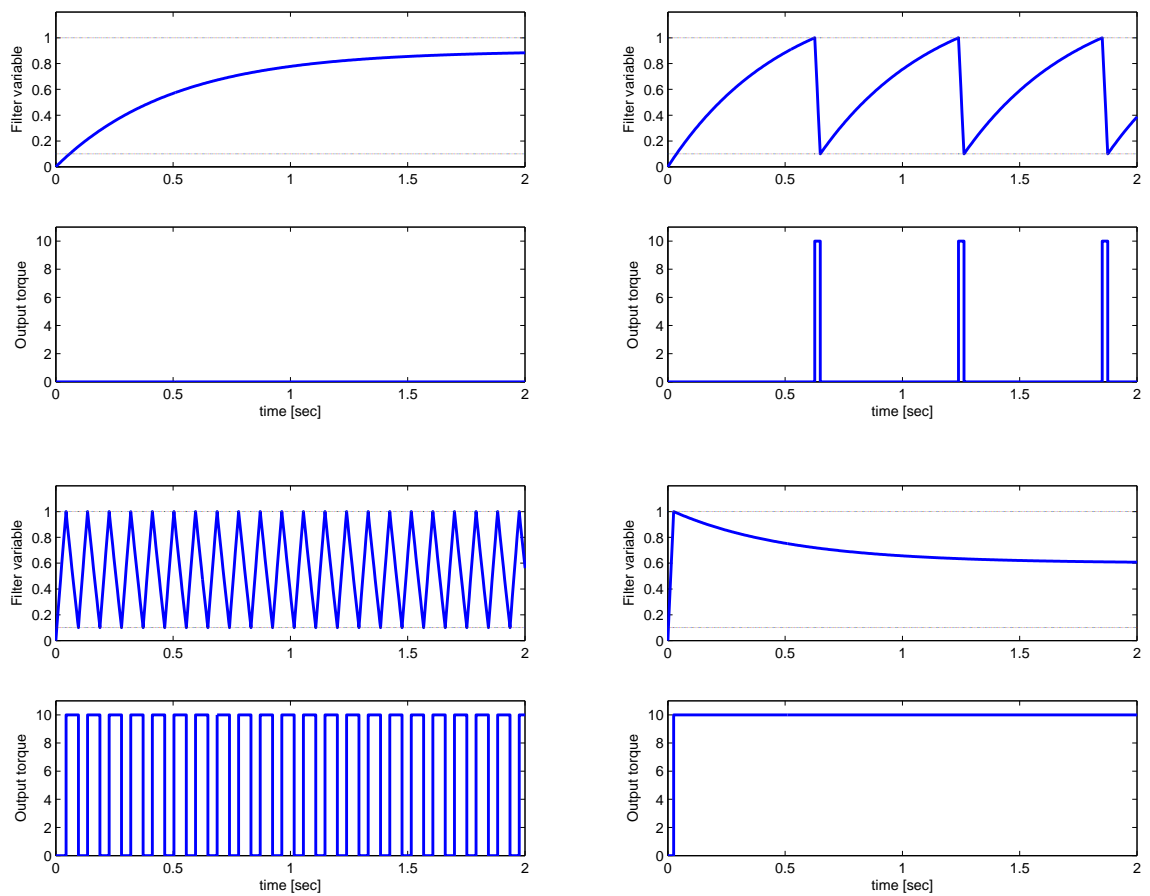


Figure 3.5: Activation sequences of a PWPF modulator for different input levels.

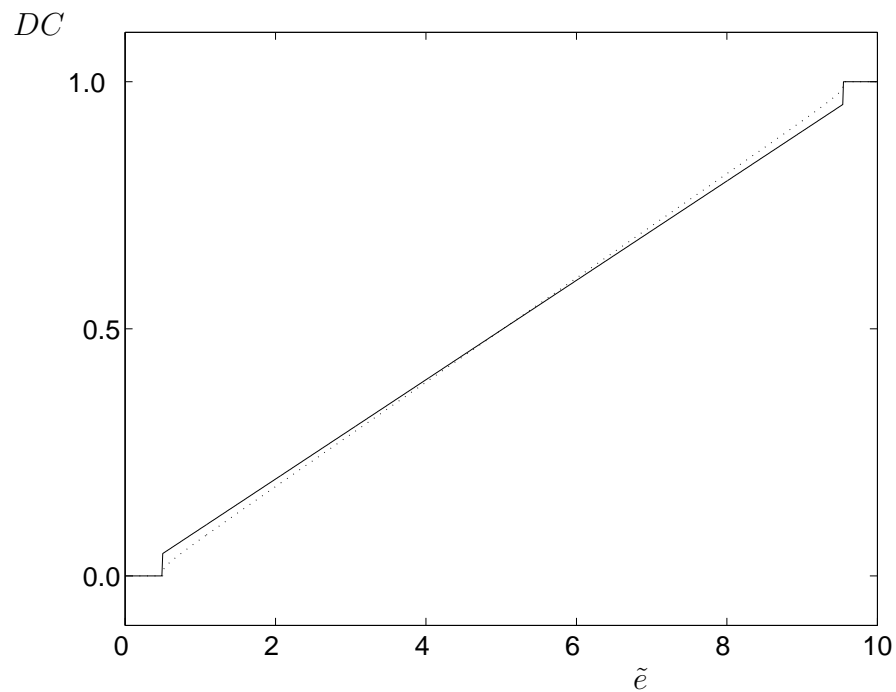


Figure 3.6: Duty cycle of the PWPF modulator.

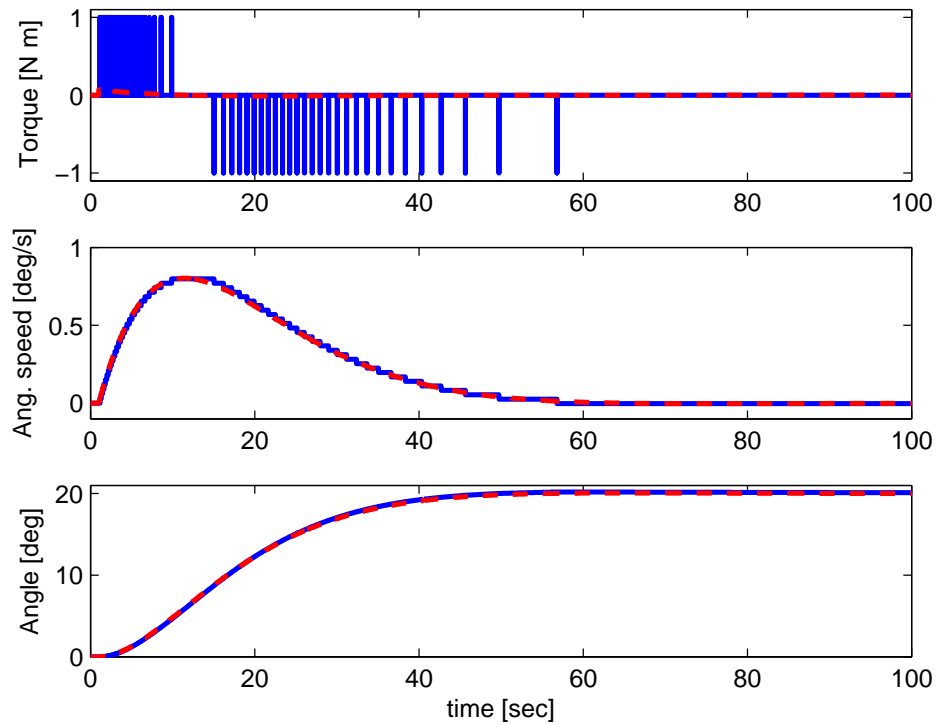


Figure 3.7: Closed-loop behaviour (short term).

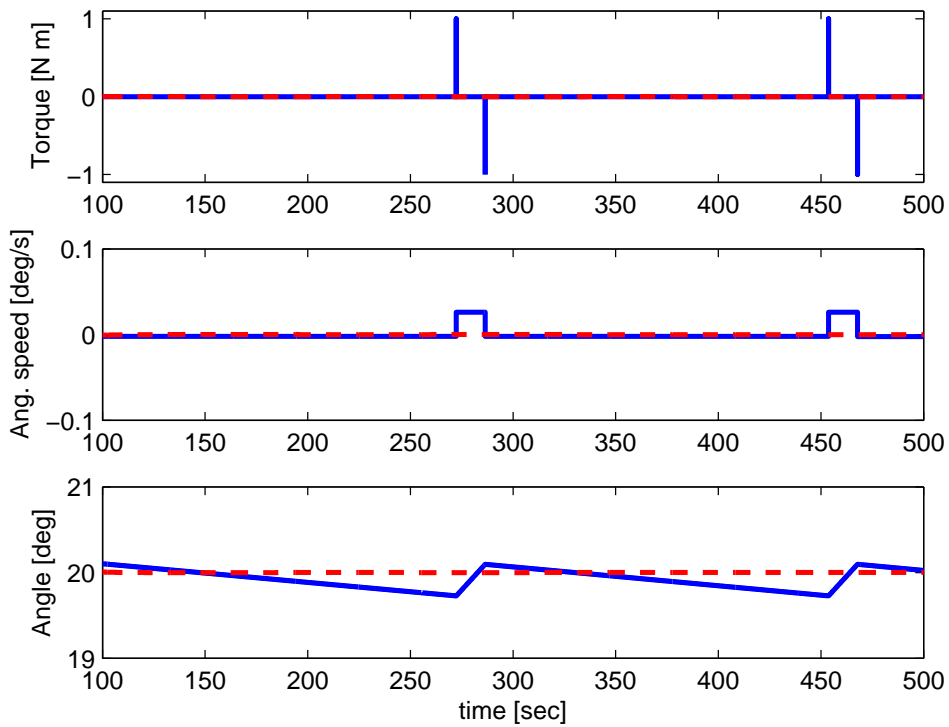


Figure 3.8: Closed-loop behaviour (long term).

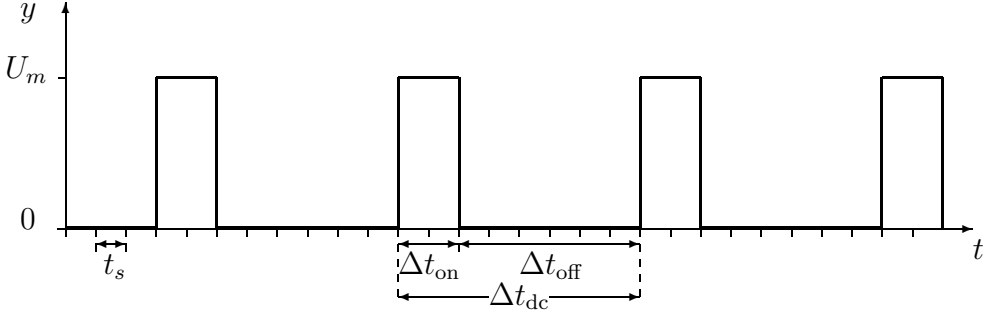
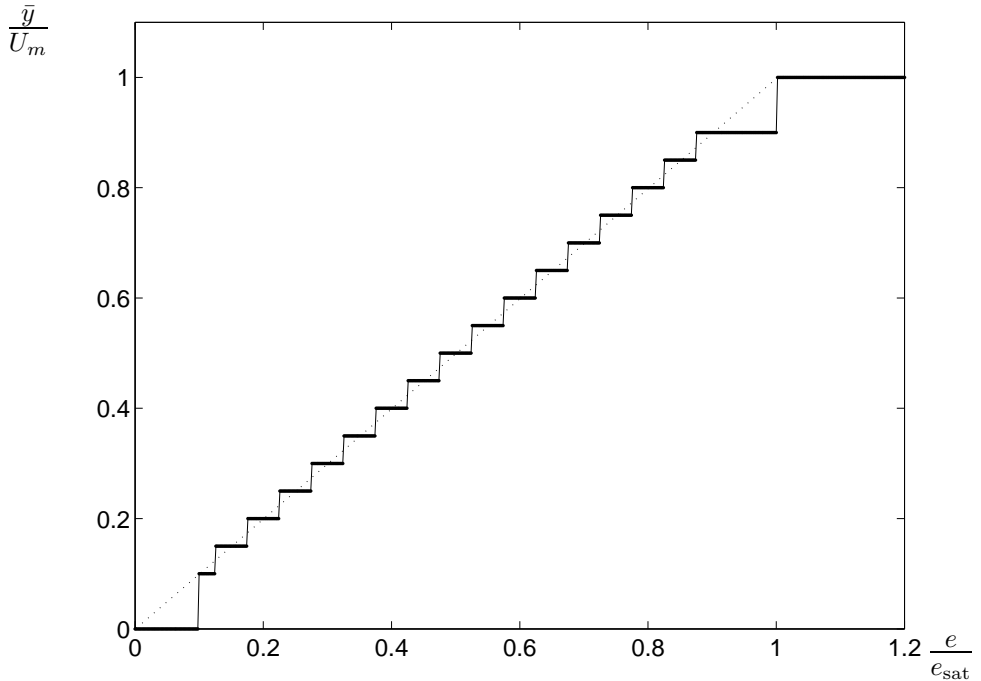


Figure 3.9: Pulse–Width Modulation.



Modulator data: $t_s = 10 \text{ ms}$; $N_{dc} = 20$; $\Delta t_{on,min} = 12 \text{ ms} \Rightarrow N_{on,min} = 2$;
 $\text{MTBP} = 17 \text{ ms} \Rightarrow N_{on,max} = 18$.

Figure 3.10: Response of a PW Modulator.

Pulse–Width Modulation

The PWPF modulator is a heritage of the analogic era, although it is still widely used. The main advantage of PWPF modulation remains the possibility of commanding a sequence of pulses with a quasi–linear response, in terms of averaged output. Nonetheless, many actuators are now commanded in the framework of a digital implementation of the control logic. It is well known that a digital controller obtained from the discretization of an analogic one can attain at most the performance of the original analogic counterpart. If a digital controller is designed directly in the discrete time domain, taking into account the sampling frequency and A/D and D/A conversions, better performance can be obtained.

Pulse–Width modulation provide a means for designing a thruster control law where the implementation of the switching logic is inherently digital. As an advantage with respect to PWPF (analogic) modulation, it is much easier to satisfy restrictions on the on–time Δt_{on} and the time–between–pulses Δt_{off} .

Figure 3.9 shows a sequence of pulses. If t_s is the sampling period of the digital controller, a pulse can be commanded for each duty cycle, the duration of which is $\Delta t_{dc} =$

Nt_s . The minimum impulse bit (MIB) $N_{\text{on,min}}$ is chosen so that $N_{\text{on,min}}t_s > \Delta t_{\text{on,min}}$. At saturation, the *on*-time is extended to the entire duty cycle. Below saturation, the maximum pulse must satisfy the constraint on minimum-time-between-pulses (MTBP), that is $\Delta t_{\text{off}} = (N - N_{\text{on}})t_s > \text{MTBP}$.

The average output of a thruster controlled in PWM is

$$\bar{y} = U_m \frac{\Delta t_{\text{on}}}{\Delta t_{\text{off}} + \Delta t_{\text{on}}} = U_m \frac{N_{\text{on}}}{N}$$

The response of the PWM to a constant input error signal \tilde{e} is depicted in Fig. 3.10, assuming that a quasi-linear average output $\bar{y} = k\tilde{e}$ is desired between a deadband e_{db} and the saturation value e_{sat} , when the *on*-time equals the duty cycle and $\bar{y} = U_m$. It should be noted that, by a proper software implementation of the activation signal, it is possible to obtain arbitrary pulse-width modulation curves.

3.6.3 Fine pointing control

After slew to target, the control system switches to fine pointing control, in order to maintain the payload aimed at the desired target with a prescribed tolerance, in presence of external disturbances. This can be done using momentum exchange devices and/or gas jets. A simple way to achieve such a fine pointing is to use cold gas jets, that produce thrust in the range between 0.05 and 20 N, with short pulse times (of the order of 10^{-2} s) for fine control. As far as the satellite will be bouncing back and forth between the edges of a limit cycle, it is important to estimate the amount of fuel necessary as a function of the prescribed pointing accuracy and thruster characteristics.

Torque-free control

Let us consider the torque-free case, that is no external disturbance acts on the spacecraft, where the payload must be pointed in a given direction, within some deadband, which in the case of astronomy payloads can become as small as $1/10$ arcsec = 0.000278 deg!

The satellite is allowed to drift slowly inside the deadband, with drift velocity $\dot{\theta}_d$. When it reaches the limit of the deadband, θ_{db} , the thruster is fired so as to revert the drift rate in the opposite direction. The satellite will drift towards the other side of the deadband, where the thruster are fired again, thus capturing the satellite into a limit cycle of width approximatley equal to $2\theta_{db}$. In what follows it will be assumed that the limit cycle is symmetric, that is, the absolute value of the angular velocity during the drifting phases is the same in both directions.¹ The thrusters generates a moment

$$M = 2F\ell = J\ddot{\theta}$$

For a thruster pulse width Δt_{on} , the change of the attitude rate is

$$\Delta\dot{\theta} = 2\frac{F\ell}{J}\Delta t_{\text{on}} = 2\dot{\theta}_d$$

¹As it was evident from the simulation in the previous paragraph, this is not what happens in reality, since there is no way of enforcing a perfectly symmetric limit cycle with a simple PD controller, unless more complex control strategies are implemented. Nonetheless, the following analysis is conservaive, inasmuch as the symmetric limit cycle is the fastes one (its period is the shortest), thus requiring the maximum number of pulses per unit time. This means that the estimate of the fuel consumption in this situation is a worst-case-scenario.

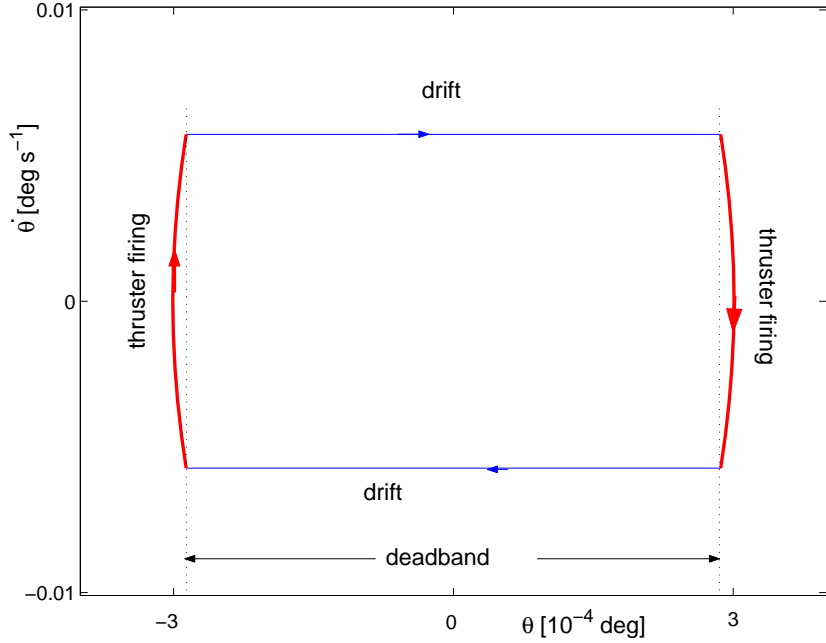


Figure 3.11: Limit cycle for gas-jet fine pointing control.

for a symmetric limit cycle, in order to exactly revert the satellite motion after the firing. Remembering that

$$I_{sp} = \frac{F \Delta t_{on}}{g \Delta m_f}$$

one gets, for each thruster firing, a fuel consumption of

$$\Delta m_f = 2 \frac{F \Delta t_{on}}{g I_{sp}} = 2 \frac{J \dot{\theta}_d}{g \ell I_{sp}}$$

Considering both sides of the deadband, the total fuel consumption per cycle is

$$\Delta m_{f,tot} = 4 \frac{J \dot{\theta}_d}{g \ell I_{sp}}$$

Ignoring the (usually negligible) thruster pulse time, the duration of the limit cycle is

$$T_{LC} \approx 4 \frac{\theta_{db}}{\dot{\theta}_d}$$

and the average fuel consumption (that is the fuel burned per unit time) is

$$\bar{m}_f = \frac{\Delta m_{f,tot}}{T_{LC}} = \frac{J \dot{\theta}_d^2}{g \ell I_{sp} \theta_{db}}$$

which can be rewritten as

$$\bar{m}_f = \frac{(F \ell \Delta t_{on})^2}{g \ell I_{sp} J \theta_{db}}$$

This latter equation shows clearly that in order to achieve a great accuracy (small value of θ_{db}) without paying too a great penalty in terms of fuel consumption, the characteristics of the thrusters are of paramount importance, inasmuch as \bar{m}_f remains small only if high specific impulse thrusters are employed, capable of delivering the force F for a very short pulse time Δt_{on} .

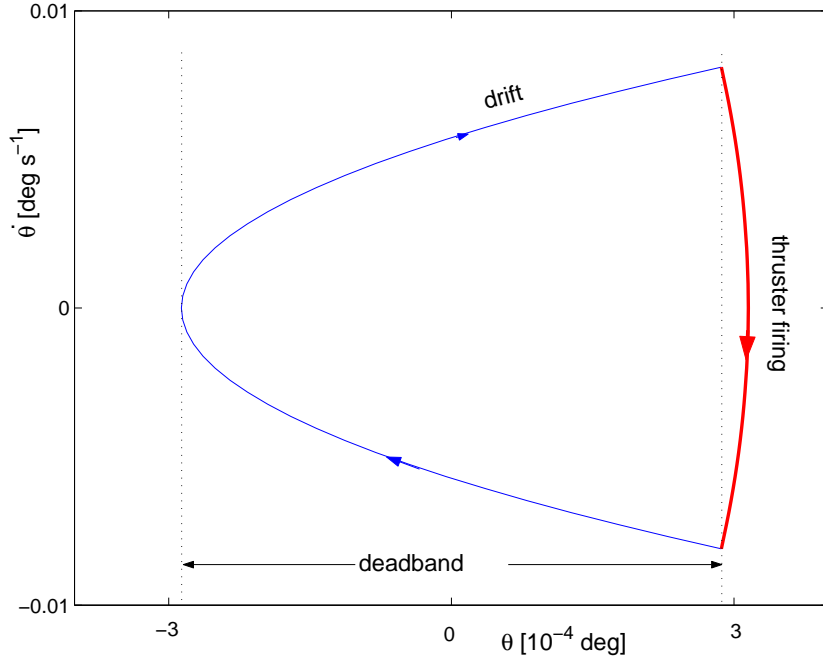


Figure 3.12: Limit cycle for gas-jet fine pointing control with constant disturbance torque.

Bias torque compensation

In most cases, the payload must be aimed at a target (be it on Earth or in the open space) in presence of external disturbances. If the resulting torque is roughly constant, such as that due to the gravity gradient, it is possible to use this torque for reversing the motion on one side of the deadband. In this case, the environmental torque will bring the spacecraft drifting towards the top of the tolerance interval. At this point the thruster are fired, to reverse the motion, that will be slowed down by the adverse disturbance torque. Rather than allowing the spacecraft to reach the other side of the deadband and fire a second thruster pulse, one allows the bias torque to slow and reverse the drift inside the deadband interval. The limit cycle will be made of two parabolic arcs, one relative to the thruster firing phase, similar to that of the previous case, that reverse the satellite motion on one side of the deadband, and the second arc, relative to the slow deceleration and motion reversal due to the external torque.

If the disturbance torque generates an angular acceleration

$$\ddot{\theta} = \alpha_D = M_D/J$$

it is

$$\begin{aligned}\dot{\theta}(t) &= \dot{\theta}_0 + \alpha_D \Delta t \\ \theta(t) &= \theta_0 + \dot{\theta}_0 \Delta t + \alpha_D \Delta t^2 / 2\end{aligned}$$

where the subscript 0 indicates the initial condition at time t_0 . From the first equation, it is $\Delta t = (\dot{\theta}(t) - \dot{\theta}_0)/\alpha_D$, that, substituted in the second one, after some simple algebra gives

$$\dot{\theta}^2 = \dot{\theta}_0^2 + 2\alpha_D(\theta(t) - \theta_0)$$

If the initial condition is on the deadband limit, it is $\theta_0 = \theta_{db}$. In order to keep the limit cycle inside the dead band, the turning point at which $\dot{\theta}$ drops to zero and reverts its sign

must be crossed on the other side of the deadband, when $\theta_0 = -\theta_{db}$. In this case, it is

$$\dot{\theta}^2 = 0 = \dot{\theta}_0^2 + 2\alpha_D(-2\theta_{db})$$

that is

$$\theta_{db} = \frac{J\dot{\theta}_0^2}{4M_D}$$

In order to close the limit cycle, the thruster pulse must be such that the total $\Delta\dot{\theta}$ is twice the drift angular velocity $\dot{\theta}_0$ at deadband crossing,

$$\Delta\dot{\theta} = 2\dot{\theta}_0 = 2F\ell\Delta t_{on}/J$$

Substituting the latter expression in the equation of θ_{db} one gets

$$\theta_{db} = \frac{(F\ell\Delta t_{on})^2}{4M_D J}$$

and again the requirement on the thruster is to deliver a small duration pulse for keeping the deadband small enough to satisfy fine pointing requirements.

Exercise

After determining the duration of the limit cycle in presence of a bias torque, where as usual the firing time can be considered negligible, prove that the average fuel consumption $\bar{m}_f = \Delta m_{f,tot}/T_{LC}$ is independent of the θ_{db} , if the motion reversal under the action of the disturbance torque exploits the whole deadband amplitude.

3.7 Momentum exchange devices for attitude control

Gas jets can deliver very high torque to manoeuvre a spacecraft and change its orientation, but they have a limited life, due to the finite propellant mass budget available. For this reason, it is important to rely on some different kind of actuators for stabilising and controlling satellite attitude during normal operations, without using propellant.

Reaction wheels (RWs) and momentum–bias wheels (MBWs) can exchange angular momentum with the spacecraft bus using only electrical power, that is obtained from the solar panels for the whole lifetime of the satellite. Each wheel is attached to the satellite structure through an electric motor, that can be used to accelerate or decelerate the wheel, relatively to the satellite. If we assume that initially both the satellite and the wheel are still in the inertial frame (zero angular momentum initial condition), spinning up the wheel in one direction will cause the bus to rotate in the opposite direction, because of conservation of overall angular momentum.

Let us consider a single axis rotation about the principal axis of inertia \hat{e}_i . The spacecraft has a total principal moment of inertia J_i about \hat{e}_i , including the wheel. The wheel spins around the axis $\hat{a} = \hat{e}_i$, having a spin moment of inertia I_s about \hat{a} and angular velocity Ω , relative to the spacecraft bus. Its rotation does not change the actual mass distribution, so that J_i is independent of the motion of the wheel.

The overall angular momentum about \hat{e}_i is

$$h_i = J_i\omega_i + I_s\Omega$$

where the first term is the angular momentum of the satellite induced by the overall rotation rate ω_i , while the second one is the relative angular momentum stored in the wheel.

Note that the absolute angular velocity of the wheel is $\Omega + \omega_i$ with respect to the inertial frame \mathcal{F}_I . If initially $\omega_i = \Omega = 0$, so that $h_i = 0$, and taking into account that the total angular momentum is conserved, inasmuch as the wheel is spun up or slowed through the exchange of internal torques applied by the electric motor, one gets

$$\omega_i = -\frac{I_s}{J_i}\Omega \quad (3.5)$$

Usually it is $I_s \ll J_i$, so that $\omega_i \ll \Omega$, that is the angular velocity achieved by the spacecraft is only a small fraction of the relative spin angular velocity of the wheel.

In order to manoeuvre the spacecraft about 3 axes, it is necessary to equip the satellite with at least 3 RWs, one for each body axis. The cluster of RWs usually contains a fourth spare wheel, the axis of which is oriented in such a way so as to exchange angular momentum components to or from any of the three axes, if one of the main wheels fails.

One of the wheels can be used to de-spin the satellite after orbit acquisition. In such a case, this wheel shall be oriented as the spin axis of the satellite and apogee kick rocket motor stack and it is called a *momentum wheel*. Its angular momentum is unlikely to drop back to zero and the control torques about its axis will be obtained accelerating and decelerating the wheel.

The MBW will also provide a certain degree of gyroscopic stability, which is an interesting feature. At the same time, the presence of the momentum bias will couple the motion about the other two axis because of the gyroscopic effect observed when deriving the equations of motion of gyrostats. As a consequence, it is no longer possible to consider separately the control problem about the principal axis of inertia. In spite of this fact, only single-axis rotations will be considered in what follows, for the sake of simplicity.

3.7.1 Open-loop control with RWs

Assuming for simplicity torque-free motion, we will size a reaction wheel with respect to requirements in single axis slew manoeuvre. Dropping the i subscript, the total angular momentum about one of the principal axis is

$$h = h_s + h_w$$

where $h_s = (J - I_s)\omega$ is the spacecraft angular momentum (without the wheel), while $h_w = J_{sw}(\Omega + \omega)$ is the spin wheel absolute angular momentum. Since there are no external torques, $h = \text{const}$ and

$$\dot{h} = \dot{h}_s + \dot{h}_w = 0 \implies \dot{h}_s = -\dot{h}_w$$

where $g_a = \dot{h}_w$ is the motor torque applied to the spin wheel.

Note that, assuming single axis rotations, it is $\omega = \dot{\theta} \Rightarrow \dot{\omega} = \ddot{\theta}$, and the equation of motion can thus be written in the form

$$(J - I_s)\ddot{\theta} = -g_a$$

which has exactly the same form derived for the RCS case, with the only difference of the sign in the control torque, which, in the case of RWs or MBWs is a reaction torque.

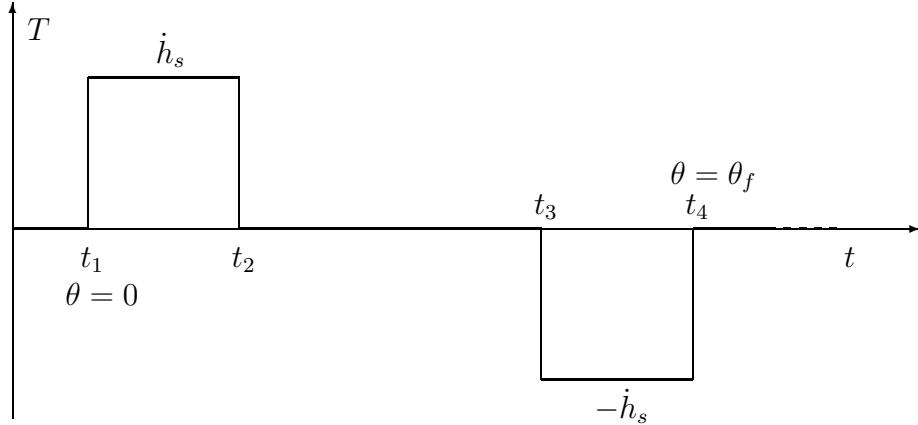


Figure 3.13: Torque profile for a single axis slew manoeuvre.

As a consequence, a similar open-loop control technique can be used, where one pulse is used for spinning up the reaction wheel and consequently the vehicle in the opposite direction, achieving a certain drift angular velocity, according to Eq. (3.5), while a second pulse will spin down both the spacecraft and the wheel, achieving at the end of the manoeuvre the desired attitude θ_f .

After the first pulse, the spacecraft gains an angular momentum equal to

$$h_s(t_2 - t_1) = (J - I_s)\dot{\theta} = -\dot{h}_w(t_2 - t_1) = -g_a(t_2 - t_1)$$

But it is also

$$\dot{h}_s = (J - I_s)\ddot{\theta} = (J - I_s)\alpha$$

where $\alpha = \ddot{\theta} = -g_a/(J - I_s)$ is the angular acceleration of the spacecraft. The evolution of the angular displacement is thus given, as in the RCS case, by

$$\begin{aligned}\theta(t_2) &= \frac{1}{2}\alpha(t_2 - t_1)^2 \\ &= -\frac{1}{2}\frac{g_a}{J - I_s}(t_2 - t_1)^2\end{aligned}$$

Note that simpler expressions can usually be employed for preliminary sizing purposes, by remembering that usually it is $J \gg I_s$. On the other side, the value of the available torque is usually much smaller than that obtained from thrusters, so that the pulse duration is not negligible with respect to manoeuvre time.

As an advantage of reaction and momentum bias wheels, the fact that electrical power (and no fuel) is employed for accelerating and decelerating the wheel make it possible to perform fast manoeuvres, without paying any penalty in terms of operational lifetime with respect to slower ones.²

3.7.2 Sizing a reaction wheel for single axis slews

For a minimum-time rotation, a bang-bang control must be used, so that $t_2 \equiv t_3$ and the final rotation angle is

$$\theta_f = 2\theta(t_2) = \frac{\dot{h}_s}{J - I_s}(t_2 - t_1)^2$$

²On the converse, a faster drifting phase requires more acceleration and deceleration from the reaction control system, which means more fuel is burned for achieving the same final attitude. This means that the satellite will run out of fuel sooner, if fast manoeuvres are performed instead of slow ones.

But assuming $t_1 = 0$, it is also $t_f = 2(t_2 - t_1)$, for bang–bang control, and one gets

$$\theta_f = \frac{1}{4} \frac{\dot{h}_s}{J - I_s} t_f^2$$

Because of conservation of angular momentum, we recall that $\dot{h}_s = -\dot{h}_w$, so that the maximum torque that the electric rotor must produce is

$$g_{a,\max} = |\dot{h}_w| = 4 \frac{(J - I_s)\theta_f}{t_f^2}$$

But for $t = t_2$, it is also

$$h_s(t_2) = (J - I_s)\dot{\theta}(t_2) = -h_w(t_2) = -\dot{h}_w(t_2 - t_1) = -\dot{h}_w t_f / 2$$

when the wheel achieves the maximum angular momentum. This means that the momentum capacity of the wheel must be

$$h_w^{\max} \geq 2(J - I_s) \frac{\theta_2}{t_f}$$

Numerical example

We require a spacecraft with $J = 100 \text{ kg m}^2$ to perform a 0.2 rad slew in 10 sec . This means that the electric motor must apply torques in both direction equal to (neglecting the unknown value of I_s)

$$\dot{h}_w \approx 4 \frac{J\theta_f}{t_f^2} \frac{4 \times 100 \times 0.2}{10^2} = 0.8 \text{ Nm}$$

The maximum momentum stored in the RW is reached when half of the reorientation is completed, so that the RW capacity must be at least

$$h_w^{\max} \approx 2J \frac{\theta_2}{t_f} = \frac{2 \times 100 \times 0.2}{10} = 4 \text{ kg m}^2 \text{s}^{-1}$$

Assuming a wheel inertia $J_{sw} = 0.03 \text{ kg m}^2$, the maximum wheel angular rate with respect to the satellite bus is

$$\begin{aligned} \Omega &= -\frac{J}{I_s}\omega = -\frac{J}{I_s} \frac{h_s}{J - I_s} \\ &\approx \frac{h_w}{J_{sw}} = 133 \text{ rad s}^{-1} = 21.2 \text{ rpm} \end{aligned}$$

3.7.3 Closed-loop control with RWs for single axis slews

With the usual meaning of the symbols, the equation of motion for single-axis rotation is

$$\frac{d}{dt} (J\dot{\theta} + I_s\dot{\Omega}) = M_{\text{ext}}$$

so that it is

$$J\ddot{\theta} + I_s\dot{\Omega} = M_{\text{ext}} \quad (3.6)$$

The reaction wheel dynamics is described by the first order equation

$$I_s (\dot{\Omega} + \ddot{\theta}) = g_a \Rightarrow I_s \dot{\Omega} = g_a - I_s \ddot{\theta}$$

Substituting the latter expression in Eq. (3.6) and assuming for simplicity that the external torque and the momentum bias are both zero, it is possible to rearrange the dynamics equation as

$$(J - I_s) \ddot{\theta} = -g_a$$

By choosing a simple PD control in the form

$$g_a = K_P(\theta_{\text{des}} - \theta) + K_D \dot{\theta} \quad (3.7)$$

the closed-loop dynamics is described by the second order differential equation

$$J^* \ddot{\theta} + K_D \dot{\theta} - K_P \theta = -K_P \theta_{\text{des}}$$

where $J^* = J - I_s$ is the moment of inertia of the platform without the spin-wheel.³

By defining the closed-loop system bandwidth as $p^2 = -K_P/J^*$ (with K_p strictly negative for static stability) and a damping parameter ζ such that $2\zeta p = K_D/J^*$ (with K_D strictly positive for asymptotic stability), the equation of motion can be rewritten in the form

$$\ddot{\theta} + 2\zeta p \dot{\theta} + p^2 \theta = p^2 \theta_{\text{des}}$$

which can be solved analytically and clearly presents a nice way of choosing the gains K_P and K_D .

3.7.4 Bias torque and reaction wheel saturation

Let us assume for simplicity that the satellite is subject to a constant disturbance torque M_D . It is easy to see that the angular displacement θ evolves according to the differential equation

$$\ddot{\theta} + 2\zeta p \dot{\theta} + p^2 \theta = p^2 \theta_{\text{des}} + M_D/J^*$$

and asymptotically converge to the steady state

$$\theta_{ss} = \theta_{\text{des}} + M_D/K_P \neq \theta_{\text{des}}$$

This means that the use of the control law of Eq. (3.7) may not guarantee a sufficient pointing accuracy. The steady state error can be made smaller by increasing the proportional gain K_P , but it will never vanish. Moreover, increasing the gain will likely degrade the performance of the real system, since the sensor noise will also be multiplied by a high gain.

It is possible to asymptotically cancel the steady state error by adding an integral term to the control law, i.e.

$$g_a = K_P(\theta_{\text{des}} - \theta) + K_D \dot{\theta} + K_I y \quad (3.8)$$

where

$$\dot{y} = \theta_{\text{des}} - \theta \Rightarrow y = \int (\theta_{\text{des}} - \theta) dt$$

³Note that the feedback control law duplicates exactly the control law employed for reaction control systems, Eq. (3.3), but because g_a is a reaction torque, the gains appears with their sign changed in the equation of the closed loop system dynamics. Their values must be chosen accordingly.

If an integral term is introduced, a steady-state can be achieved only if $\dot{y} = 0$, i.e. $\theta = \theta_{\text{des}}$, with a value of y such that

$$K_I y = M_D \Rightarrow g_{a,ss} = M_D$$

This means that if the spacecraft is subject to a constantly not null external torque, the average value of which is not zero (aerodynamic torque, gravity gradient), the platform can be maintained aimed at a fixed position only if an equivalent motor torque is delivered to the reaction wheel. As a consequence, the wheel will absorb these disturbances by spin-up and fix the orientation, but its angular velocity will constantly increases. Should the wheel reach the maximum spinning speed, the attitude control system is saturated.

In order to avoid such a problem, before reaching saturation it is necessary to dump the angular momentum excess. This can be done simply braking the wheel and firing the thrusters in the opposite direction. In this way the momentum accumulated in the wheel is brought back to zero, because of the external torque produced by the thrusters. During wheel desaturation the pointing accuracy of the control system is usually reduced.

The use of thrusters for despinning the wheels shows that also when using RWs for attitude control it is necessary to carefully design the propellant mass budget. Thruster firings will be also in this case the main source of fuel consumption during the station keeping phase, and will be the main limit to the satellite operative life.

3.7.5 Roll–yaw axes control in presence of momentum bias using reaction wheels

In order to derive the (linearized) equation of motion of a satellite equipped with a momentum wheel parallel to the pitch axis and two reaction wheels for roll and yaw control, the angular momentum can be expressed as

$$\mathbf{h}_B = \mathbf{I}\boldsymbol{\omega}_B + \mathbf{H}_B$$

where

$$\mathbf{H}_B = I_b(\Omega_0 + \Delta\Omega)\mathbf{e}_{2B} + I_r\Omega_1\mathbf{e}_{1B} + I_r\Omega_3\mathbf{e}_{3B}$$

is the angular momentum stored in the spinning wheel, I_b being the moment of inertia of the pitch-axis bias-momentum wheel while I_r is the moment of inertia of the two reaction wheels. Writing \mathbf{H}_B as

$$\mathbf{H}_B = \mathbf{H}_{0B} + \Delta\mathbf{H}_B = (0, h_0, 0)^T + (\Delta h_1, \Delta h_2, \Delta h_3)^T = (0, I_b\Omega_0, 0)^T + (I_r\Omega_1, I_b\Delta\Omega, I_r\Omega_3)^T$$

and assuming that $\|\mathbf{I}\boldsymbol{\omega}_B\|, \|\Delta\mathbf{H}_B\| \ll h_0$, the equation of motion can be written as

$$\mathbf{I}\dot{\boldsymbol{\omega}}_B + I_b\Delta\dot{\Omega}\mathbf{e}_{2B} + I_r\dot{\Omega}_1\mathbf{e}_{1B} + I_r\dot{\Omega}_3\mathbf{e}_{3B} + \boldsymbol{\omega}_B \times I_b\Omega_0 = \mathbf{M}_B$$

where higher order terms have been neglected. Each wheel is characterized by a dynamics in the form

$$I\ddot{\Omega} = g_a - I\dot{\omega}$$

Assuming finally a small angular displacement, so that $\dot{\boldsymbol{\omega}}_B = \ddot{\boldsymbol{\theta}}$, the pitch equation is decoupled from the others and takes the form already discussed in the previous paragraph, while the coupled roll–yaw dynamics is described by the following system of ordinary differential equation:

$$\begin{aligned} J_1\ddot{\theta}_1 + I_r\dot{\Omega}_1 - I_b\Omega_0\dot{\theta}_3 &= M_1 \\ J_3\ddot{\theta}_1 + I_r\dot{\Omega}_3 + I_b\Omega_0\dot{\theta}_1 &= M_3 \end{aligned}$$

Coupling these equation with the dynamics of the reaction-wheels

$$\begin{aligned}\dot{\Omega}_1 &= g_{a_1}/I_r - \ddot{\theta}_1 \\ \dot{\Omega}_3 &= g_{a_3}/I_r - \ddot{\theta}_3\end{aligned}$$

one gets the system of (linear) equations

$$\begin{aligned}(J_1 - I_r)\ddot{\theta}_1 - I_b\Omega_0\dot{\theta}_3 &= -g_{a_1} + M_1 \\ (J_3 - I_r)\ddot{\theta}_3 + I_b\Omega_0\dot{\theta}_1 &= -g_{a_3} + M_3\end{aligned}$$

Choosing for both reaction wheels spin-torque command laws in the form

$$g_{a_i} = K_{P_i}\theta_i + K_{D_i}\dot{\theta}_i$$

and taking the Laplace transform of the system of linear ordinary differential equation, one gets for the torque-free case ($M_1 = M_3 = 0$) the following algebraic equation in the Laplace variable s :

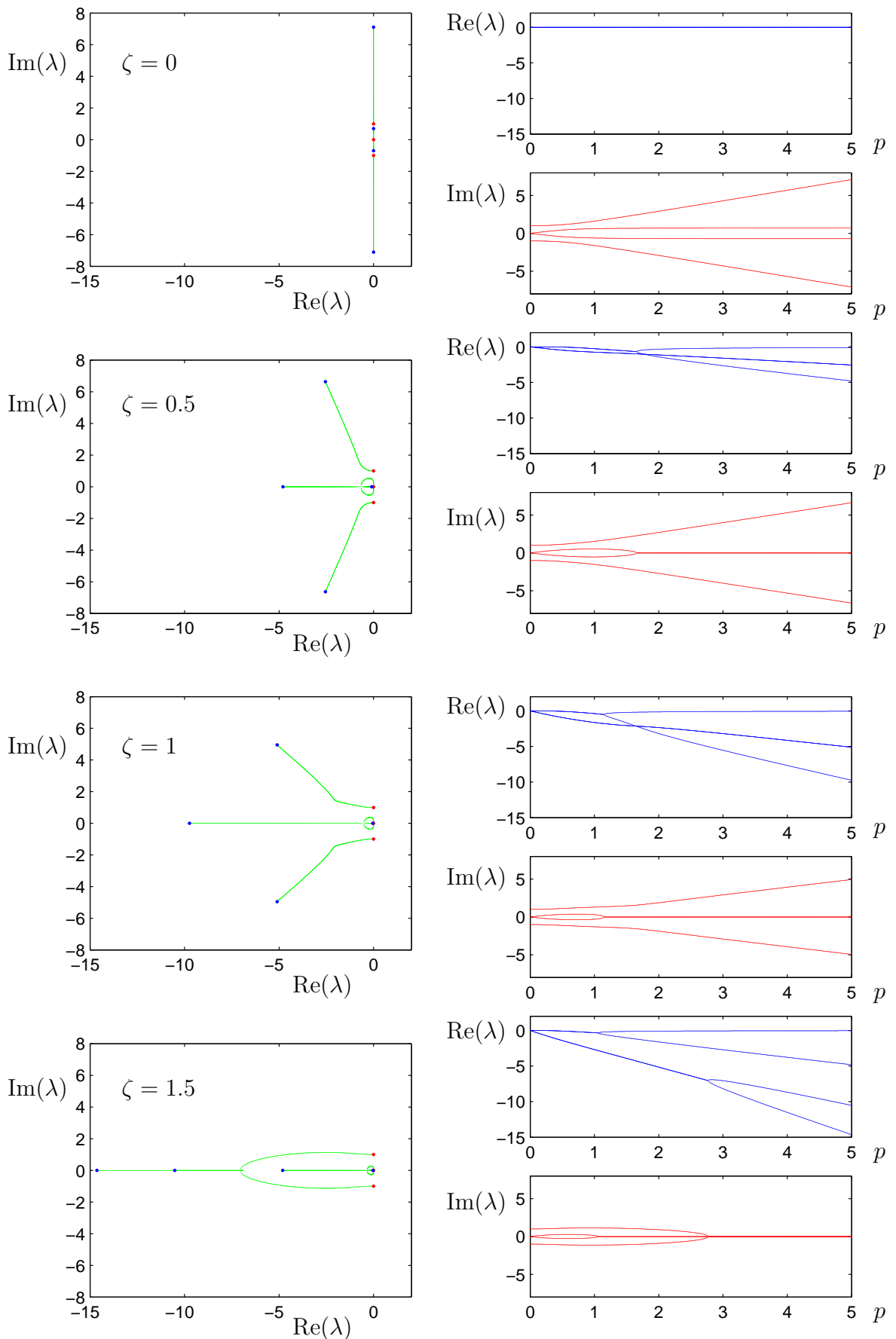
$$\begin{bmatrix} s^2 + 2\zeta_1 p_1 s + p_1^2 & -\gamma_1 s \\ \gamma_2 s & s^2 + 2\zeta_2 p_2 s + p_2^2 \end{bmatrix} \begin{pmatrix} \bar{\theta}_1(s) \\ \bar{\theta}_3(s) \end{pmatrix} = \begin{pmatrix} 0 \\ 0 \end{pmatrix}$$

where $p_i^2 = K_{P_i}/(J_i - I_r)$ and $2\zeta_i p_i = K_D/(J_i - I_r)$, while the gyroscopic coupling term is represented by the coefficient $\gamma_i = I_b\Omega_0/(J_i - I_r)$. With a proper choice of the gains, it is possible to have $p_1 = p_2$ and $\zeta_1 = \zeta_2$, which means that perturbations about roll and yaw axes are damped with similar time behaviour. Moreover, in such a case the number of design parameter is reduced to two and a simple parametric study is possible. It should be noted that, independently of the choice of the controller parameters, the proposed control law requires an explicit estimate of the yaw angle, which may not be a trivial task. A direct measure of the roll angle is usually available from a Earth horizon sensor, while the yaw angle can be measured directly only with the aid of an expensive star tracker. As an alternative, a rate-integrating gyro may be used, where care must be taken on the closed loop dynamics of the effects of gyro drift and integration of the sensor noise over large period of time.

Figure 3.14 shows this study for $\gamma = 1$. As it can be observed, for $\zeta = 0$, the closed loop dynamics presents undamped oscillations for all the values of p , which means that, as usual, a feedback on angular displacement only is not capable of providing asymptotic stability to the origin. For subcritical damping ($\zeta \leq 1$), the eigenstructure is characterized by two pairs of complex conjugate eigenvalues, for low values of the proportional gain K_P . Beyond a certain critical value (corresponding to $p_{cr} = 1.65$, for $\zeta = 0.5$), a couple of complex conjugate roots collapses and two real negative eigenvalues are found for higher values of p . One of them tends towards the origins, as p is increased, so that extremely high proportional gains are not convenient. The critical value at which a pair of complex conjugate roots is replaced by two real eigenvalues decreases as ζ is increased. In the supercritical range, for $\zeta > 1$, the root locus changes its structure and regions of p can be found where all the eigenvalues are real.

3.7.6 Roll-yaw axes control using a double-gimbal momentum wheel

An approach very similar to that used for the case of a pitch axis momentum bias wheel plus two reaction wheels can be used of deriving the equation of motion of a satellite

Figure 3.14: Root locus as a function of p for different values of ζ .

equipped with a double-gimbal momentum wheel. The angular momentum can be expressed again as

$$\mathbf{h}_B = \mathbf{I}\boldsymbol{\omega}_B + \mathbf{H}_B$$

where

$$\mathbf{H}_B = I_b(\Omega)\mathbf{a}_B$$

is the angular momentum stored in the spinning wheel, I_b being the moment of inertia of the pitch-axis momentum wheel, while the spin axis can be deflected by the gimbals from its nominal position parallel to the pitch axis, so that

$$\mathbf{a}_B = (-\cos \delta_2 \sin \delta_1, \cos \delta_1 \cos \delta_2, \sin \delta_2)^T$$

Assuming that the gimbal rotation angles δ_1 and δ_2 are small, it is $\mathbf{a}_B \approx (-\delta_1, 1, \delta_2)^T$. In this case \mathbf{H}_B can be written in the form

$$\begin{aligned} \mathbf{H}_B = \mathbf{H}_{0B} + \Delta \mathbf{H}_B &= (0, h_0, 0)^T + (\Delta h_1, \Delta h_2, \Delta h_3)^T \\ &= (0, I_b \Omega_0, 0)^T + (-I_b \Omega_0 \delta_1, I_b \Delta \Omega, I_b \Omega_0 \delta_2)^T \end{aligned}$$

Assuming again that $\|\mathbf{I}\boldsymbol{\omega}_B\|, \|\Delta \mathbf{H}_B\| \ll h_0$, the linearized equation of motion for small amplitude angular displacement is obtained neglecting higher order terms as

$$\mathbf{I}\dot{\boldsymbol{\omega}}_B + \Delta \dot{\mathbf{H}}_B + \boldsymbol{\omega}_B \times I_b \Omega_0 = \mathbf{M}_B$$

which becomes, choosing the set of principal axes of inertia as the body frame,

$$\begin{aligned} J_1 \ddot{\theta}_1 + \Delta \dot{H}_1 - h_0 \dot{\theta}_3 &= M_1 \\ J_2 \ddot{\theta}_1 + \Delta \dot{H}_2 &= M_2 \\ J_3 \ddot{\theta}_1 + \Delta \dot{H}_3 + h_0 \dot{\theta}_1 &= M_3 \end{aligned}$$

As usual, the pitch dynamics is decoupled and is not repeated here, while roll and yaw equation of motion are coupled by the gyroscopic term. Letting $u_r = -\Delta \dot{h}_1$ and $u_y = -\Delta \dot{h}_3$ be the control variables, the coupled roll–yaw dynamics is described by the following set of linear second order equations:

$$\begin{aligned} J_1 \ddot{\theta}_1 - h_0 \dot{\theta}_3 &= u_r + M_1 \\ J_3 \ddot{\theta}_3 + h_0 \dot{\theta}_1 &= u_y + M_3 \end{aligned}$$

where the gimbal rotation command is

$$\begin{aligned} \dot{\theta}_1 &= u_r / h_0 \\ \dot{\theta}_2 &= -u_y / h_0 \end{aligned}$$

It is clear that the same control law derived for the cluster of momentum bias wheel and reaction wheels can be implemented with a double-gimbal hardware, provided that the control power made available by the rotation of the gimbals is sufficient for the prescribed stabilization and control purposes.

3.8 Quaternion feedback control

Many satellites are reoriented performing successive rotation about the control axis, in order to achieve the desired attitude. Unfortunately, this strategy, although very simple to be implemented, is not time-optimal nor optimal in terms of fuel or energy consumption. The overall angular path is far in excess the minimum one described by the Euler rotation about the Euler's axis. The quaternion feedback control provides a means for obtaining a nearly-optimal reorientation, with a control logic only marginally more complex.

3.8.1 Derivation of a globally asymptotically stabilizing controller: Lyapunov method

The potential function method for nonlinear control stems directly from Lyapunov's second method: an extended form of the Lyapunov function, referred to as the potential function, is analytically defined with a global minimum at the target state. According to Lyapunov's second theorem, the state vector converges to the goal point if the rate of change of the potential is negative definite. The mechanism which drives the convergence is thus based upon the rate of change of the potential function $V = V(\mathbf{x})$: whenever the rate of change of V is positive for the unforced system, the state vector will diverge from the goal point unless some form of control over the system is available, in which case it is possible to make negative by properly tailoring the control action. In this way, given a dynamical system described by a set of differential equations in the form $\dot{\mathbf{x}} = \mathbf{f}(\mathbf{x}, \mathbf{u})$, where \mathbf{u} indicates a set of available control variables, it is possible to derive a control methodology which forces the convergence to the desired goal condition, indicated by the symbol $\bar{\mathbf{x}}$.

Convergence to $\bar{\mathbf{x}}$ and global stability can be enforced by building a candidate Lyapunov potential function that has a global minimum in $\bar{\mathbf{x}}$, that is, such that

- 1) $V(\bar{\mathbf{x}}) = 0$
- 2) $V(\mathbf{x}) = 0$ for $\mathbf{x} \neq \bar{\mathbf{x}}$
- 3) $V(\mathbf{x}) \rightarrow \infty$ for $\|\mathbf{x}\| \rightarrow \infty$

Once a candidate Lyapunov function is available, its rate of change is given by

$$\dot{V}(\mathbf{x}) = \frac{\partial V}{\partial \mathbf{x}} \frac{d\mathbf{x}}{dt} = \frac{\partial V}{\partial \mathbf{x}} \mathbf{f}(\mathbf{x}, \mathbf{u})$$

By choosing a control action $\mathbf{u} = \mathbf{u}(\mathbf{x})$ such that

$$4) \quad \dot{V}(\mathbf{x}) < 0 \text{ for } \mathbf{x} \neq \bar{\mathbf{x}}$$

Lyapunov theorem guarantees that the resulting closed loop system is globally asymptotically stable in $\bar{\mathbf{x}}$ and thus, once the final target state has been defined, controllable. This method for the generation of closed-loop control functions has the advantage of allowing the implementation of non-linear controls for wide amplitude manoeuvres, since the method does not hinge on linearization.

3.8.2 Application of Lyapunov method to nonlinear spacecraft attitude control

The rigid body dynamic equations written in vector form are given by

$$\mathbf{I}\dot{\boldsymbol{\omega}}_B + \boldsymbol{\omega}_B \times (\mathbf{I}\boldsymbol{\omega}_B) = \mathbf{M}_B$$

while the equation that describe the evolution of the quaternions is

$$\begin{aligned} \dot{q}_0 &= -\frac{1}{2}\mathbf{q}^T \boldsymbol{\omega}_B \\ \dot{\mathbf{q}} &= \frac{1}{2}(\mathbf{q}_0 \boldsymbol{\omega}_B - \boldsymbol{\omega}_B \times \mathbf{q}) \end{aligned}$$

By assuming that the fixed reference frame coincides with the desired attitude, it is possible to express a good candidate Lyapunov function as

$$V = \frac{1}{2}\boldsymbol{\omega}_B^T \mathbf{I} \boldsymbol{\omega}_B + k\mathbf{q}^T \mathbf{q}$$

where $k > 0$ is an arbitrary positive constant. It is easy to show that V satisfies conditions (1), (2) and (3). By evaluating \dot{V} from the equations of motion,

$$\begin{aligned}\dot{V} &= \boldsymbol{\omega}_B^T (\mathbf{I} \dot{\boldsymbol{\omega}}_B) + 2k\mathbf{q}^T \dot{\mathbf{q}} \\ &= \boldsymbol{\omega}_B^T [M_B - \boldsymbol{\omega}_B \times (\mathbf{I} \dot{\boldsymbol{\omega}}_B)] + k\mathbf{q}^T (q_0 \boldsymbol{\omega}_B - \boldsymbol{\omega}_B \times \mathbf{q}) \\ &= \boldsymbol{\omega}_B^T (M_B + kq_0 \mathbf{q})\end{aligned}$$

it is immediate to show that, for any positive definite matrix \mathbf{C} , the choice of a control torque in the form

$$\mathbf{M}_B = -\mathbf{C} \boldsymbol{\omega}_B - kq_0 \mathbf{q}$$

makes $\dot{V} = -\boldsymbol{\omega}_B^T \mathbf{C} \boldsymbol{\omega}_B$ strictly negative definite, unless the spacecraft is at rest ($\boldsymbol{\omega}_B = 0$) in the reference attitude ($\mathbf{q} = (0, 0, 0)^T$), that is, also condition (4) is satisfied and M_B provides a globally asymptotically stabilising control law.

It should be noted that the extreme flexibility in choosing both the gain matrix \mathbf{C} and the quaternion coefficient k , which are required only to be positive definite, make the control law stabilising also in the presence of saturation of one or more of the control channels.

3.8.3 Generalization of the Quaternion Feedback Control law

Quaternions can be easily computed by modern attitude determination systems and for this reason their use is nowadays very common. As a consequence, a simple feedback control law based on the information obtained from the attitude sensors is very easily implementable on-board for autonomous manoeuvre management.

It is possible to demonstrate that, by means of the use of the quaternion error vector \mathbf{q}_e , a feedback law in the form

$$\mathbf{M}_B = -\mathbf{K} \mathbf{q}_e - \mathbf{C} \boldsymbol{\omega}_B$$

where $\mathbf{q}_e = (q_{1e}, q_{2e}, q_{3e})^T$ is the attitude error quaternion vector, is globally asymptotically stabilizing onto any arbitrary desired attitude, $(q_{0,d}, \mathbf{q}_d^T)^T$, for a wide choice of the gain matrices \mathbf{K} and \mathbf{C} .

When the desired attitude is fixed, it is possible to assume without loss of generality that the “absolute” reference frame coincides with the desired attitude (and in case switch to another absolute frame if a new attitude needs to be acquired), so that $(q_{0,d}, q_{1,d}, q_{2,d}, q_{3,d})^T = (1, 0, 0, 0)^T$ and $\mathbf{q}_e \equiv \mathbf{q}$. In this case the control logic can be rewritten as

$$\mathbf{M}_B = -\text{sign}(q_{0,c}) \mathbf{K} \mathbf{q} - \mathbf{C} \boldsymbol{\omega}_B$$

where the $\text{sign}(q_{0,c})$ coefficient is introduced in order to accept as possible target attitudes both $(\pm 1, 0, 0, 0)^T$ unit quaternions.⁴ Note that the interpretation of the gain matrices \mathbf{K} and \mathbf{C} as artificial stiffness and damping coefficients allows to size the gains using procedures similar to those employed for single axis control.

Among the simplest possible globally stabilizing controllers, we have

⁴Remember that the quaternions $(q_0, q_1, q_2, q_3)^T$ and $(-q_0, -q_1, -q_2, -q_3)^T$ represent the same attitude.

$$\begin{aligned}
\text{Controller 1: } \mathbf{K} &= k\mathbf{1}, & \mathbf{C} &= \text{diag}(c_1, c_2, c_3) \\
\text{Controller 2: } \mathbf{K} &= \frac{k}{q_4^3}\mathbf{1}, & \mathbf{C} &= \text{diag}(c_1, c_2, c_3) \\
\text{Controller 3: } \mathbf{K} &= k \text{ sign}(q_4)\mathbf{1}, & \mathbf{C} &= \text{diag}(c_1, c_2, c_3) \\
\text{Controller 4: } \mathbf{K} &= [\alpha\mathbf{I} + \beta\mathbf{1}]^{-1}, & \mathbf{C} &= \text{diag}(c_1, c_2, c_3)
\end{aligned}$$

where k and c_i are positive scalar constants, $\mathbf{1}$ is the 3×3 identity matrix, $\text{sign}(q_4)$ is the sign function,⁵ and α and β are non-negative scalars.

Controller 1 is a special case of controller 4, when $\alpha = 0$. It is possible to choose $\beta = 0$ only if $\alpha \neq 0$. Controllers 2 and 3 approach the origin $(1, 0, 0, 0)^T$ taking the shorter angular path, that is, tracking an Euler rotation.

All these control laws can be implemented under the assumption that there is a set of actuators that can deliver the required amount of external torque \mathbf{M}_B , that is a set of thruster. The problem of the jet selection logic and torque saturation are beyond the scope of the present discussion.

3.9 Control Moment Gyroscopes

When using momentum management devices for attitude stabilisation and control it can be useful to write the attitude equation of motion in terms of angular momentum, instead than working with the angular velocity. Although this is true in general, it becomes practically unavoidable for modeling a satellite equipped with a cluster of Control Moment Gyroscopes (CMG).

A CMG is made of a spinning wheel mounted on a pivoting gimbal, the axis of which is perpendicular to the wheel spin axis. Instead than accelerating and decelerating the wheel for obtaining the proper reaction from the spacecraft platform, the momentum exchange between the wheel and the bus is achieved rotating the wheel spin axis about the gimbal. In this way a gyroscopic torque is obtained in a direction perpendicular to both the spin and the gimbal axes. At least three gimballed wheels are necessary for full three-axis control, but a minimum of 4 CMG's is usually employed. A higher number of wheels can be considered for increasing system redundancy and overall control power. Figure 3.15 shows a cluster of 4 CMG's in a pyramid mounting, that for a skew angle $\beta \approx 53$ deg produces a quasi-spherical angular momentum envelope, that is, the maximum angular velocity that can be commanded by the cluster is almost independent of the direction of the desired rotation axis.

3.9.1 Model of a spacecraft controlled by a cluster of CMG's

When the dynamic state of the spacecraft is expressed in terms of the (conserved) angular momentum vector, the equation of motion is rewritten as

$$\dot{\mathbf{h}}_B + \boldsymbol{\omega}_B \times \mathbf{h}_B = \mathbf{M}_B$$

where \mathbf{h}_B is the overall angular momentum (expressed in body-frame components). If the spacecraft is a rigid body, it is simply

$$\mathbf{h}_B = \mathbf{I}\boldsymbol{\omega}_B$$

⁵The sign function is 1 when the argument is positive, -1 when it is negative.

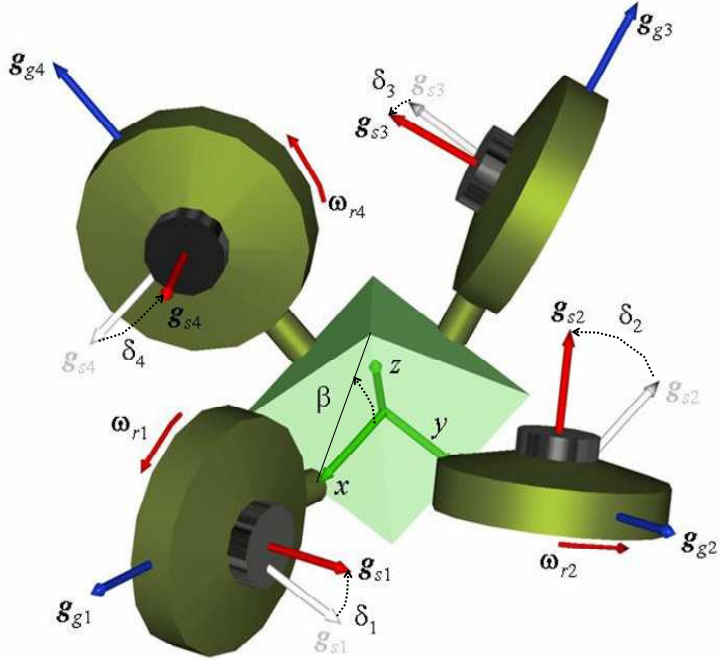


Figure 3.15: Pyramid mounting for a cluster of 4 CMG's.

and the equation can be trivially rewritten in the previous formulation. If on the converse the spacecraft has n rotating parts, it is

$$\mathbf{h}_B = \mathbf{I}\boldsymbol{\omega}_B + \sum_{i=1}^n \mathbf{h}_{i_B}$$

where \mathbf{h}_{i_B} is the relative angular momentum vector stored inside the i -th spinning wheel.⁶ Letting

$$\mathbf{H}_B = \sum_{i=1}^n \mathbf{h}_i$$

it is

$$\mathbf{h}_B = \mathbf{I}\boldsymbol{\omega}_B + \mathbf{H}_B$$

and the equation of motion becomes

$$\mathbf{I}\dot{\boldsymbol{\omega}}_B + \boldsymbol{\omega}_B \times (\mathbf{I}\boldsymbol{\omega}_B) + \dot{\mathbf{h}}_B + \boldsymbol{\omega}_B \times \mathbf{h}_B = \mathbf{M}_B$$

where \mathbf{M}_B is the external torque acting on the spacecraft. Assuming for the sake of simplicity a torque-free environment and a zero initial angular momentum, it is possible to write the last equation as

$$\mathbf{I}\dot{\boldsymbol{\omega}}_B + \boldsymbol{\omega}_B \times (\mathbf{I}\boldsymbol{\omega}_B) = \mathbf{u}$$

where

$$\mathbf{u} = -\dot{\mathbf{H}}_B - \boldsymbol{\omega}_B \times \mathbf{H}_B$$

⁶The inertia tensor \mathbf{I} is assumed to take into consideration the contribution of the spin-wheels to the mass distribution as if they were still. For this reason only the relative contribution to angular momentum is added.

is the control torque generated by a proper action on the spinning wheels inside the spacecraft bus. The control torque demand can be determined on the basis of some feedback control logic, such as the quaternion feedback control presented in the previous section. Once the control torque demand \mathbf{u} is known, the CMG steering logic can be determined as

$$\dot{\mathbf{H}}_B = -\mathbf{u} - \boldsymbol{\omega}_B \times \mathbf{H}_B \quad (3.9)$$

For a cluster of n CMG, the internal angular momentum vector \mathbf{H}_B is a function of the rotation angles $\delta_1, \delta_2, \dots, \delta_n$ of each wheel about its gimbal axis, that is

$$\mathbf{H}_B = \mathbf{H}(\boldsymbol{\delta}) \quad (3.10)$$

Taking the time derivative of this latter equation, one gets

$$\frac{d\mathbf{H}_B}{dt} = \frac{\partial \mathbf{H}}{\partial \boldsymbol{\delta}} \frac{d\boldsymbol{\delta}}{dt}$$

that can be rewritten in compact form as

$$\dot{\mathbf{H}}_B = \mathbf{A}(\boldsymbol{\delta}) \dot{\boldsymbol{\delta}} \quad (3.11)$$

where \mathbf{A} is the jacobian matrix

$$\mathbf{A} = \frac{\partial \mathbf{H}}{\partial \boldsymbol{\delta}}$$

The problem is now that of finding a proper inversion of the equation $\dot{\mathbf{H}}_B = \mathbf{A}\dot{\boldsymbol{\delta}}$, that provides a gimbal rate command $\dot{\boldsymbol{\delta}}$ capable of delivering the required control torque \mathbf{u} for the current gimbal position $\boldsymbol{\delta}$ and angular velocity $\boldsymbol{\omega}_B$.

3.9.2 Gimbal rate command with Moore–Penrose pseudo-inverse

The case of a cluster of 4 CMG mounted with the gimbal axis perpendicular to the faces of a pyramid the sides of which are inclined of a skew angle β is the most popular in the literature. This CMG configuration, where the angular momentum vectors of each wheel span one of the faces of the pyramid, is particularly popular as it delivers a nearly spherical momentum envelope, when $\beta = 54.73$ deg and each wheel spins at the same angular velocity relative to the spacecraft bus. Assuming that the x and y body axes are perpendicular to the sides of the base of the pyramid and that the z axis is parallel to the pyramid height, it is

$$\begin{aligned} \mathbf{H}_B &= \mathbf{H}(\boldsymbol{\delta}) = \sum_{i=1}^n \mathbf{h}_{i_B} \\ &= h \left(\begin{bmatrix} -c\beta \sin \delta_1 \\ \cos \delta_1 \\ s\beta \sin \delta_1 \end{bmatrix} + \begin{bmatrix} -\cos \delta_2 \\ -c\beta \sin \delta_2 \\ s\beta \sin \delta_2 \end{bmatrix} + \begin{bmatrix} c\beta \sin \delta_3 \\ -\cos \delta_3 \\ s\beta \sin \delta_3 \end{bmatrix} + \begin{bmatrix} \cos \delta_4 \\ c\beta \sin \delta_4 \\ s\beta \sin \delta_4 \end{bmatrix} \right) \end{aligned}$$

where h is the angular momentum stored inside each CMG, while $s\beta = \sin \beta$ and $c\beta = \cos \beta$.

In order to perform the reorientation, it is necessary to drive the gimbal according to Eq. (3.11), where, for the case of the pyramid mounting, it is

$$\mathbf{A} = \begin{bmatrix} -c\beta \cos \delta_1 & \sin \delta_2 & c\beta \cos \delta_3 & -\sin \delta_2 \\ -\sin \delta_1 & -c\beta \cos \delta_2 & \sin \delta_3 & c\beta \cos \delta_4 \\ s\beta \cos \delta_1 & s\beta \cos \delta_2 & s\beta \cos \delta_3 & s\beta \cos \delta_4 \end{bmatrix}$$

and the CMG angular momentum rate is given by Eq. (3.9). A possible inversion of Eq. (3.11) is given by the Moore–Penrose pseudo–inverse matrix

$$\dot{\boldsymbol{\delta}} = \mathbf{A}^\# \dot{\mathbf{H}}_B \quad (3.12)$$

where

$$\mathbf{A}^\# = \mathbf{A}^T (\mathbf{A} \mathbf{A}^T)^{-1}$$

3.9.3 Cluster singular states

Although most of the CMG steering logic proposed in the literature are variants of this form, it should be noted that the pseudo–inverse does not exists when the matrix $\mathbf{A} \mathbf{A}^T$ becomes singular. The singular points where the determinant $\det(\mathbf{A} \mathbf{A}^T) = 0$ are characterized by a gimbal configuration such that the CMG cluster cannot deliver torque in one direction, called the singular direction. These points are distributed along hypersurfaces in the $\boldsymbol{\delta}$ –space that satisfy the singularity condition

$$\det(\mathbf{A} \mathbf{A}^T) = 0$$

or, upon transformation according to Eq. (3.10), in the angular momentum space.

The presence of singularities in the $\boldsymbol{\delta}$ space has to major consequences: (i) When approaching a singular point the gimbal rate command goes to infinity because of the increasing norm of the matrix $(\mathbf{A} \mathbf{A}^T)^{-1}$, and (ii) it is not possible to implement the steering logic with an arbitrary torque demand \mathbf{u} , because of the presence of the singular direction along which the CMG cluster is not capable of producing a torque component.

Several singularity avoidance strategies have been developed and discussed in the literature. The most common approach, derived from the solution derived for problem of similar nature in robotic manipulators, is based on the general solution to Eq. (3.11), which can be written in the form

$$\dot{\boldsymbol{\delta}} = \mathbf{A}^T (\mathbf{A} \mathbf{A}^T)^{-1} \dot{\mathbf{H}}_B + \gamma \mathbf{n}$$

where the null vector \mathbf{n} satisfies the relation

$$\mathbf{A} \mathbf{n} = 0$$

that is, \mathbf{n} spans the null space of the jacobian matrix \mathbf{A} . In this way, the steering logic (3.12) is complemented with some null motion, where the parameter γ represents the amount of null motion that must be added in order to “stay away” from the singularities. The null vector can be expressed as

$$\mathbf{n} = [\mathbf{I} - \mathbf{A}^T (\mathbf{A} \mathbf{A}^T)^{-1} \mathbf{A}] \mathbf{d}$$

where \mathbf{d} is an arbitrary non–zero n –dimensional vector.

Although there are several possible approaches for determining a proper value for γ , depending on the current value of the gimbal angles, in general it is necessary to add null motion only when approaching a singularity. In fact, the Moore–Penrose pseudo–inverse represents the minimum norm solution for Eq. (3.11), and as such it can be considered an optimal solution, when singularities are not an issue. On the converse, a proper amount of null motion needs to be added when approaching a singular gimbal configuration, in order to avoid the increase of $\|\boldsymbol{\delta}\|$. In this way, on one side the control torque demand is

always satisfied, and at the same time the control effort is increased, with respect to the pseudo-inverse steering logic, only when this is necessary to avoid a singularity. For this reason the parameter γ is usually chosen as a function of the singularity measure

$$m = \sqrt{\det(\mathbf{A}\mathbf{A}^T)}$$

where m quantifies the distance from a singular state. As an example, it is possible to set

$$\begin{aligned}\gamma &= m^6, & \text{for } m \geq 1 \\ \gamma &= m^{-6}, & \text{for } m < 1\end{aligned}$$

A variety of heuristic approaches have also been proposed, in order to solve the problem of the presence of singular states, while keeping the computational burden of the steering logic to a minimum. A heuristic approach is represented by the so-called singularity robust pseudo-inverse, written in the form

$$\mathbf{A}^* = \mathbf{A}^T(\mathbf{A}\mathbf{A}^T + \lambda\mathbf{1})^{-1}$$

where $\mathbf{1}$ is the identity matrix and λ is a positive scalar, that is tuned as a function of m as

$$\begin{aligned}\lambda &= 0, & \text{for } m \geq m_0 \\ \lambda &= \lambda_0(1 - m/m_0)^2, & \text{for } m < m_0\end{aligned}$$

where λ_0 and m_0 are small positive constants to be properly selected. In this case, the pseudo-inverse steering logic is “altered” when approaching the singular state in such a way so as to avoid the singularity of the matrix $(\mathbf{A}\mathbf{A}^T)^{-1}$ simply by the addition of a small contribution to its principal diagonal.

Chapter 4

References

1. B. Wie, *Space vehicle dynamics and control*, AIAA Education Series, Reston, 1998.
2. M.J. Sidi, *Spacecraft dynamics and control. A practical engineering approach*, Cambridge Univ. Press, New York, 1997.
3. M.H. Kaplan, *Modern Spacecraft Dynamics and Control*, J.Wiley& Sons, New York, 1976.
4. G. Mengali, *Meccanica del Volo Spaziale*, Edizioni Plus, Pisa, 2001.